A FAR-INFRARED MICHELSON INTERFEROMETER AND ITS APPLICATION TO THE STUDY OF PHOTOCONDUCTIVITY IN ULTRA-PURE GERMANIUM

H.W.H.M. JONGBLOETS

A FAR-INFRARED MICHELSON INTERFEROMETER AND ITS APPLICATION TO THE STUDY OF PHOTOCONDUCTIVITY IN ULTRA-PURE GERMANIUM

PROMOTOR:
PROF.DR.P. WYDER

CO-REFERENT
DR. J.H.M. STOELINGA

A FAR-INFRARED MICHELSON INTERFEROMETER AND ITS APPLICATION TO THE STUDY OF PHOTOCONDUCTIVITY IN ULTRA-PURE GERMANIUM

PROEFSCHRIFT

TER VERKRIJGING VAN DE GRAAD VAN DOCTOR IN DE
WISKUNDE EN NATUURWETENSCHAPPEN
AAN DE KATHOLIEKE UNIVERSITEIT TE NIJMEGEN, OP GEZAG VAN
DE RECTOR MAGNIFICUS PROF. DR. P.G.A.B. WIJDEVELD,
VOLGENS BESLUIT VAN HET COLLEGE VAN DECANEN
IN HET OPENBAAR TE VERDEDIGEN
OP DONDERDAG 13 MAART 1980
DES NAMIDDAGS TE 4.00 UUR

door

HENDRIKUS WILHELMUS HUBERTUS MARIA JONGBLOETS
geboren te Nijmegen

1980
Druk: Krips Repro Meppel

The investigations described in this thesis have been carried out in the group "Experimentele Natuurkunde IV" of the Research Institute for Materials of the Faculty of Science at the Catholic University of Nijmegen under the direction of Prof. Dr. P. Wyder.

Part of this work has been supported by the "Stichting voor Fundamenteel Onderzoek der Materie" (FOM) with financial support from the "Nederlandse Organisatie voor Zuiver Wetenschappelijk Onderzoek" (ZWO).

We acknowledge the permission to reprint previously published papers, obtained from the publishers of Physica and Physical Review.

Aan mijn ouders

Op deze plaats wil ik allen bedanken die op enigerlei wijze hebben bijgedragen aan de totstandkoming van dit proefschrift. In het bijzonder wil ik vermelden dr. H.J.A. van Dijk van het Philips Natuurkundig Laboratorium te Eindhoven, die door het beschikbaar stellen van een aantal ultra-zuivere germanium preparaten het onderzoek, beschreven in hoofdstuk IV van dit proefschrift, mogelijk heeft gemaakt.

Verder dank ik Martien van de Steeg, die als doctoraal-student op uiterst plezierige wijze heeft meegewerkt bij veel van de hier beschreven experimenten, en die ook in de laatste fase van het schrijven van dit manuscript is bijgesprongen. Zeer bijzonder ook Riki Gommers, die het meeste type-werk voor haar rekening heeft genomen. Zeer zeker ook Evert-Jan van der Werf die als student uiterst geduldig een enorme reeks metingen heeft verricht die ons uiteindelijk het vertrouwen gaven dat het reflectie-effect, beschreven in hoofdstuk III, geen hersenschim was.

En natuurlijk dank ik de medewerkers van de dienstverlenende afdelingen van de faculteit der wiskunde en natuurwetenschappen en, last but not least, alle medewerkers van Experimentele Natuurkunde IV, met wie ik jarenlang op uiterst plezierige wijze heb mogen samenwerken. In dit verband wil ik in het bijzonder noemen de technische medewerkers, Kees Beers en Jan Hermsen.

CONTENTS

In solid state physics, the relevant energies of many interesting effects correspond with temperatures of the order of 1 - 1000 degrees Kelvin. This range covers the binding energies of impurities in semiconductors, the ordering temperatures in ferromagnetism, antiferromagnetism and ferroelectricity, the transition temperatures of superconductors, phonon- and Debije-energies, etc. To study this interesting region, sometimes high magnetic fields can be applied. Field strengths up to 25 Tesla, corresponding to 16.7 K, are available at the Nijmegen High Magnetic Field installation.

In this framework it is obviously very much worthwile to have electromagnetic radiation available of comparable energy. This is the far infrared (FIR) or submillimetre wave region (wave length range 50 - 1000 μm or wave number range 10 - 200 cm^{-1}), which connects the optical and microwave parts of the electromagnetic spectrum. This is a most awkward regime because of the lack of broadband sources of sufficient power. It is true that nowadays FIR lasers are available with output power up to 0.4 W [1,2], but these have the disadvantage of not being continuously tunable nor being very stable. The FIR region can also be approached from the microwave side by the technique of harmonic generation which offers a higher stability and so a higher resolution. With this method the range of 2 - 25 cm^{-1} can easily be spanned with an output power decreasing from 10^{-2} to 10^{-8} W with increasing wave number.

The most widely used technique is that where the FIR region is penetrated from the optical side by employing a broadband source (medium pressure mercury arc lamp) in combination with a dispersive optical device, such as a grating monochromator[4,5,6], or an interferometric device such as a lamellar grating interferometer[7,8] or a Michelson interferometer[9]. These instruments deliver only a radiation power which at low wave numbers is less than 10^{-9} W within a bandwidth of 1 cm^{-1}, but they cover the whole FIR region.

In chapter II of this thesis the hardware of a modern commercial Grubb Parsons FIR Michelson interferometer system is described, originally developed by Chantry et al.[9]. This system has been modified and improved in our laboratory by the author with the help of the instrument and electronics workshops of our Faculty. This instrument now covers the range 5 - 350 cm^{-1}. A short summary of the theory underlying the technique of Fourier spectroscopy is given in chapter III (section III.1). This more conventional part of the

theory does not take into account the radiation which returns to the interferometer due to reflection of the sample. It is shown that this can lead to significant distortions in the spectra, as is analyzed both theoretically and experimentally in chapter III (section III.2) and Ref. 10. In an appendix to this thesis the computer programs, developed for the processing of the data and the execution of the Fourier transform needed to obtain a frequency spectrum, are collected.

The application of the Michelson interferometer to the study of the properties of impurity states in semiconductors is described in chapter IV. This study has been stimulated greatly by the very advanced crystal growing techniques which exist nowadays. It has become possible to fabricate ultrapure crystals with impurity concentrations smaller than 10^{10} atoms/cm^3. In other words, only one out of every 10^{12} atoms is an impurity. It is extremely difficult to identify these impurities by conventional methods, e.g. Hall effect measurements. However, photothermal ionization spectroscopy (PTIS) in the far infrared region, first developed by Russian scientists[11,12], offers a possibility to study the impurities both qualitatively and quantitatively. With this technique FIR spectroscopy can be used as a tool for chemical analysis.

It is well known that the group V donor and group III acceptor impurities in group IV semiconductors (e.g. in germanium, silicon) exhibit "hydrogen-like" energy level schemes for the single bound electron/hole, with binding energies in the order of 10 meV. The PTIS technique is based on the two-step photothermal ionization process where the electron/hole is excited from the impurity groundstate to a higher level by the FIR radiation, and then subsequently thermally ionized into the band continuum, where it contributes to the electrical conductivity. Therefore, in the photoconductivity line spectra, which reflect the discrete energy level structure of the impurity, the line intensity will be temperature dependent.

Up to now little was known about the detailed mechanism of this thermal ionization, nor was the temperature dependence exactly known. The ad hoc assumption often mentioned in the literature[13-16] of a simple exponential behaviour seems not to fit the experimental results. Therefore the statistical problem was studied in detail (i.e. the transition from a localized impurity state to a delocalized bandstate); we have been able to show that a detailed theoretical understanding is possible and gives very good agreement with our experimental observations. An expression was derived for the temperature

dependence, which includes not only the energy difference between band edge and excited level, but also the degeneracy of the relevant level and the band. Moreover it contains a factor proportional to the impurity concentration.

Preliminary results are given in chapter IV, section IV.2 and Ref. 17. In section IV.3 (Ref. 18) very accurate values for the ground state energies of the Al, B and P impurities in germanium are derived from the temperature dependence. These values are in excellent agreement with existent theories [19,20]. In addition, the ratio of the concentrations of the two acceptors present in our sample, is derived. This ratio is in accordance with the value obtained from the concentration profile in the original crystal from which our sample was cut. The determination of this profile is explained in section IV.4. In section IV.5 (Ref. 21) a detailed theoretical derivation of the temperature dependence is given, not only for the line intensity in a photothermal conductivity spectrum, but also for the signal strength in a photoconductivity experiment.

Photoconductivity measurements in magnetic fields are described in section IV.6 (Ref. 22). The linear and quadratic Zeeman terms are determined for all lines of the boron excitation spectrum. In the literature [23,24] only values for the lowest levels are available; the corresponding values of our investigation agree with these. Some of the lines showing up in a magnetic field can be identified as states associated with light-hole Landau levels. Values for the magnetic field dependence of these Landau levels, derived from the measurements, agree very well with values from the literature [25].

References.

1. T.Y. Chang, IEEE Trans. Microwave Theory and Tech. MTT-22, 983 (1974).
2. D.T. Hodges, Infrared Phys. 18, 375 (1978).
3. M.J. Huijben, C.G.C.M. de Kort, J.H.M. Stoelinga and P. Wyder, Infrared Phys. 19, 257 (1979).
4. M. Tinkham, Science 145, 240 (1964).
5. J.H.M. Stoelinga en P. Wyder, Nederlands Tijdschrift voor Natuurkunde 36, 107 (1970).
6. M.V. Dorigo, J.H.M. Stoelinga and P. Wyder, Z. f. angew. Math. u. Phys. 20, 565 (1969).
7. J. Strong and G.A. Vanasse, J. Opt. Soc. Am. 50, 113 (1960).
8. R.C. Milward, Infrared Phys. 6, 59 (1969).

9. G.W. Chantry, H.W. Evans, J. Chamberlain and H.A. Gebbie, Infrared Phys. 9, 85 (1969).
10. H.W.H.M. Jongbloets, M.J.H. van de Steeg, E.J.C.M. van der Werf, J.H.M. Stoelinga and P. Wyder, accepted for publication in Infrared Phys. (1980).
11. T.M. Lifshits and F. Ya. Nad', Sov. Phys. Doklady 10, 532 (1965).
12. Sh. M. Kogan and T.M. Lifshits, Phys. Status Solidi A39, 11 (1977).
13. T.M. Lifshits, N.I. Likhtman and V.I. Sidorov, Sov. Phys. Semicond. 2, 652 (1968).
14. S. Dana Seccombe and D.M. Korn, Solid State Commun. 11, 1539 (1972).
15. E.M. Bykova, L.A. Goncharov, T.M. Lifshits, V.I. Sidorov and R.N. Hall, Sov. Phys. Semicond. 9, 1223 (1976).
16. P.E. Simmonds, J.M. Chamberlain, R.A. Hoult, R.A. Stradling and C.C. Bradley, J. Phys. C: Solid St. Phys. 7, 4164 (1974).
17. H.W.H.M. Jongbloets, J.H.M. Stoelinga, M.J.H. van de Steeg and P. Wyder, Physica 89B, 18 (1977).
18. H.W.H.M. Jongbloets, J.H.M. Stoelinga, M.J.H. van de Steeg and P. Wyder, Phys. Rev. B 20, 3328 (1979).
19. R.L. Jones and P. Fisher, J. Phys. Chem. Solids 26, 1125 (1965).
20. J.H. Reuszer and P. Fisher, Phys. Rev. 135, A1125 (1965).
21. H.W.H.M. Jongbloets, M.J.H. van de Steeg, J.H.M. Stoelinga and P. Wyder, accepted for publication in J. Phys. C: Solid St. Phys. (1980).
22. H.W.H.M. Jongbloets, M.J.H. van de Steeg, J.H.M. Stoelinga and P. Wyder, submitted for publication.
23. A.P. Soepangkat and P. Fisher, Phys. Rev. B 8, 870 (1973).
24. J. Broeckx, P. Clauws, K. van den Steen and J. Vennik, J. Phys. C: Solid St. Phys. 12, 4061 (1979).
25. J.C. Hensel and K. Suzuki, Phys. Rev. B 9, 4219 (1974).

1. Introduction.

For all far infrared spectroscopic experiments described in this thesis the technique of Fourier transform spectroscopy (FTS) was used. The principle of FTS involves the recording of interference fringes formed by radiation which has propagated through an interferometer. This interferogram is a function of path difference between two optical beams formed in the interferometer, and is uniquely related to the spectral distribution of the radiation. This information is recovered by the process of Fourier transformation (see chapter III).

The FTS technique offers several advantages over conventional dispersive techniques:

1. The multiplex advantage, first pointed out by Fellgett[1], that each spectral element is observed for the whole duration of the experiment. The signal-to-noise ratio of an interferometric system will therefore be superior to that of a dispersive system (at least as long as detector noise is the dominant source of noise).

2. Jacquinot[2] showed that the information throughput of cylindrically symetrical systems such as an interferometer, could be much higher than in systems where a slit has to be used.

3. An interferometer is mechanically extremely simple as compared with a grating instrument. And it has the added advantage that the problem of stray light is not very severe, because only radiation that has undergone interference contributes to the interferogram.

Once the problem of transforming interferograms into spectra was overcome with the advance of modern computers, the advantages mentioned before made the FTS technique the most widely applied technique in far infrared spectroscopy. Extensive reviews of FTS have been given by Chantry[3] and Bell[4]; a short summary of the most important aspects is given in chapter III (section III.1).

2. Spectrometer hardware

A typical far infrared interferometric spectrometer consists of the following sub-systems:

a). A broad band source of far infrared radiation, and optics for beam collimation.

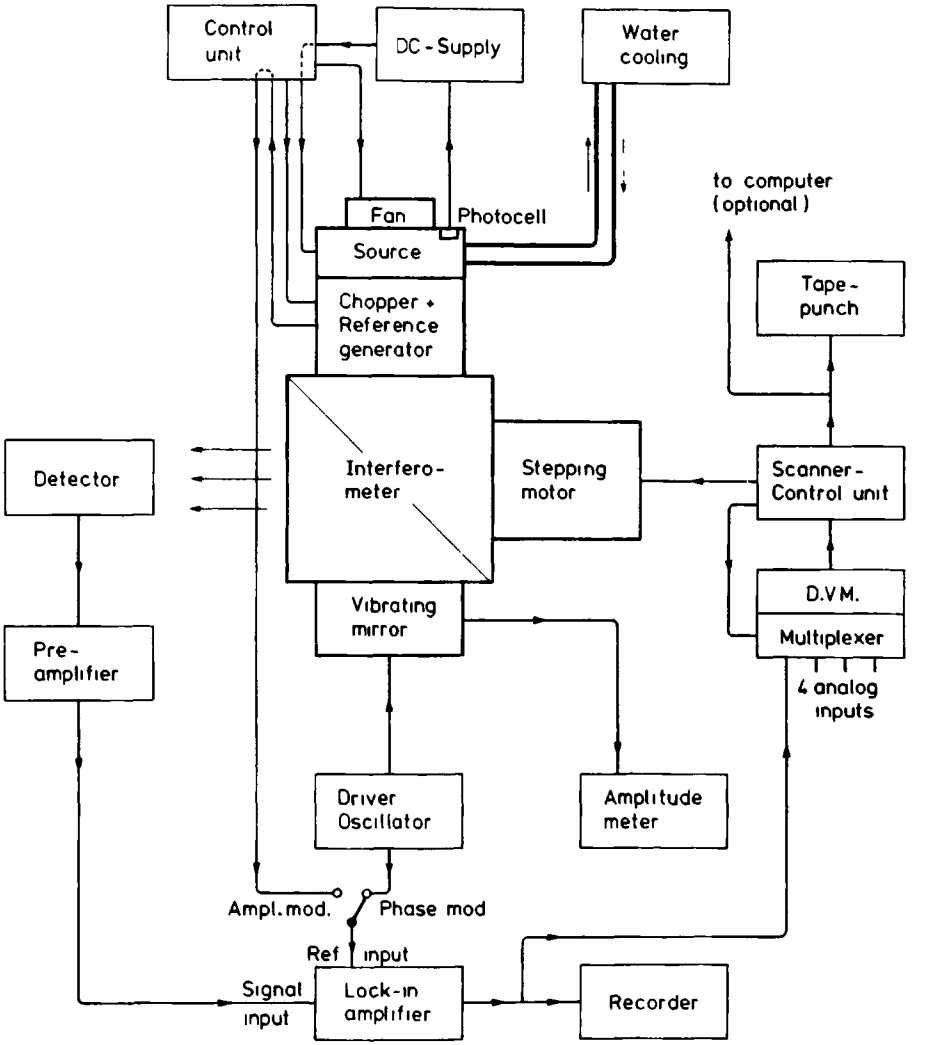

SCHEMATIC DIAGRAM OF FOURIER SPECTROMETER

Figure 1

F.I.R. MICHELSON INTERFEROMETER

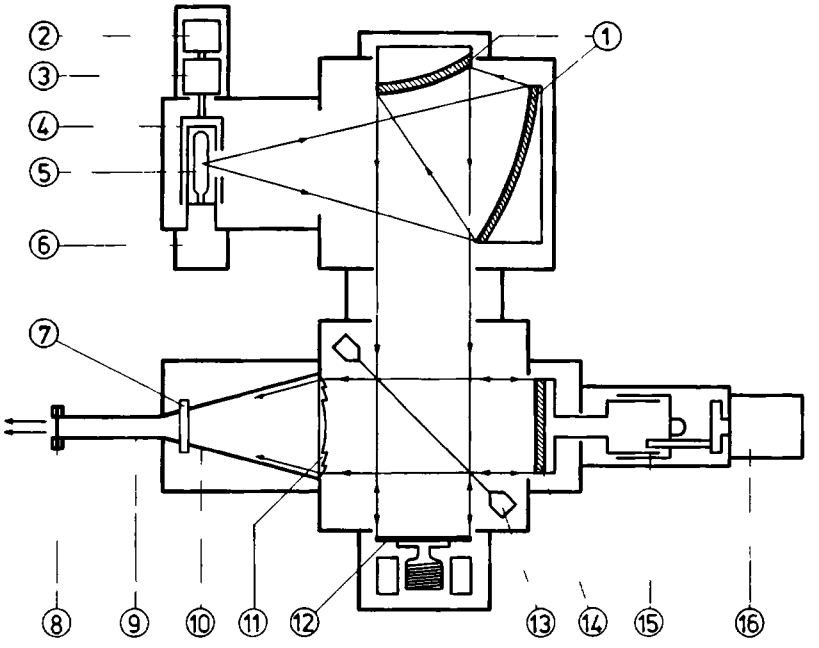

① Collimator mirrors
② Reference signal generator
③ Chopper motor
④ Chopper
⑤ Medium pressure mercury lamp
⑥ Water-cooled lamp mount
⑦ Transmission filter
⑧ Black polyethylene window
⑨ Lightpipe (polished brass)
⑩ Brass cone
⑪ TPX Fresnel lens
⑫ Vibrating mirror
⑬ Beamsplitter (mylar film)
⑭ Moving mirror
⑮ Micrometer
⑯ Stepping motor

Figure 2

b). The interferometer itself to create the necessary interferogram-function from the broad band radiation.

c). A far infrared detector and signal amplifying system for recording analogue interferogram signals.

d). A Scanner-Control Unit to drive the interferometer and containing a digital data system to digitize interferogram signals and store the data, so that they can be processed by a computer.

These subsystems can easily be recognized in the schematic diagram (figure 1) of the Fourier spectrometer, which was used for the experiments described in this thesis. The interferometer is of the Michelson type, with a thin film dielectric beamsplitter (figure 2). This modular instrument was developed at the National Physical Laboratory (Teddington, England) [5] and manufactured by Grubb Parsons Company[6]. Several details of this basic machine have been modified and improved in our laboratory.

a) Source

The medium pressure mercury arc lamp is still the best continuous broad band far infrared source available today, particularly at wave numbers below 100 cm^{-1} where emission from the hot electron plasma predominates. Unfortunately its power output is rather low. In the whole 10 - 300 cm^{-1} band it delivers $\sim$5 $mW.cm^{-2}.sterad^{-1}$. Above 100 cm^{-1}, strong absorption and reemission from the fused quartz outer mantle takes place, which makes the total radiative output extremely sensitive to effects of convective cooling. For high stability, the lamp operates on d.c., under constant vacuum and in a water-cooled jacket. The special d.c. power supply for the Philips HPK 125 W mercury lamp was custom-built by Heinzinger [7]; it uses a photo-cell feed-back circuit to stabilize the radiation output of the source.

The radiation can be chopped by a cylindrical chopper around the lamp (amplitude modulation; see chapter III, section III.1), and the emergent beam is collimated by a combination of a concave and convex mirror.

b) Michelson interferometer

The radiation from the source is divided by the beamsplitter into two beams, which are sent to two plane mirrors. One mirror can be translated over a distance of 2 cm by a micrometer screw driven by a stepping motor (Slo-Syn SS25-1002). The beams are reflected by the mirrors and, as they are mutually coherent, interference will occur as they are recombined at the beamsplitter

and travel to the detector. The emergent beam is focussed on the entrance of a polished brass lightpipe by a TPX Fresnel lens. A low-pass transmission filter and a vacuum-tight black polyethylene window remove the unwanted part of the Planck-spectrum of the source.

The division of the incident wavefront into two is achieved by a free-standing dielectric film beamsplitter; Mylar films of thicknesses between 6 μm and 100 μm are available, covering the spectral range of 5-350 cm^{-1}. (For a description of the properties of thin film beamsplitters: see Ref. 3, chapter 3).

An alternative way of modulating the radiation is the so-called phase modulation (see chapter III, section III.1), achieved by a sinusoidal variation of the optical path difference. For this purpose, one of the plane mirrors is mounted on a vibration generator manufactured by Ling Dynamic Systems Ltd[8].

c) Far infrared detector

The important criteria for a detector for use in combination with a far infrared interferometer are that it should have a high sensitivity (low noise equivalent power, NEP) and high responsivity, a uniform spectral response over a wide wave number range, and a high linearity of output over a wide dynamic range of input signals. In practice these criteria are only met by thermal detectors, which use the heating by the radiation to measure the absorbed power.

Most commercial far infrared interferometers use a room temperature Golay detector[9], which has the disadvantage of a moderate NEP ($\sim 10^{-10}$ $W.Hz^{-\frac{1}{2}}$) and slow response time ($\sim$ 30 msec). Low[10] was the first to describe a germanium bolometer operated at liquid helium temperatures. Nowadays both germanium and silicon bolometers[11] are used, and often a ^3He cooling system is employed to reach a temperature of 0.35 K [12], yielding a NEP of 10^{-12} - 10^{-14} $W.Hz^{-\frac{1}{2}}$. An extensive review of these cryogenic semiconductor bolometers was given by Pankratov and Korotkov [13].

Figure 3 shows a typical example of a basic detection system; various modifications for specific experiments are used in our laboratory. The FIR radiation enters the system via a black polyethylene window, which blocks out all visible and near infrared radiation. A lightpipe directs the radiation through a cooled low-pass filter (removing room temperature radiation) and a conical lightpipe to an integrating cavity wherein the bolometer has been

CRYOSTAT WITH FAR INFRARED DETECTOR

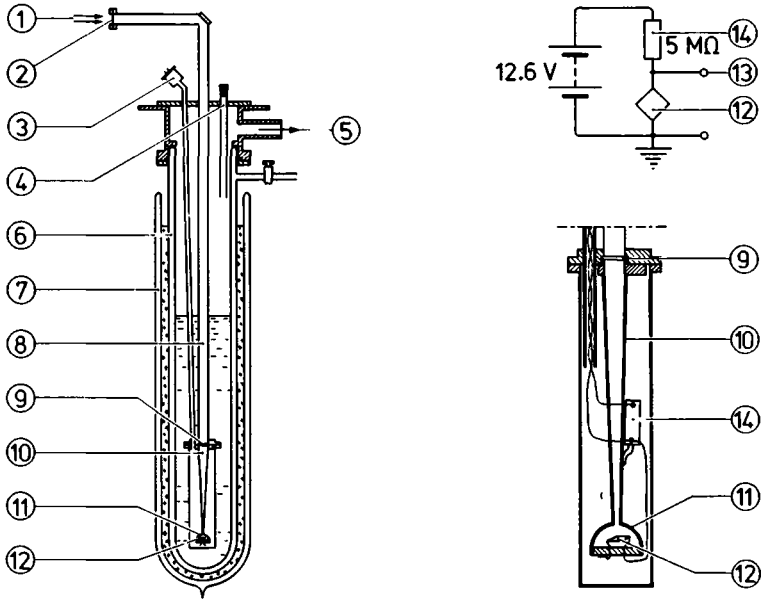

① Incident radiation
② Polyethylene window
③ Electrical connections
④ Helium fill port
⑤ To helium pump
⑥ Liquid helium dewar
⑦ Liquid nitrogen dewar
⑧ Light pipe (stainless steel)
⑨ Sapphire filter
⑩ Cone (gold plated copper)
⑪ Cavity („ „ „)
⑫ Bolometer
⑬ To amplifier
⑭ Load resistor (5 MΩ)

Figure 3

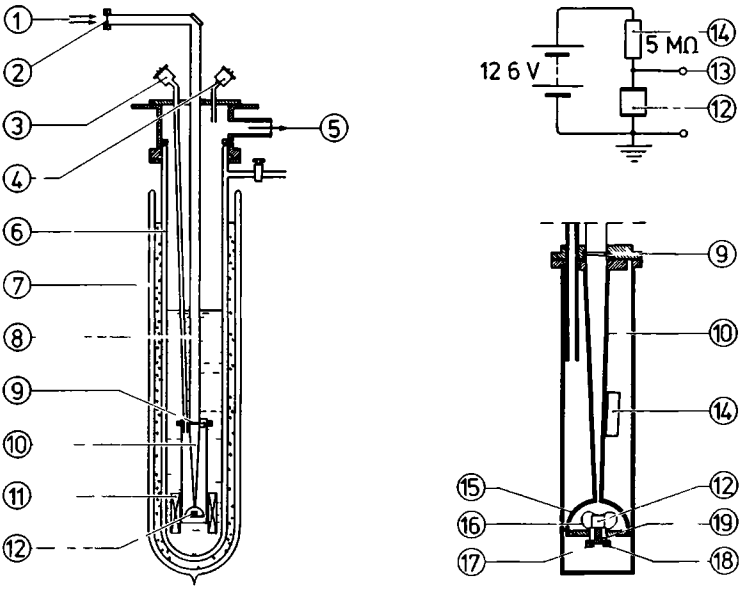

① Incident radiation
② Polyethylene window
③ Electrical connections for Ge-sample
④ Electrical connections for s.c magnet
⑤ To helium pump
⑥ Liquid helium dewar
⑦ Liquid nitrogen dewar
⑧ Light pipe (stainless steel)
⑨ Sapphire filter
⑩ Cone (gold plated copper)
⑪ Superconducting magnet
⑫ Germanium sample
⑬ To amplifier
⑭ Load resistor (5 MΩ)
⑮ Cavity (gold plated copper)
⑯ Clamp
⑰ Thermometer
⑱ Heater
⑲ Tufnol insulation

Figure 4

mounted. The absorbed radiation causes an increase in temperature of the bolometer element; this temperature change manifests itself as a change in the electrical conductance. The bolometer is connected to an electric circuit which delivers a bias current provided by a 12.6 Volt mercury battery via a 5 MΩ cooled load resistor. The variation in the voltage drop across the bolometer, due to the chopped radiation, is measured with a lock-in amplifier.

d) Scanner-Control Unit

The Scanner-Control Unit contains a preset indexer to drive the stepping motor a preset number of steps for discrete sampling of the interferogram. The step-length (i.e. the number of steps between two consecutive interferogram points) is chosen appropiate to the spectrum high wave number cutoff (see also chapter III). The waiting time between sampled points is about twice the integration time of the detector lock-in amplifier. A digital volt meter (4½ digit), preceded by a 4-channel multiplexer, digitizes the analogue output of the lock-in amplifier, and eventually the data are punched on papertape. The data are processed on a PDP-12 (DEC) laboratory computer, linked to a Houston incremental plotter. The relevant computer program is shown in an appendix to this thesis.

3. Experimental arrangement for photo-conductivity measurements.

For the photoconductivity experiments, described in chapter IV, no bolometer is needed, as the sample itself is the detector. Figure 4 shows the cryostat insert. As can be seen, the construction is almost identical to that of the bolometer system (figure 3). Only the semispherical cavity at the end of the conical lightpipe is enlarged so that it can contain the cubic sample of dimensions 1 x 1 x 1 cm^3.

The sample is clamped onto the base of the cavity with only a small heat leak to the base. The clamp and the sample can be heated above the temperature of the surrounding helium bath by a resistance wire wrapped around the mounting stud. The temperature of the sample is measured with an Allen Bradley carbon resistor and can be stabilized within 0.1 K. Electric contacts are made by pressing flat copper disks against two sides of the sample which are wetted with a mixture of In-Hg (50-50). The sample is connected to an electric circuit, identical to the bolometer circuit, so the variation of the conductivity due to chopped radiation can be measured with a lock-in amplifier.

References

1. P. Felgett, J. de Physique C.2 28, 165 (1967).
2. P. Jacquinot, J. Opt. Soc. Am. 44, 761 (1954).
3. G.W. Chantry, Submillimetre Spectroscopy, Academic Press, N.Y. (1971).
4. R.J. Bell, Introductory Fourier Transform Spectroscopy, Academic Press, N.Y. (1972).
5. G.W. Chantry, H.M. Evans, J. Chamberlain and H.A. Gebbie, Infrared Phys. 9, 85 (1969).
6. Sir Howard Grubb Parsons and Company Limited, Walkergate, Newcastle upon Tyne NE62YB, England.
7. Heinzinger Regel- und Messtechnik, 82 Rosenheim, Happingerstr. 71, West Germany.
8. Ling Dynamic Systems Limited, Royston Herts SG85BQ, England.
9. M.J.E. Golay, Rev. Sci. Instrum. 20, 816 (1949).
10. F.J. Low, J. Opt. Soc. Am. 51, 1300 (1961).
11. I.F. Silvera and G. Birnbaum, J. Opt. Soc. Am. 58, 718 (1968).
12. H.D. Drew and A.J. Sievers, Appl. Opt. 8, 2067 (1969).
13. N.A. Pankratov and V.P. Korotkov, (Sov. Phys.) Opt. Technology 14, 106 (1974).

III.1 GENERAL INTRODUCTION

1. The interferogram-function.

In a Michelson interferometer radiation from the source is divided into two beams, one is sent to a fixed mirror, and the other is sent to another mirror which can be driven along one arm of the interferometer (Fig. 1). Assume the source to be monochromatic, emitting radiation of amplitude $\sqrt{S}$ (intensity S) and of wave number $\sigma(=1/\lambda)$. This radiation falls onto a dielectric beam divider to which can be assigned a complex reflectivity $\hat{r}$ and transmissivity $\hat{t}$; these functions are complex because of the phase shifts introduced into the optical beam by the phenomena that occur in the

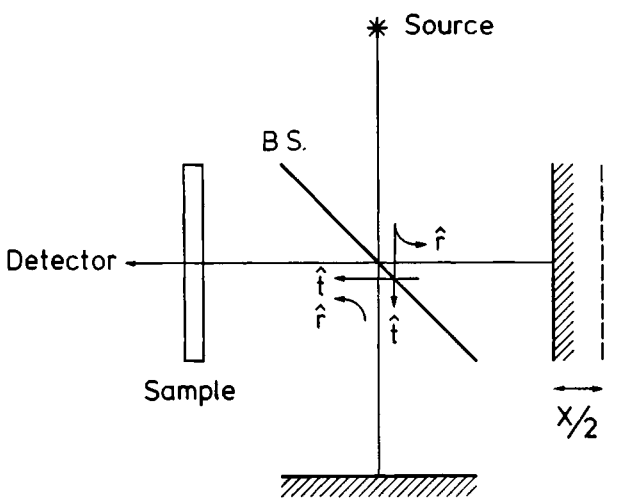

Fig. 1 : The division of complex amplitudes in a Michelson interferometer; $\hat{r}$ and $\hat{t}$ are the complex reflectivity and transmissivity of the dielectric film beam splitter (B.S.).

beam divider. (See e.g. Chantry[1], chapter 3.) Therefore $\hat{r}$ and $\hat{t}$ can be written as

$$\begin{aligned} \hat{r} &= r \cdot e^{i\theta} \\ \hat{t} &= t \cdot e^{i\varphi} \ . \end{aligned} \tag{1}$$

A displacement x/2 of the moving mirror in one arm of the interferometer produces a phase delay Δ between the two beams, given by

$$\Delta = 2\pi\sigma x \ . \tag{2}$$

From Fig. 1 it can easily be seen that the amplitude $\hat{a}_{det}$ of the recombined beam going to the detector, and the amplitude $\hat{a}_{source}$ of the beam going back to the source, are given by

$$\begin{aligned} \hat{a}_{det} &= \sqrt{S}(\hat{r}\hat{t}+\hat{t}\hat{r} \cdot e^{i\Delta}) \\ \hat{a}_{source} &= \sqrt{S}(\hat{t}^2+\hat{r}^2 \cdot e^{i\Delta}) \ . \end{aligned} \tag{3}$$

These equations illustrate the dissymmetry of the two beams. For the one travelling towards the detector, the beams traversing the two arms each suffer one transmission and one reflection at the beam splitter; for the other case one beam is reflected twice and the other transmitted twice. Using equation (1) this leads to

$$\begin{aligned} \hat{a}_{det} &= \sqrt{S}rt(1+e^{i\Delta})e^{i(\theta+\varphi)} \\ \hat{a}_{source} &= \sqrt{S}(t^2 \cdot e^{i2\varphi}+r^2 \cdot e^{i2\theta} \cdot e^{i\Delta}) \ . \end{aligned} \tag{4}$$

The intensity of the beams is given by the square of the modulus of the complex amplitude. Therefore, one gets at the detector and at the source respectively

$$\begin{aligned} I_{det} &= 2r^2t^2S(1+\cos\Delta) \\ I_{source} &= S[\, r^4+t^4+2r^2t^2 \cdot \cos(2\theta-2\varphi+\Delta)\,] \ . \end{aligned} \tag{5}$$

In the case of a non-absorbing beam splitter it can be shown (Chantry[1], chapter 3) that

$$2\theta - 2\varphi = (2n+1)\pi \qquad n = 1,2,3,\ldots \; . \tag{6}$$

This leads to

$$I_{source} = S(r^4+t^4-2r^2t^2\cdot\cos\Delta) \; . \tag{7}$$

The properties of the beam splitter can be combined in two parameters A and B given by

$$\begin{aligned} A &= r^4+t^4 \\ B &= 2r^2t^2 \; . \end{aligned} \tag{8}$$

The quality B is often called the efficiency of the beam splitter. If a sample with energy transmission-coefficient T is placed into the beam going to the detector (see Fig. 1), the intensity of the relevant beams can finally be expressed as

$$\begin{aligned} I_{det}(\Delta) &= TSB(1+\cos\Delta) \\ I_{source}(\Delta) &= S(A-B\cdot\cos\Delta) \end{aligned} \tag{9}$$

So far the source was assumed to be monochromatic with wave number σ and intensity S. If the source emits a broad spectrum with distribution $S(\sigma)$, the total intensity $I'(x)$ reaching the detector can be found by integrating $I_{det}(\Delta)$ over all wave numbers σ. It has to be noted that the quantities A, B and T are functions of σ as well. The interferogram-function $I'(x)$ for a broad spectrum is thus found to be

$$\begin{aligned} I'(x) &= \int_0^\infty T(\sigma)\cdot S(\sigma)\cdot B(\sigma)\cdot(1+\cos 2\pi\sigma x)\cdot d\sigma \\ &= 2\int_0^\infty Q(\sigma)\cdot(1+\cos 2\pi\sigma x)\cdot d\sigma \; , \end{aligned} \tag{10}$$

where $Q(\sigma) \equiv \frac{1}{2}\, T(\sigma)\cdot S(\sigma)\cdot B(\sigma)$.

2. Amplitude and phase modulation.

Since the intensity of the source in the far infrared region is very weak, the voltage output of the detectors is very small. Therefore it is necessary to modulate the radiation and to use phase sensitive detection (PSD) techniques. In a Michelson interferometer this modulation can be done in two ways: 1) Amplitude Modulation (AM), where the light beam emerging from the source is chopped; 2) Phase Modulation (PM), where the optical path difference between the two interfering beams is modulated. This is achieved by a vibration with small amplitude a of one of the mirrors in the interferometer. The modulation frequency ω for AM and PM is optimized with respect to the response time of the detector.

In the previous section the unmodulated interferogram-function I'(x) was calculated and is given by equation (10). When some form of periodic modulation is used, the interferogram-function becomes time-dependent and the intensity reaching the detector can be resolved into Fourier components. Since phase sensitive detection selects out only the fundamental Fourier-component of the signal, the ideal form of modulation is a pure sine-function of time. Obviously, the resulting interferograms and spectra will depend on which of the two modulation techniques, AM or PM, is used.

When AM is used the source intensity $S(\sigma)$ in equation (10) becomes time-dependent. If the modulation has the ideal sine-form, the intensity $I'_{AM}(x,t)$ reaching the detector becomes

$$I'_{AM}(x,t) = I'(x)\cdot(1+\sin\omega t) \ . \tag{11}$$

After PSD, the registered interferogram-function will be proportional to

$$\begin{aligned} I'_{AM}(x) &= \tfrac{1}{2}\, I'(x) \\ &= \tfrac{1}{2} \int_0^\infty 2Q(\sigma)\cdot(1+\cos 2\pi\sigma x)\cdot d\sigma \ . \end{aligned} \tag{12}$$

This proportionality-factor is determined by the detector sensitivity and the amplification of the phase sensitive detector (lock-in amplifier). If a more practical square function is used for the modulation, the factor $\frac{1}{2}$ in equation (12) has to be replaced by $2/\pi$. The actual spectral information is contained in the x-dependent part of equation (12), called the interferogram.

This interferogram $I_{AM}(x)$ is obtained from expression (12) by subtracting the constant level $\int Q(\sigma)\cdot d\sigma$, leading to

$$I_{AM}(x) = \tfrac{1}{2} \int_{o}^{\infty} 2Q(\sigma)\cdot\cos(2\pi\sigma x)\cdot d\sigma \ . \qquad (13)$$

Notice that $I_{AM}(x)$ is an even function of x!

When PM is applied the optical path difference x is modulated. If a sinusoidal modulation of amplitude a is used, in equation (10) x has to be replaced by $x+a\cdot\sin\omega t$. Using the Bessel series expansions of $\cos(z\cdot\sin\theta)$ and $\sin(z\cdot\sin\theta)$, the cos-term in equation (10) can be written as

$$\cos[\,2\pi\sigma(x+a\cdot\sin\omega t)\,] = \sum_{m=-\infty}^{\infty} J_m(2\pi\sigma a)\cdot\cos(2\pi\sigma x+m\omega t) \ . \qquad (14)$$

Since phase sensitive detection is used, only the component with the fundamental frequency has to be considered. The intensity $I'_{PM}(x,t)$ of this component is given by

$$I'_{PM}(x,t) = \int_{o}^{\infty} 2Q(\sigma)\cdot(-2J_1(2\pi\sigma a))\cdot\sin 2\pi\sigma x\cdot\sin\omega t\cdot d\sigma \ , \qquad (15)$$

where the relation $J_{-m}(z) = (-1)^m J_m(z)$ has been used. After PSD, the registered interferogram is therefore proportional to

$$I_{PM}(x) = \int_{o}^{\infty} 2Q(\sigma)\cdot(-2J_1(2\pi\sigma a))\cdot\sin 2\pi\sigma x\cdot d\sigma \ . \qquad (16)$$

Notice that this interferogram is an odd function of x and that this expression has no constant term as in equation (12).

3. Spectra calculated by Fourier transformation.

Expressions for the observed interferograms were given in equations (13) and (16) for the case of AM and PM respectively. An extension can be made to negative wave numbers by stating that $Q(-\sigma) = Q(\sigma)$. Since $J_1(-2\pi\sigma a) = -J_1(2\pi\sigma a)$ it follows that $-2J_1(2\pi\sigma a)\cdot Q(\sigma)$ is an odd function of σ. With this

extension equations (13) and (16) can be rewritten in a complex form as

$$I_{AM}(x) = \tfrac{1}{2} \int_{-\infty}^{\infty} Q(\sigma) \cdot e^{i2\pi\sigma x} \cdot d\sigma$$

$$I_{PM}(x) = \frac{-2}{i} \int_{-\infty}^{\infty} Q(\sigma) \cdot J_1(2\pi\sigma a) \cdot e^{i2\pi\sigma x} \cdot d\sigma \quad . \tag{17}$$

From these equations it is clear that the interferograms $I_{AM}(x)$ and $I_{PM}(x)$ have a Fourier-type of relationship with the spectral functions $\frac{1}{2}\, Q(\sigma)$ and $\frac{-2}{i}\, Q(\sigma) \cdot J_1(2\pi\sigma a)$ respectively. The latter two functions can be recovered from $I_{AM}(x)$ and $I_{PM}(x)$ by an inverse complex Fourier transform. Since in practise a complex Fourier transform yields a complex spectrum, one usually calculates the modulus of this spectrum, i.e.

$$P(\sigma) = \left| \int_{-\infty}^{\infty} I(x) \cdot e^{-2\pi i\sigma x} \cdot dx \right| \quad , \tag{18}$$

yielding

$$P_{AM}(\sigma) = \tfrac{1}{2}\, Q(\sigma) \qquad \text{and}$$

$$P_{PM}(\sigma) = 2\left|J_1(2\pi\sigma a)\right| \cdot Q(\sigma).$$

From these considerations, some advantages of PM are immediately evident:

1. In order to obtain the spectral information from the interferogram-function $I'_{AM}(x)$ (equation (12)), the constant term in this expression has to be subtracted. Fluctuations in the source intensity and detector sensitivity affect this constant term and therefore can falsefy the spectrum. Since the expression for $I_{PM}(x)$ (equation (16)) contains no constant term, greater immunity from fluctuations in source intensity and detector sensitivity is obtained with PM.

2. The ratio of $P_{PM}(\sigma)$ and $P_{AM}(\sigma)$ is $4\left|J_1(2\pi\sigma a)\right|$. This factor is wave number dependent and is > 1 for wave numbers between 0.08/a and 0.51/a. It reaches zero at $\sigma_o = 0.611/a$ and has a maximum of 2.3 at $\sigma_{max} = 0.29/a$. This means that in case of PM the signal-to-noise ratio exceeds that of AM over 75% of the range between 0 and σ_o and is twice as high near σ_{max}. A physical

way of looking at this is that there is no chopper to interrupt the optical beam, so that the detector views the source for a greater length of time with PM, thus leading to an increase in the signal-to-noise ratio.

3. The wave number dependent multiplicative factor $4|J_1(2\pi\sigma a)|$ can be used to act as a non-absorbtive filter. The Bessel function falls to zero when $\sigma = 0.611/a$. By an appropriate choice of the modulation amplitude a, a certain spectral region can be suppressed. Thus in combination with suited low-pass transmission filters an effective suppression of radiation with high wave numbers can be achieved.

A more detailed description of AM and PM was given by Chamberlain[2,3,4] and Chantry[1].

4. Effects due to sampling of the interferogram over a finite length.

The optical path difference x is usually assumed to be a continuous variable ranging from $-\infty$ to $+\infty$. Actually, however, interferograms are recorded in discrete steps Δx, over a finite range. If N datapoints are recorded symmetrically around zero path difference, i.e. x ranging from -L to +L with $L = (N/2)\cdot\Delta x$, then expression (18) for the modulus spectrum has to be modified into

$$P(\sigma) = \Delta x \cdot \sum_{n=-N/2}^{+N/2} I(n\Delta x)\cdot e^{-2\pi i\sigma n\Delta x} \quad . \tag{19}$$

This expression relates $P(\sigma)$ uniquely with $I(n\Delta x)$ for a limited range of values for σ only. This can be seen by considering the source to be monochromatic with wave number $\sigma_o = (1/\lambda_o)$. According to equation (9), this results in a cosine-like interferogram. To determine the value of σ_o from the interferogram, the sampling theorem states that at least two points have to be sampled within one wave length. Therefore, this leads, for a given value of Δx, to a limit for the highest wave number σ_{max}, given by $\sigma_{max} = 1/(2\Delta x)$. However, it is obvious that an infinite number of waves with higher wave numbers will also fit through the points in the range of observation. Therefore, the information contained in the interferogram can be attributed to higher wave numbers as well; this phenomenon is called "aliasing" (Chantry[1], chapter 3). If low pass filters are used, which block out the radiation with wave numbers above σ_{max}, using expression (19) the original spectrum can be

recovered uniquely from the recorded interferogram.

In addition, the limitation of recording the interferogram over a finite range of x-values, $-L \leq x \leq L$, also confines the spectral resolution. It can easily be shown (Chantry[1], chapter 3), that the power spectrum of a truncated interferogram of a monochromatic line is proportional to

$$\frac{\sin 2\pi(\sigma_o-\sigma)L}{2\pi(\sigma_o-\sigma)L} \cdot \qquad (20)$$

This function has a half-width of approximately $1/(2L)$, and has large and slowly decaying sidelobes. If the resolution is taken as the minimum wave number distance at which another line of equal intensity can just be observed in the transformed discrete spectrum, then one gets a resolution of $1/(2L)$. Therefore, spectra with a higher resolution can be obtained simply by moving the mirror over a longer distance, parallel to its original position. In practice, the resolution is restricted by the signal-to-noise-ratio, the finite aperture of the source and detector, and by tilt adjustments (i.e. the image of one mirror in the beam splitter is not perfectly parallel to the surface of the other).

The sidelobes mentioned above can easily be mistaken for real spectral features. If the recorded interferogram is multiplied with a so-called apodization-function, these sidelobes can be suppressed effectively. Usually a cosine squared function (which is 1 at $x = 0$ and 0 at $x = \pm L$) is chosen; this is also done in our computer program, described in the Appendix. It should be noted however, that this procedure broadens the central line, degrading the resolution by a factor 1.5.

An example of an interferogram of a monochromatic line, recorded with amplitude modulation, is shown in figure 2a. This line originated from a home-built grating monochromator, described in refs. 5 and 6. Figure 2b shows the corresponding power spectrum, calculated with equation (19). From figure 2a it can be seen that the interference pattern decays within the interferogram length; therefore figure 2b represents the actual lineshape. In fact, the lineshape is determined by the width of the exit-slit of the grating monochromator. From the interferogram, the wavelength λ_o is seen to have a value of 0.370 mm, while the central position σ_o of the line in the spectrum is situated at 27 cm^{-1}. So for these values the relation $\sigma_o = 1/\lambda_o$ holds.

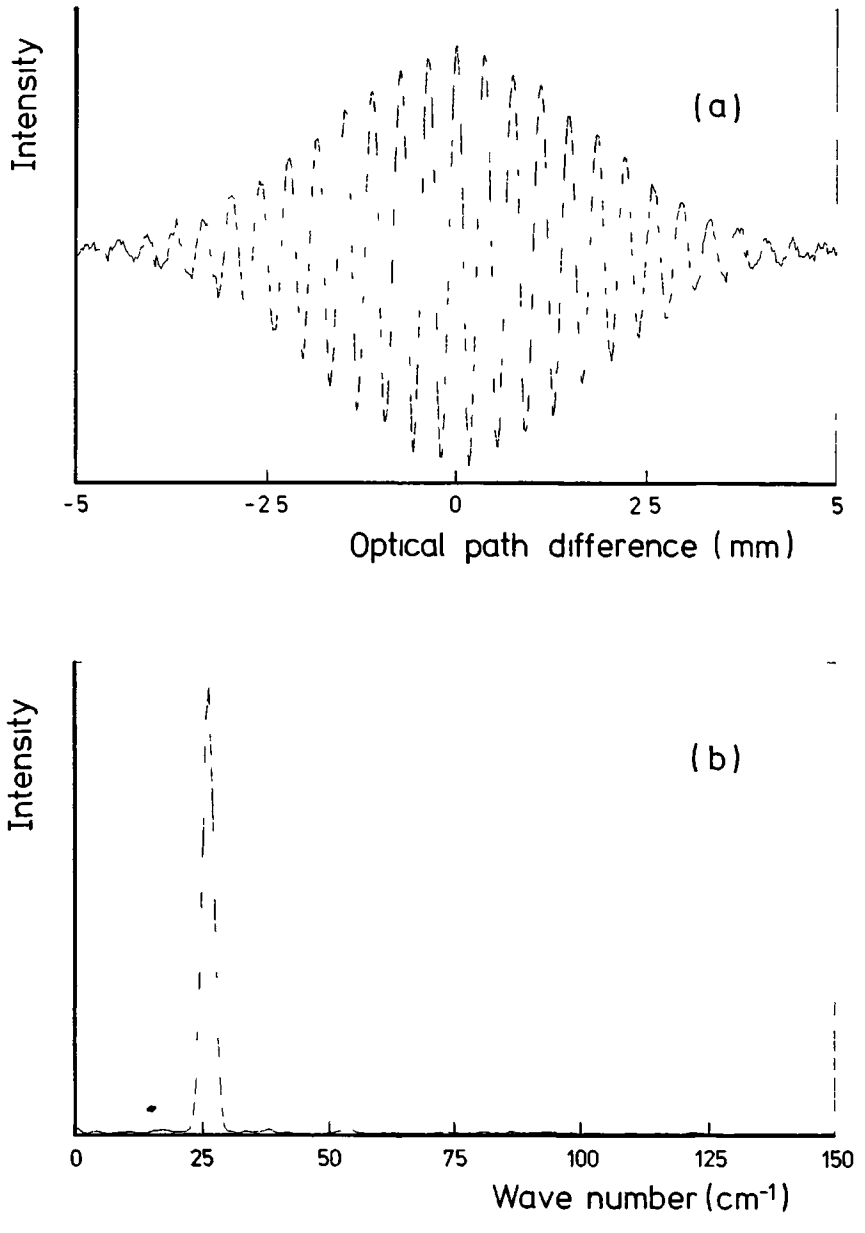

Fig. 2 : Figure (a) and (b) show respectively the interferogram and spectrum of a monochromatic line, originating from a grating monochromator.

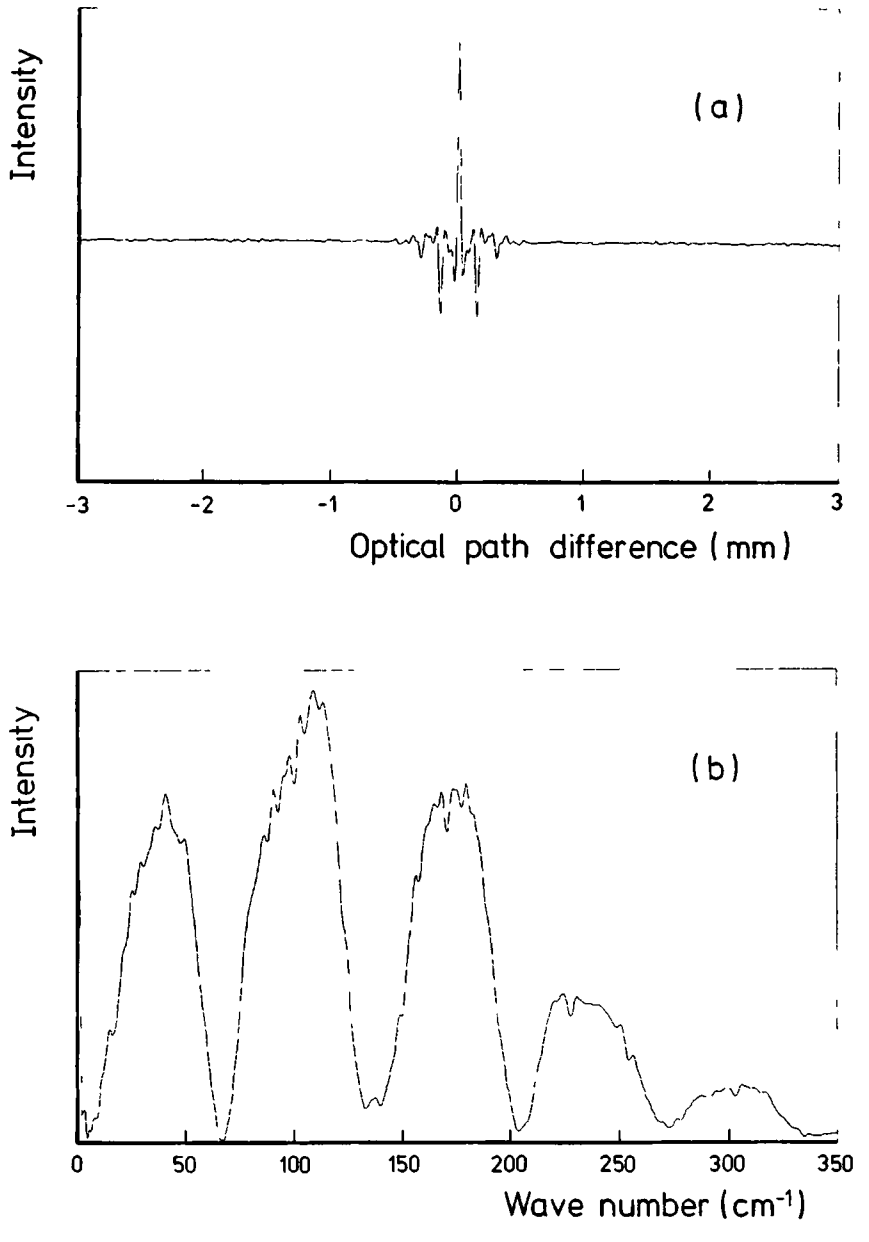

Fig. 3 : Figure (a) and (b) show respectively the interferogram and spectrum of a continuous broad band spectrum. The structure is determined by the efficiency of the 50 µm Mylar beamsplitter.

In the previous section it was demonstrated that the spectral output was determined by the properties of the thin film beam splitter as well. The disadvantage of these thin films is that due to standing wave interference effects, caused by multiple reflections within the thin transparant films, the beam splitter efficiency $B(\sigma)$ is a periodic archlike function of wave number, reaching zero at multiple values of $1/(2nd\cos\theta')$. Here d is the thickness of the film, n the refractive index and θ' the angle of the refracted beam inside the film. The function $B(\sigma)$ was first introduced in equation (8); its exact form has been calculated by several authors[7-10]. An example of the influence of a beam splitter is shown in figure 3a and 3b, where a Mylar beam splitter of 50 μm thickness was used, with an angle of incidence for the broad band radiation of 45°. Using $n = 1.72$[9] the wave numbers where $B(\sigma)$ reaches 0, are found to be multiple values of 64 cm^{-1}, in accordance with figure 3b.

Interferograms such as in figure 2a and 3a, which are recorded symmetrically around zero path difference, are called double-sided interferograms. In principle, if the interferogram is exactly symmetrically sampled, it is sufficient to record one side only (single-sided interferograms). Actually, often the sampling comb is not positioned so as to record an ordinate at exactly zero path difference. It can easily be shown (Chantry[1], chapter 3) that this does not affect the modulus spectrum of a double-sided interferogram. In case of a single-sided interferogram symmetry must be restored by numerical computation[11,12]. Single-sided interferograms (not used in the present investigations) are treated in details in textbooks (see Bell[13] or Vanasse and Sakai[14]).

References.

1. G.W. Chantry, Submillimetre Spectroscopy, Academic Press, New York (1971).
2. J. Chamberlain, Infrared Physics 11, 25 (1971).
3. J. Chamberlain and H.A. Gebbie, Infrared Physics 11, 57 (1971).
4. J. Chamberlain, J. Haigh and M.J. Hine, Infrared Physics 11, 75 (1971).
5. M.V. Dorigo, J.H.M. Stoelinga and P. Wyder, Z. ang. Math. Phys. (ZAMP) 20, 565 (1969).
6. J.H.M. Stoelinga and P. Wyder, Nederlands Tijdschrift voor Natuurkunde 36, 107 (1970).
7. D.J. James and J. Ring, J. Phys. (Paris) 28, 150 (1967).
8. E.V. Loewenstein and A. Engelsrath, J. Phys. 28, 153 (1967).
9. D.R. Smith and E.V. Loewenstein, Appl. Opt. 14, 2473 (1975).
10. D.A. Naylor, R.T. Boreiko and T.A. Clark, Appl. Opt. 17, 1055 (1978).
11. M.L. Forman, W.H. Steel and G.A. Vanasse, J. Opt. Soc. Am. 56, 59 (1966).
12. H. Sakai, G.A. Vanasse and M.L. Forman, J. Opt. Soc. Am. 58, 84 (1968).
13. R.J. Bell, Introductory Fourier Transform Spectroscopy, Academic Press, New York (1972).
14. G.A. Vanasse and H. Sakai, Progress in Optics, E. Wolf ed., 6, 259 (1967), North Holland, Amsterdam.

III.2 SPECTRUM DISTORTION IN FAR-INFRARED FOURIER SPECTROSCOPY BY MULTIPLE REFLECTIONS BETWEEN SAMPLE AND MICHELSON INTERFEROMETER

ABSTRACT

In far-infrared Fourier spectroscopy with a Michelson interferometer deviations in the measured transmission spectra of samples with non-negligible reflection can be observed. This effect is investigated both theoretically and experimentally. It is shown that the spectral element at a certain wave number contains contributions of subharmonics of that wave number.

1. Introduction.

One of the most widely used instruments in far-infrared spectroscopy is the Michelson interferometer with thin film beamsplitter. An extensive review of the Fourier spectroscopic technique on which this instrument is based has been given by Chantry[1]. In order to determine the transmission spectrum of some sample one usually performs two measurements: 1) A sample interferogram with a sample in the light-path between interferometer and detector, and: 2) A background interferogram without the sample. These interferograms are Fourier transformed, and the ratio of the two obtained spectra then yields the desired transmission spectrum.

However, it should be noted that a non-negligible amount of radiation can be reflected back into the interferometer system by a reflecting sample. This can lead to significant distortions in the spectra. This effect seems to have escaped notice until now. It is the purpose of this paper to present results of a theoretical and experimental investigation into the effect of this reflected radiation on the measured transmission spectrum.

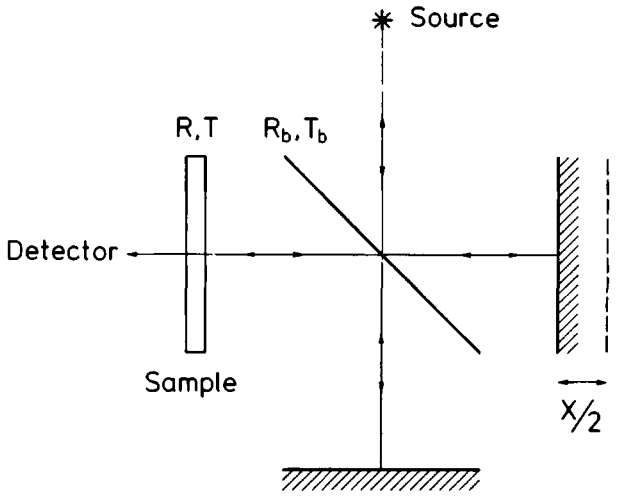

Fig. 1 : Schematic diagram of a Michelson interferometer in a configuration for transmission measurements. The energy reflection and transmission coefficients of the beamsplitter are R_b and T_b respectively, those of the sample are R and T.

2. Theory.

Fig. 1 shows schematically a Michelson interferometer with an incident beam of radiation. There are two emergent beams, one towards the sample and detector, the other towards the source. In the following calculations we neglect the effect of absorption in the beamsplitter, which is a good approximation for the first lobe of the interference pattern of a Mylar beamsplitter[2].

We assume the source to be monochromatic with wave number σ and intensity S, and the optical path difference between the two arms of the interferometer to be x. Then the phase difference between the beams recombining at the beamsplitter will be $\Delta = 2\pi\sigma x$, the energy I_o arriving at the sample will be given by

$$I_o(\Delta) = SB(1 + \cos\Delta) \quad , \tag{1}$$

and the energy I_o' returning to the source by

$$I'_o(\Delta) = S(A - B\cdot\cos\Delta) \ . \qquad (2)$$

(See for instance: Loewenstein and Engelsrath[3].) The beamsplitter properties are represented by the quantities $A = R_b^2 + T_b^2$ and $B = 2R_bT_b$, where R_b and T_b denote the energy reflection and transmission coefficients of the beamsplitter respectively. For a non-absorbing beamsplitter we have $R_b + T_b = 1$ and $A + B = 1$. The quantity B is often called the efficiency of the beamsplitter.

The sample will transmit a fraction T of the incident radiation towards the detector, and will reflect a fraction R back into the interferometer ($R < 1$). To simplify the calculations it will be assumed that the reflected radiation has a random phase relation with the original beam, so that no interference will occur and one can simply add the intensities. The sample can then be considered as an extra radiation source with intensity $RI_o(\Delta)$. According to Eq. (2) a fraction with energy

$$I_1(\Delta) = RI_o(\Delta)(A - B\cdot\cos\Delta)$$

will return to the sample, and will again be partly reflected, etc. The total energy I reaching the detector, after transmission through the sample, will therefore be

$$I(\Delta) = TSB(1 + \cos\Delta) \sum_{n=0}^{\infty} R^n(A - B\cdot\cos\Delta)^n \ . \qquad (3)$$

The term in the infinite sum is < 1 (because $R < 1$ and $A + B = 1$), so the geometrical series can be summed. Introducing the quantity C, defined as

$$C = \frac{RB}{1 - RA} \ , \qquad (4)$$

the summation of Eq. (3) yields:

$$I(\Delta) = \frac{TS}{R}\left[1 - \frac{1 - C}{1 + C\cdot\cos\Delta}\right] \ . \qquad (5)$$

It follows from Eq. (4) that $0 \leq C < 1$. In order to perform the Fourier transform it is convenient to write Eq. (5) in the form of a Fourier series. It is shown in the Appendix that the function

$$f(\Delta) = (1 + C \cdot \cos\Delta)^{-1}$$

can be represented by a Fourier series

$$f(\Delta) = \frac{a_o}{2} + \sum_{n=1}^{\infty} a_n \cdot \cos(n\Delta)$$

with coefficients a_n given by

$$a_n = \frac{2}{\sqrt{1 - C^2}} \left(\frac{\sqrt{1 - C^2} - 1}{C} \right)^n . \qquad (6)$$

Defining the coefficients B_n as:

$$B_o = \frac{1}{R} \left[1 - (1 - C) \frac{a_o}{2} \right] \qquad (7.a)$$

$$B_n = \frac{C - 1}{nR} \cdot a_n \qquad \text{for } n = 1,2,3,\ldots, \qquad (7.b)$$

the Fourier series representation of $I(\Delta)$ can be expressed as:

$$I(\Delta) = TS \left[B_o + \sum_{n=1}^{\infty} B_n \cdot n \cdot \cos(n\Delta) \right] . \qquad (8)$$

Fig. 2 shows the calculated B_o, B_1, B_2 and B_3 as functions of R for various values of the beamsplitter efficiency B. It can easily be shown that for $R \to 0$ the values $B_o \to B$, $B_1 \to B$ and $B_n \to 0$ for $n \geq 2$, so that in this limit Eq. (8) reduces to the well known form of Eq. (1)

$$\lim_{R \to 0} I(\Delta) = TSB(1 + \cos\Delta) .$$

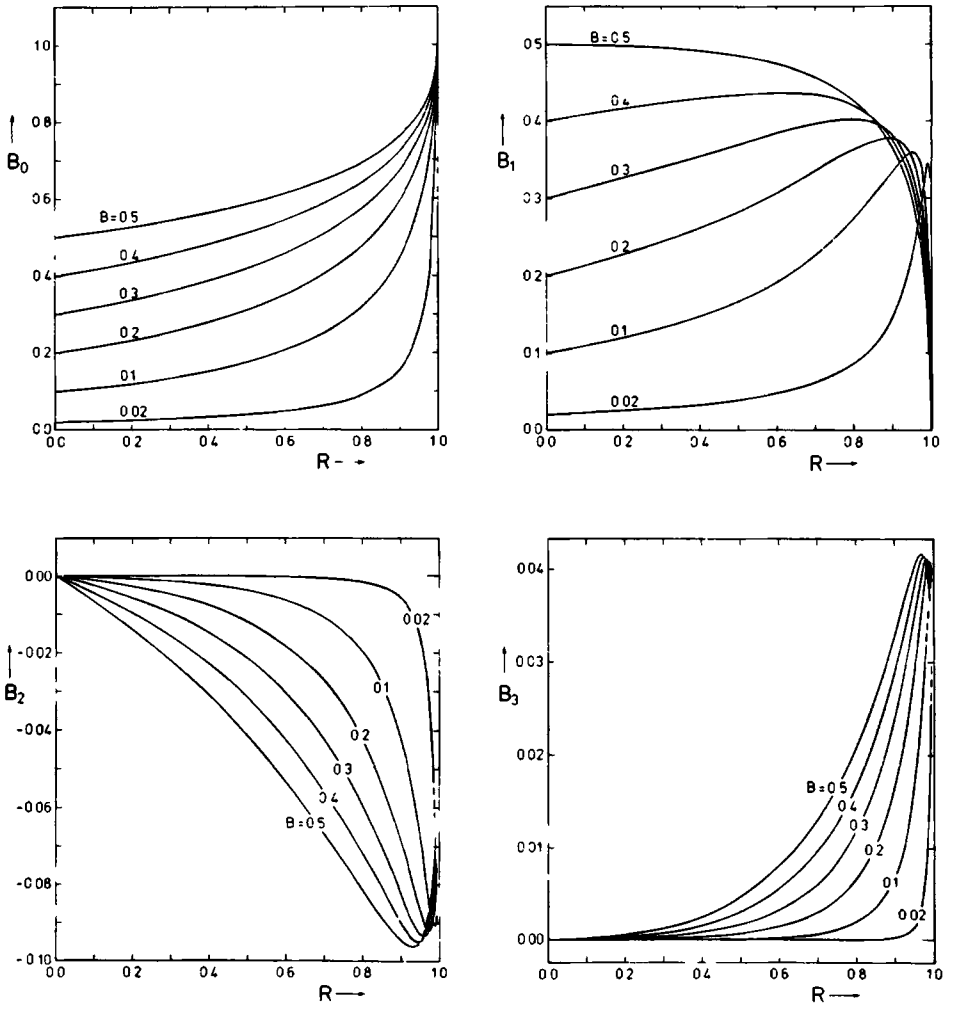

Fig. 2 : The calculated values of the quantities B_0, B_1, B_2 and B_3 as functions of R for various values of the beamsplitter efficiency B (non-absorbing beamsplitter).

It is obvious from Eq. (8) that the interferogram-function $I(\Delta)$ contains higher harmonics of the basic frequency due to the reflected radiation.

So far the source was assumed to be monochromatic with wavenumber σ and intensity S. If the source emits a broad spectrum $S(\sigma)$, the total energy $I'(x)$ reaching the detector can be found by integrating $I(\Delta)$ over all wavenumbers σ. In doing so one has to take into account that the quantities A,B,T,R,C and B_n may also be functions of σ. The interferogram-function $I'(x)$ for a broad spectrum is thus found to be

$$I'(x) = \int_0^\infty T(\sigma)\cdot S(\sigma)\cdot B_o(\sigma)\cdot d\sigma + \int_0^\infty \sum_{n=1}^{\infty} T(\sigma)\cdot S(\sigma)\cdot B_n(\sigma)\cdot n\cdot\cos(2\pi n\sigma x)\cdot d\sigma \quad . \tag{9}$$

The first integral in Eq. (9) is independent of x, and corresponds to the average of $I'(x)$ over all x. The second integral in Eq. (9) is the proper interferogram $I(x)$, which, by changing the variable σ to σ/n, can be written as

$$I(x) = \int_0^\infty \sum_{n=1}^{\infty} T(\tfrac{\sigma}{n})\cdot S(\tfrac{\sigma}{n})\cdot B_n(\tfrac{\sigma}{n})\cdot\cos(2\pi\sigma x)\cdot d\sigma \quad . \tag{10}$$

In most experiments the intensity of the source is chopped and the detector provides a signal proportional to $I'(x)$. After phase-sensitive detection and subtraction of the average level one obtains an interferogram proportional to $I(x)$. The spectrum one is interested in is then calculated as the Fourier transform of this interferogram. One sees immediately from Eq. (10) that this spectrum $P(\sigma)$, omitting multiplicative constants, is given by:

$$P(\sigma) = \sum_{n=1}^{\infty} T(\tfrac{\sigma}{n})\cdot S(\tfrac{\sigma}{n})\cdot B_n(\tfrac{\sigma}{n}) \quad . \tag{11}$$

This means that the spectral element with wavenumber σ contains not only information about the sample, source and instrument for wavenumber σ, but

also for a series of subharmonics of σ.

For small values of R Eq. (11) reduces to the well known undistorted spectrum:

$$\lim_{R\to 0} P(\sigma) = T(\sigma)\cdot S(\sigma)\cdot B(\sigma) \ .$$

The background spectrum (without the sample) is simply $S(\sigma)\cdot B(\sigma)$, so that for $R\to 0$ the transmission spectrum, calculated as the ratio of the sample and background spectrum, is indeed equal to $T(\sigma)$. However, for non-negligible values of R one does not obtain the proper transmission spectrum in this simple way, and the corrections discussed above have to be taken into account.

3. Experiment.

In order to test the analysis of section 2 we performed some experiments in which the transmission spectra of samples with high reflection were measured and compared with the known transmission. A modular FIR interferometer[4], manufactured by Grubb Parsons Company, was employed with a 12.5 μm Mylar beamsplitter. One of the modifications allowed the use of both the standard broadband source (i.e. a mercury lamp) or an external monochromatic source (i.e. a FIR-laser or a monochromator). A TPX lens focussed the radiation emerging from the interferometer onto the entrance hole of a lightpipe which contained the sample-holder. The reflected radiation re-entered the interferometer along the reversed path, while the transmitted power was detected at the exit of the lightpipe.

a. Monochromatic source.

The properties of an interferometer are most clearly studied by employing a monochromatic source. In our experiments this was an optically pumped FIR laser, operating at the 118.8 μm (σ_o = 84.2 cm^{-1}) transition of methanol[5]. The radiation was coupled into the interferometer via a lightpipe and collimated by a TPX lens; the emerging power was measured with a Molectron P3 pyro-electric detector. A 750 lines/inch nickel mesh (manufactured by Buckbee and Mears Company, Minnesota) was used as reflecting sample; the measured transmission coefficient at 84.2 cm^{-1} was T = 0.15.

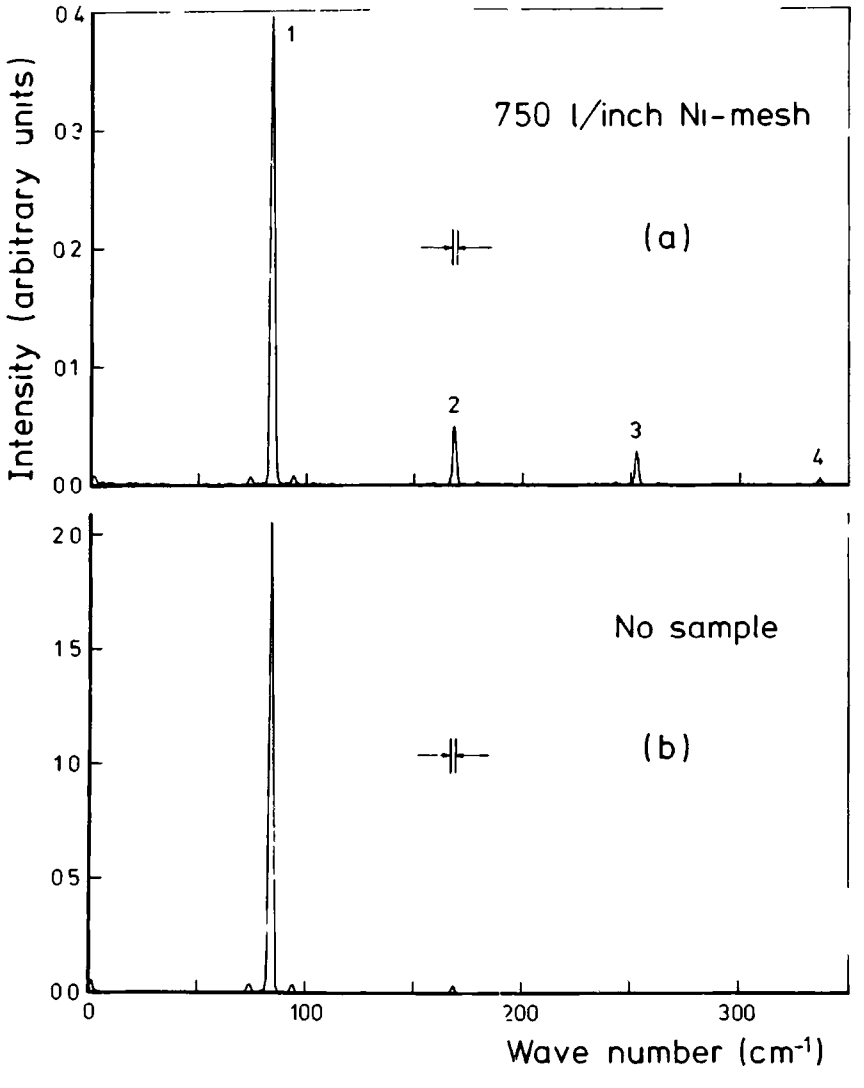

Fig. 3 : The transmission spectrum of a 750 lines/inch nickel mesh, showing the effect on the transformed spectrum of the reflected radiation (a). The source was monochromatic with radiation wave number σ_o = 84.2 cm^{-1}; the background spectrum is shown as curve (b). The transmission of the sample at 84.2 cm^{-1} is τ = 0.15.

The measured background interferogram was an almost perfect cosine of which the Fourier transform yields the monochromatic peak at $\sigma_o = 84.2\ cm^{-1}$ shown in Fig. 3b. A very small harmonic component at $2\sigma_o$ can be seen which may be due to a reflection at the detector or to a possible non-linearity of the detector sensitivity. The small side-peaks at 10 cm^{-1} to the left and right of the main peak are caused by a small periodical pitch error in the micrometer screw of the mirror drive of the interferometer[6].

The measured transmission spectrum (see Fig. 3a) of the sample shows very clearly the peaks at harmonics of σ_o as predicted by the theory of section 2. As our computer program calculated the modulus of the complex transformed spectrum, the negative sign of the peaks at even multiples of σ_o does not show up in Fig. 3a. The intensities of the peaks relative to the background peak are given in Table 1. We also calculated the relative peak intensities with the formula $T(\sigma_o)\cdot B_n(\sigma_o)/B(\sigma_o)$ given by the theory; the results are also given in Table 1, where the negative signs for the even peaks have been omitted. In the calculations a loss of 5% of the radiation was assumed so that the effective reflection coefficient of the sample was taken as R = 0.8.

In calculating the efficiency of the beamsplitter the polarization properties have to be taken into account[2,3]. The originally polarized radiation of the laser proved to be totally depolarized by entering the interferometer through a lightpipe and collimator lens. The calculations were performed separately for the parallel and perpendicularly polarized components of the incident radiation, and the results were averaged. For a non-absorbing 12.5 μm Mylar beamsplitter and 45° angle of incidence, the calculated efficiency of the two components was found to be $B_{\parallel} = 0.11$ and $B_{\perp} = 0.46$ respectively.

As can be seen from Table 1 the agreement between theory and experiment is rather good. It is interesting to note that the efficiency of the beamsplitter has a minimum at 250 cm^{-1} so that without the reflection effect discussed in this paper there could not be a noticeable intensity in the region where peak no. 3 is located.

b. Broadband source.

In order to investigate the influence of the reflection effect on broadband spectra, we measured the transmission of polished brass disks

Table 1 : The experimentally and theoretically determined relative peak intensities in the transmission spectrum of a 750 lines/inch nickel mesh with a monochromatic source of wave number 84.2 cm^{-1}.

peak no.	1	2	3	4
Experiment	0.19	0.024	0.012	0.002
Theory	0.19	0.026	0.006	0.002

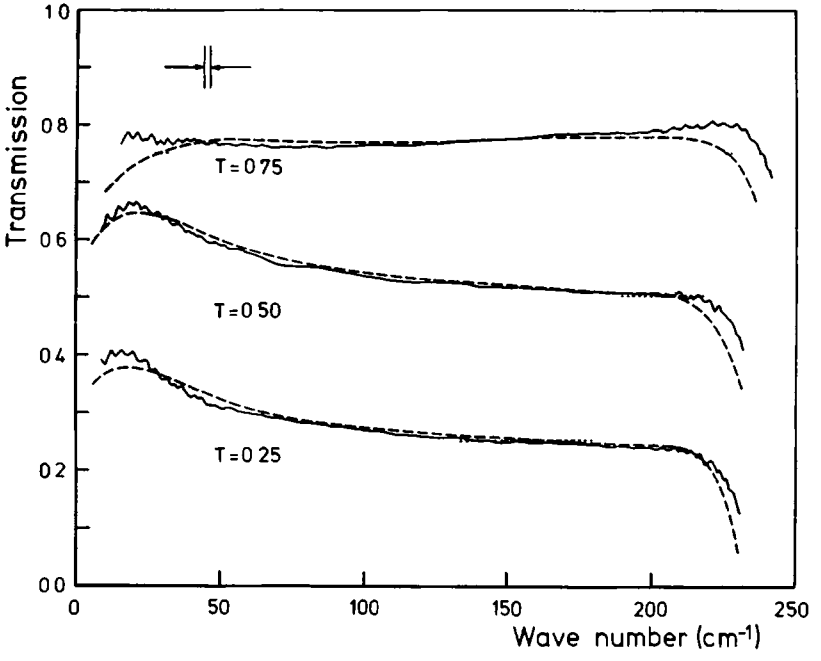

Fig. 4 : The measured (solid curves) and calculated (dashed curves) transmission spectra of polished brass disks from which sectors of 90^{o}, 180^{o} and 270^{o} were removed. The deviation due to the reflection effect from the ideal constant transmission coefficients T = 0.25, 0.50 and 0.75 respectively is clearly demonstrated.

from which sectors of 90^{o}, 180^{o}, and 270^{o} were removed. The broadband source was a medium pressure mercury lamp (Philips HPK 125 W). An IR50 Golay cell was used as detector. Without the reflection effect under study, the expected transmission spectra should have a constant level at T = 0.25, 0.50, and 0.75 respectively. But, as can be seen in Fig. 4, the experimental results exhibit a distinct deviation from this ideal behaviour. Only the spectrum with the lowest reflection (T = 0.75) approximates the real transmission spectrum almost up to the regions near 0 cm^{-1} and 250 cm^{-1}, where the ratio of sample and background spectrum becomes inaccurate because of the minima in the beamsplitter efficiency. However, the measured transmission spectra conform very well to the calculated spectra (dashed curves in Fig. 4) if the reflection effect is included. In these calculations effective reflection coefficients were chosen by assuming a loss of 5% of the radiation, yielding R = 0.70, 0.45, and 0.20 respectively. The beamsplitter efficiency $B(\sigma)$ was calculated as in Ref. 2, ignoring absorption, and averaging over all polarization directions. The combination of source-spectrum and transmission of the present filters and windows was approximated by an analytical function $S(\sigma)$, which fitted the experimental curve within 10%.

As the spectral level at wavenumber σ is mainly determined by the first two terms of the infinite series of Eq. (11), i.e. $T(\sigma)\cdot S(\sigma)\cdot B_1(\sigma)$ and $T(\frac{1}{2}\sigma)\cdot S(\frac{1}{2}\sigma)\cdot B_2(\frac{1}{2}\sigma)$, the main result of the reflection effect will be an increase of the level for low wavenumbers, and a decrease near 250 cm^{-1}. This is due to the maximum in the beamsplitter efficiency at 125 cm^{-1}, and the minima at 0 cm^{-1} and 250 cm^{-1}.

4. Conclusions.

We have shown theoretically and experimentally that due to reflections from the sample the measured transmission spectrum can exhibit a substantial deviation from the real spectrum if a Michelson interferometer is employed. The best way to avoid this effect is to arrange the optical set-up in such a way that the reflected radiation is prevented to re-enter the interferometer.

Appendix.

In this appendix the calculation will be given of the coefficients of the Fourier series representation of the function:

$$f(\Delta) = (1 + C\cdot\cos\Delta)^{-1} \quad , \tag{A1}$$

where $0 \leqslant C < 1$. This function $f(\Delta)$ is a bounded periodic function of period 2π (i.e. $f(\Delta + 2\pi) = f(\Delta)$), and satisfies the Dirichlet conditions:
a) In any period $f(\Delta)$ is continuous;
b) In any period $f(\Delta)$ has only a finite number of maxima and minima.
In addition, $f(\Delta)$ is even (i.e. $f(-\Delta) = f(\Delta)$). Then $f(\Delta)$ may be represented by a Fourier series

$$f(\Delta) = \frac{a_o}{2} + \sum_{n=1}^{\infty} a_n\cdot\cos(n\Delta) \tag{A2}$$

where

$$a_n = \frac{1}{\pi} \int_{-\pi}^{\pi} f(\Delta)\cdot\cos(n\Delta)\cdot d\Delta \quad . \tag{A3}$$

Writing the Euler definition for the cosine, and using the fact that $f(\Delta)$ is even one obtains the complex form of a_n:

$$a_n = \frac{2}{\pi} \int_{-\pi}^{\pi} \frac{e^{in\Delta}}{2 + C(e^{i\Delta} + e^{-i\Delta})} \, d\Delta \quad .$$

Substituting $z = e^{i\Delta}$ and integrating along the unity circle yields:

$$a_n = \frac{2}{\pi} \oint \frac{z^n}{2 + C(z + z^{-1})} \cdot \frac{dz}{iz} \quad . \tag{A4}$$

Introducing the quantities E and F, defined as:

$$E = (\frac{-1}{C})(1 + \sqrt{1 - C^2}) \tag{A5a}$$

$$F = (\frac{-1}{C})(1 - \sqrt{1 - C^2}) \tag{A5b}$$

Eq. (A4) can be written as:

$$a_n = \frac{4}{C} \cdot \frac{1}{2\pi i} \oint \frac{z^n}{(z - E)(z - F)} dz \ . \tag{A6}$$

Since $0 \leqslant C < 1$ we have $E < -1$ and $-1 < F \leqslant 0$, so that F lies inside the unity circle and E does not. The residu theorem is stated as

$$\frac{1}{2\pi i} \oint \frac{g(z)}{z - a} dz = g(a)$$

if a lies inside the closed integration path, and g(z) does not have any singularities inside this path. This can be applied to Eq. (A6) by substituting a = F and

$$g(z) = \frac{z^n}{z - E} \ ,$$

yielding:

$$a_n = \frac{4}{C} \cdot \frac{F^n}{F - E}$$

or, using the definitions for E and F:

$$a_n = \frac{2}{\sqrt{1 - C^2}} \left(\frac{\sqrt{1 - C^2} - 1}{C}\right)^n \ . \tag{A7}$$

References.

1. Chantry G.W., Submillimetre Spectroscopy, Academic Press, London and New York (1971).
2. Naylor D.A., R.T. Boreiko & T.A. Clark, Appl. Opt. 17, 1055 (1978).
3. Loewenstein E.V. & A. Engelsrath, J. de Phys. 28, C2-153 (1967).
4. Chantry G.W., H.M. Evans, J. Chamberlain & H.A. Gebbie, Infrared Phys. 9, 85 (1969).
5. Chang T.Y., T.J. Bridges & E.G. Burkhardt, Appl. Phys. Lett. 17, 249 (1970).
6. Steeg M.J.H. van de, H.W.H.M. Jongbloets, J.H.M. Stoelinga, R.W. van der Heijden, R.J.M. van Vucht & P. Wyder, to be published.

CHAPTER IV PHOTOTHERMAL IONIZATION SPECTROSCOPY OF SHALLOW IMPURITIES IN ULTRA-PURE GERMANIUM

IV.1 INTRODUCTION TO PHOTOTHERMAL IONIZATION SPECTROSCOPY (PTIS)

1. General introduction.

In the last decade extensive investigations into the ultrapurification of germanium have taken place, mainly with the purpose of fabrication of nuclear radiation detectors[1,2,3].

As criterion for the purity of germanium is currently used the total concentration of shallow donors and acceptors (i.e. elements like As, Sb, P, Li, Al, B, etc.). One of the difficulties which were met for many years was that while the net concentration of the residual donors and acceptors in the Ge crystals could be measured, one had very little information about the chemical identities of these impurities. However, a knowledge of the chemical identities is obligatory for the improvement in the technology of preparation of ultrapure germanium.

Here a new technique, developed by Russian scientists[4,5,6], came to the rescue, which could be used to detect and identify impurities in germanium in concentrations down to the 10^9 cm^{-3} range and possibly even lower. This technique of photothermal ionization spectroscopy (PTIS) is based on two experimentally established facts: 1) Under very definite conditions the spectrum of the extrinsic photoconductivity is a line spectrum which reflects the energy level structure of the impurities; 2) The magnitude of the photoresponse is independent of the concentrations of the impurities down to very low concentrations. A recent review of the PTIS technique was given by Kogan and Lifshits[7]. Since 1970 many experimentalists have used PTIS for the investigation of ultra-pure Ge. (See for instance Refs. 3, 8-13.)

In our laboratory we have performed measurements on ultra-pure germanium samples obtained from Dr. H.J.A. van Dijk of Philips Research Laboratories in Eindhoven.

Before explaining the PTIS technique a brief review will be given of the essential details of the theory of shallow donors and acceptors in germanium.

2. Theoretical considerations.

Kittel and Mitchell[14] and Kohn and Luttinger[15] presented the first comprehensive theoretical model for shallow donors in germanium; the so-called "effective mass approximation". The model is based on the following qualitative picture: The group V donor has five electrons outside of closed shells. Four of these complete the bonds with neighbouring Ge atoms. The fifth finds itself in the Coulomb field of the singly-charged impurity ion.

A series of quantum states can be assigned to this additional electron similar to those of the single electron in the hydrogen atom, but with some important modifications. First, the "hydrogenic" impurity is not in a vacuum but in a lattice with dielectric constant, ε, so that all binding-energies emerging from the hydrogen atom are reduced by a factor ε^2 and the linear dimensions of the wave functions are increased by a factor ε. Furthermore, the electric charge moving in the field of the impurity ion does not have the mass m_o of the free electron but has an effective mass m^*, which is anisotropic. The dielectric constant and the reduced mass together result in approximately 1000 times smaller energies than in the hydrogen atom. The wave functions of the excited states extend over thousands of crystal cells, but are zero in the central cell occupied by the impurity. The corresponding energy levels are therefore almost insensitive to the chemical nature of the impurity atoms, and the "effective mass theory" provides a very accurate description of the excited levels.

The differences that make the identification of the individual impurities possible are due to departures of the lowest levels from the effective mass approximation. The ground state wave function has a maximum in the crystal central cell. Therefore the ground state energy is sensitive to the form of the crystal field in the central cell and depends on the chemical nature of the impurity. This "central cell correction" to the effective mass approximation causes a "chemical shift" of the ground state level, characteristic for the impurity in question. Theoretical calculations were performed by Philips[16], while Reuszer and Fisher[17] deduced the chemical shifts for various donors from measured absorption spectra.

Most of the considerations above apply mutatis mutandis also to acceptors in Ge. On the other hand, acceptor states represent a rather different situation, because of the special structure of the top of the valence band. The acceptor problem was first formulated by Kohn[18], while numerical calculations were performed by Schechter[19], Mendelson and James[20] and

more recently by Baldereschi and Lipari[21,22]. A very extensive review of the theory of acceptors and donors in Ge was given by Bassani et al.[23].

The chemical shifts of the ground states of several shallow acceptors in germanium were determined by Jones and Fisher[24] from transmission measurements on samples with impurity concentrations of 10^{15} cm^{-3}. The absorption peaks they observed were interpreted as optical transitions from the ground state of the impurities to bound excited states. From a combination of theory and experiment they deduced the energy level schemes shown in Fig. 1. As can be seen the higher excited states of all acceptors are virtually the same, as was predicted by the effective mass theory. Only the

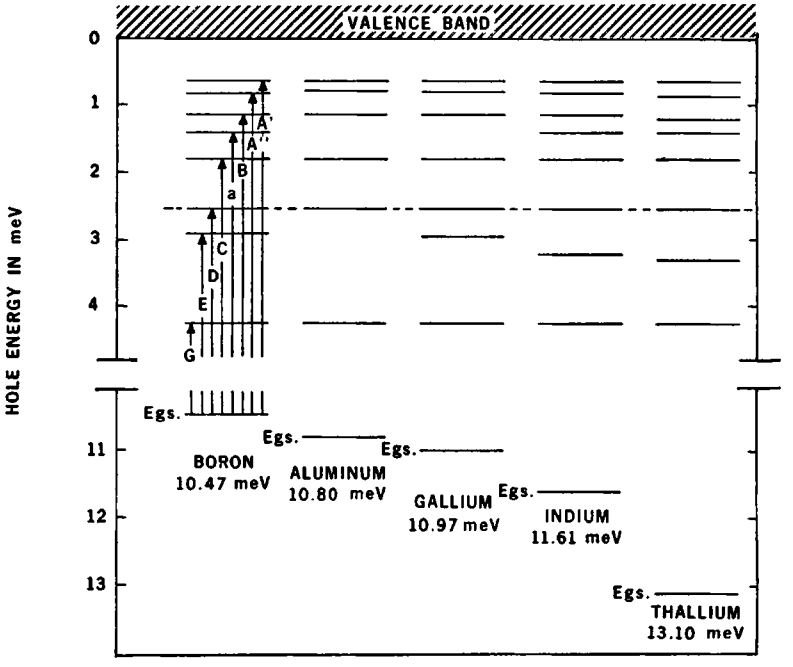

Fig. 1 : The bound states of some shallow acceptors in germanium, as determined by Jones and Fisher[24]. The numbers in the figure give the ground state energies ($E_{g.s.}$) of the impurities relative to the valence band.

most strongly bound states, and especially the ground state $E_{g.s.}$, differ among different impurities. The resulting absorption spectra therefore have the same structure but are shifted versus each other, the shifts depending on the differences in ground state energies.

The disadvantage of using transmission spectroscopy for the study of impurities is that this technique asks for samples with a high impurity concentration. However, the size of the wave functions then produces a severe overlapping between the impurity atoms, resulting in a relatively low resolution in the spectra. In contrast with this PTIS on very pure samples, where the impurity atoms are far apart, produces spectra with very narrow lines.

3. Photothermal ionization spectroscopy (PTIS).

In PTIS one measures the change in conductivity of a sample under illumination with radiation in the same region as used in transmission spectroscopy. For shallow donors and acceptors in germanium this is the far infrared region (wave number 10 - 200 cm^{-1}).

As an example we show in Fig. 2 the photoconductivity spectra at several temperatures of a polycrystalline sample, containing residual impurities in a concentration of $\sim 10^{10} - 10^{11}$ cm^{-3}. It is seen that above a temperature of 5 K a photoconductivity spectrum with a distinct line structure arises for photon energies below the impurity ionization energy (i.e. the onset of the continuum at ~ 85 cm^{-1}). The positions of the peaks on the energy scale coincide with the peaks in the optical absorption spectrum of the boron and aluminum acceptors known from the literature[24]. This proves that the lines are due to optical transitions of the charge carriers from the ground state to bound excited states of the impurity. However, in order to contribute to the conductivity the charge carriers must be released into the free band. We see in Fig. 2 that the heights of the peaks increase with increase in temperature. This suggests that the ionization of the impurity is a two-step process: 1) charge carriers in the ground state are optically excited to some intermediate state; 2) Subsequently a fraction of these excited charge carriers may be promoted thermally into the free band, producing an increase in conductivity of the sample. This is why the name of photothermal ionization was introduced for this two-step process.

In order to obtain enough phonons of sufficient energy one would like to keep the Ge sample at high temperatures, while to keep most of the impurities in their ground state low temperatures would be prefered. This leads to an experimentally-determined optimum temperature of around 8 K for observation of shallow impurities in germanium.

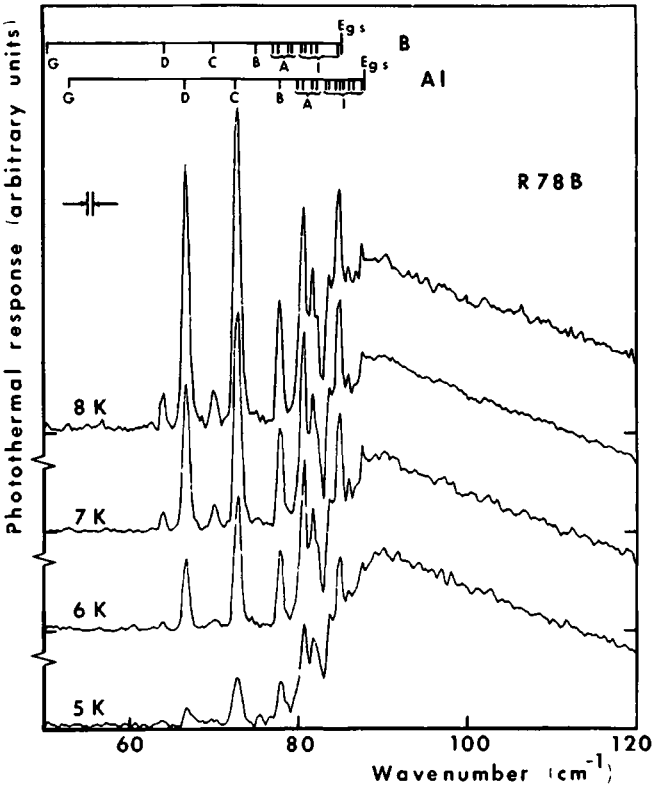

Fig. 2 : Photoconductivity spectra at several temperatures of a polycrystalline Ge sample, containing aluminum and boron in a concentration of $\sim 10^{10} - 10^{11}$ cm^{-3}.

The most important and essential difference between PTIS and other analysis methods is that the recorded signal does not decrease with decrease of impurity concentration down to a very low concentration[7]. This is a consequence of the fact that both the average number of current carriers, n, and the change Δn under illumination depend equally on the concentration of the impurities. The voltage sensitivity of the photo-response is proportional to the relative change of the carrier concentration $\Delta n/n$. This enables one to detect the impurities even if their concentration is extremely low and undetectable by all other analysis methods.

As the positions of the spectral lines reflect the energy spectrum of the impurity atoms PTIS enables the determination of the chemical nature of

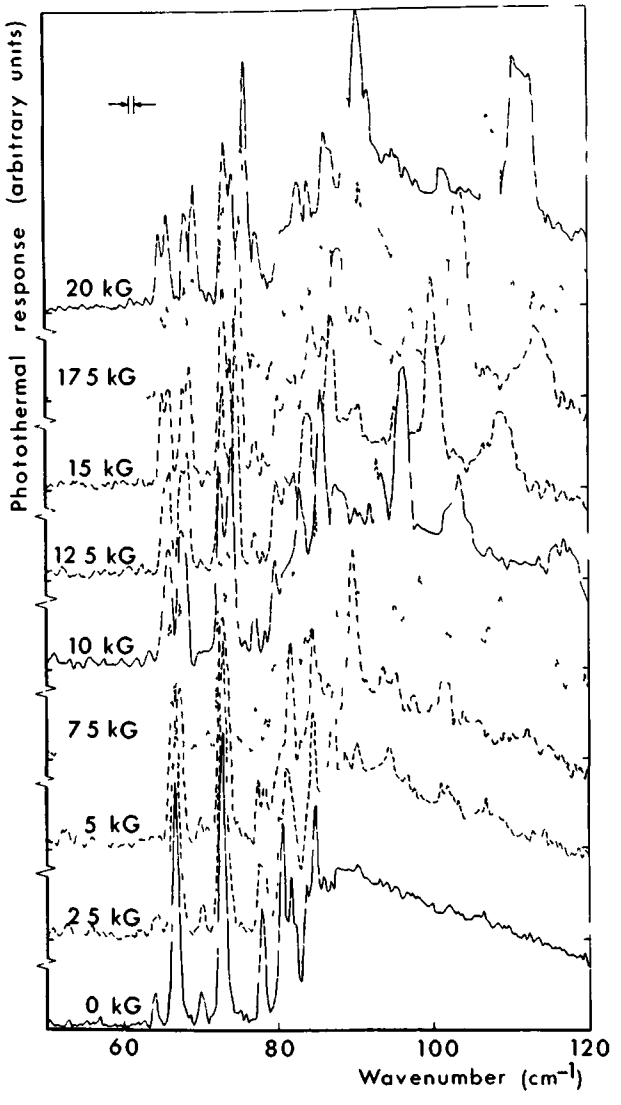

Fig. 3 : Photoconductivity spectra at 7.5 K of shallow acceptors in germanium for several values of the applied magnetic field (same sample as in Fig. 2).

the impurities. Accurate spectra for a number of donors and acceptors can be found in the literature (for instance in Refs. 8,9 and 10). The identification of the impurities in the spectra of Fig. 2 was done by comparison with the B and Al spectra given by Haller and Hansen[9]; these spectra are shown in the top of Fig. 2.

4. Applications of PTIS.

Originally the PTIS technique was only used as an analytical tool in the production of ultra-pure germanium. However, the inherent advantages over other analysis methods, such as the much better spectral resolution, have predicted PTIS to become one of the most powerful tools for the study of the basic physical aspects of germanium and a variety of other semiconductors.

The research subjects in which we have been engaged are:

1. An accurate determination of the ground state energies of some impurities from the temperature dependence of the peak intensities in the photoconductivity spectra;
2. The influence of a magnetic field on the energy level scheme of acceptors in germanium.

Figure 2 showed the effect of the temperature on the intensity of the peaks in a spectrum, whereas Fig. 3 shows the effect of a magnetic field on the same spectrum. As can be seen from Fig. 3 the spectrum not only exhibits a splitting or shift of the peaks below the continuum onset, but also develops a set of peaks in the continuum.

The results of our investigations will be presented in the form of a set of papers. Preliminary results are presented in Section IV.2, while in Sections IV.3 and IV.5 the temperature effect is explained in more detail. Section IV.4 is a supplement to Section IV.3. In Section IV.6 we present measurements in a magnetic field on a monocrystalline sample, where the orientation was known. The experimental results will be discussed in terms of existing theories about Zeeman effect and Landau levels in germanium.

References.

1. R.D. Baertsch and R.N. Hall, IEEE Trans. Nucl. Sci. 17, 235 (1970).
2. R.N. Hall and T.J. Soltys, IEEE Trans. Nucl. Sci. 18, 160 (1971).
3. R.N. Hall, R.D. Baertsch, T.J. Soltys, and L.J. Petrucco, Annual Report No. 6 (Aug. 73), General Electric Co.
4. T.M. Lifshits and F.Ya. Nad', Sov. Phys. Doklady 10, 532 (1965).
5. V.I. Sidorov and T.M. Lifshits, Sov. Phys. Solid State 8, 2000 (1967).
6. T.M. Lifshits, N.I. Likhtman, and V.I. Sidorov, Sov. Phys. Semicond. 2, 652 (1968).
7. Sh.M. Kogan and T.M. Lifshits, Phys. Status Solidi A 39, 11 (1977).
8. S. Dana Seccombe and D.M. Korn, Solid State Commun. 11, 1539 (1972).
9. E.E. Haller and W.L. Hansen, Solid State Commun. 15, 687 (1974).
10. M.S. Skolnick, L. Eaves, R.A. Stradling, T.C. Portal and S. Askenazy, Solid State Commun. 15, 1403 (1974).
11. E.E. Haller, W.L. Hansen and F.S. Goulding, IEEE Trans. Nucl. Sci. NS-22, 127 (1975).
12. E.M. Bykova, L.A. Goncharov, T.M. Lifshits, V.I. Sidorov, and R.N. Hall, Sov. Phys. Semicond. 9, 1223 (1976).
13. E.E. Haller, Phys. Rev. Letters 40, 584 (1978).
14. C. Kittel and A.H. Mitchell, Phys. Rev. 96, 1488 (1954).
15. W. Kohn and J.M. Luttinger, Phys. Rev. 98, 915 (1955).
16. J.C. Phillips, Phys. Rev. B1, 1540 (1970).
17. J.H. Reuszer and P. Fisher, Phys. Rev. 135, A1125 (1965).
18. W. Kohn, Solid-State Physics, Vol. 5, p. 257 (ed. by F. Seitz and D. Turnbull), Academic Press, New York (1957).
19. D. Schechter, J. Phys. Chem. Solids 23, 237 (1962).
20. K.S. Mendelson and H.M. James, J. Phys. Chem. Solids 25, 729 (1964).
21. A. Baldereschi and N.O. Lipari, Phys. Rev. B8, 2697 (1973).
22. A. Baldereschi and N.O. Lipari, Phys. Rev. B9, 1525 (1974).
23. F. Bassani, G. Iadonisi and B. Preziosi, Rep. Prog. Phys. 37, 1099 (1974).
24. R.L. Jones and P. Fisher, J. Phys. Chem. Solids 26, 1125 (1965).

MAGNETO-OPTICAL DETERMINATION OF THE GROUND STATE LEVELS OF SOME SHALLOW IMPURITIES IN HIGH PURITY GERMANIUM

H W H M JONGBLOETS, J H M SIOFLINGA, M J H VAN DE STEEG and P WYDER

Physics Laboratory and Research Institute for Materials, University of Nijmegen, Toernooiveld, Nijmegen, The Netherlands

We determine the impurity ground state levels of aluminium, boron and phosphor in germanium from very accurate measurements of the photo thermal conductivity as a function of the frequency of the incident radiation, the temperature and the magnetic field strength. From our magnetic data information is obtained on the field dependence of even the highest levels observed up to now.

1. Introduction and experimental method

During the last decade there has been considerable interest in the study of the energy levels of the impurity states in germanium and silicon. The experimental techniques used fall mainly into two groups: far infrared transmission measurements using spectrometers or interferometers on samples containing impurities at concentrations of $\sim 10^{15}$–10^{16} at./cm^3, and photo-thermal conductivity measurements which enable investigation of high-purity samples with 10^{10}–10^{11} impurities/cm^3. Here also far infrared grating spectrometers or interferometers and sometimes lasers are used. The experimental results of these two methods are in good agreement both with each other and with theoretical calculations. For a review see Bassani et al. [1].

However, up to now the precise determination of the ground state levels of the impurities has met difficulties. Seccombe and Korn [2] assume that the two step photo thermal conductivity process has a relative ionization probability which varies as $P_{i,n}(T) \propto \exp\{-(E_B - E_i)/kT\}$, where E_i is the energy of the intermediate level and E_B is the energy of the banded higher energy levels. From the measured temperature dependence they find activation energies $E_B - E_i$ which lie about 3 cm^{-1} below the ionization energy of the isolated impurity which is attributed to impurity banding. The same temperature dependence has been assumed by Simmonds et al. [3] and previously by Nagasaka [4] whereby the latter remarks that the measured temperature dependence deviates from an exponential behaviour. This is tentatively attributed to the effect of clustering of the impurities.

Haller and Hansen [5] on the other hand determine the energy difference of the ground state energy and the band edge from the shape of the onset of the continuum observed in their photo thermal conductivity data. They assume that this shape is due to the Fermi distribution of the electron energy at the top of the (valence) band. Their obtained values for the ground state energies are about 1 cm^{-1} higher than the theoretical values from the literature. However, since the shape of the onset of the continuum, according to our observations, does not change with the temperature between 2 and 8 K, this shape cannot be due to the Fermi distribution but may be caused for instance by an averaging over k space by the effect of two phonon processes in the thermal process. Although the frequency of the onset of the continuum gives information over the ground state energy its value cannot be obtained from this with high accuracy.

It is our aim to derive the right temperature dependence of the photo thermal conductivity response and to obtain accurate values for the ground state energies for some shallow acceptors and donors in high purity germanium from detailed measurements of the photo-thermal conductivity as a function of the temperature. For the determination of the ground state levels the degeneracy of the intermediate levels has to be known. This degeneracy is obtained from measured level splittings in a magnetic field up to 20 kG. The field dependencies of the energy levels are compared with current theories of both the low and high field region.

The measurements were performed both on polycrystalline and on monocrystalline samples obtained from the same ingot of high purity

Physica 89B (1977) 18–21

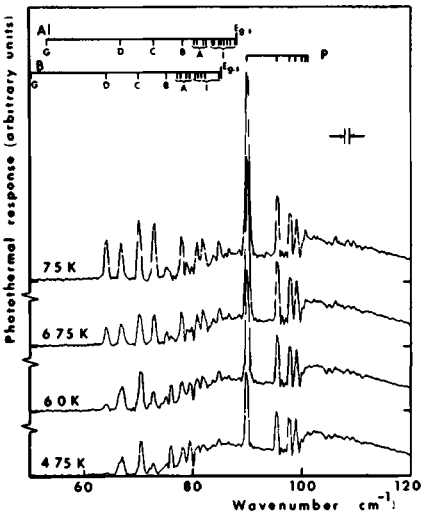

Fig 1 Photoconductivity spectra at several temperatures of a Ge sample containing both donors (P) and acceptors (B and Al) The Al and B spectra at the top are after Haller and Hansen [5], the P spectrum after Seccombe [2]

germanium containing aluminium, boron and phosphor in concentrations ranging from 10^{10} to 10^{11} at./cm^3. The concentrations of the impurities of the two monocrystalline samples J78A and J78B were (2×10^{11} at./cm^3 B, 4.7×10^{10} at./cm^3 Al, 1.9×10^{10} at./cm^3 P) and (1.5×10^{11} at./cm^3 P, 4.7×10^{10} at./cm^3 Al), respectively. These concentrations were determined with the method outlined in ref. 6 where also the experimental details will be given.

As is shown in fig. 1 with this method both donor and acceptor impurities present in the same sample can be investigated. Using a superconducting coil magnetic fields up to 20 kG could be applied.

2. Determination of the ground state energy

Generalizing the calculations of Spenke [7] it can be shown that the thermal ionization mechanism associated with the two-step photothermal conductivity process leads to a line intensity I given by:

$$I = A\left[1+\left(\frac{1}{gg'}\right)\exp(\Delta E/kT)\right]^{-1} \qquad (1)$$

for both donors and acceptors. Here ΔE is the energy-difference between the intermediate level and the band, g is the degeneracy of the excited level and g' is the degeneracy of the band at $k=0$. The factor A is proportional to the concentration of the impurity and to the optical transition probability of the spectral line.

We measured the temperature dependence of the line intensities at temperatures ranging from 2 to 10 K. As an example some of these spectra are shown in fig. 1. All spectra were corrected for the spectral background of the far infrared interferometer and were normalized to the same continuum height. This continuum is caused by direct optical excitations to the band edge. The relative line intensities were plotted on a logarithmic scale versus $10/T$ as is shown in fig. 2 for boron in the monocrystalline sample J78A. In this figure the solid curves represent computer fits of the experimental data to eq. (1) using ΔE and A as parameters. The degeneracy factors g were deduced from the measured level splittings in a magnetic field (see the next section). The degeneracy of the conduction band of germanium is $g'=1$ and that of its valence band is $g'=2$. As is shown in fig. 2 the measured temperature dependencies of the line intensities are fully in agreement with eq. (1) within the experimental error.

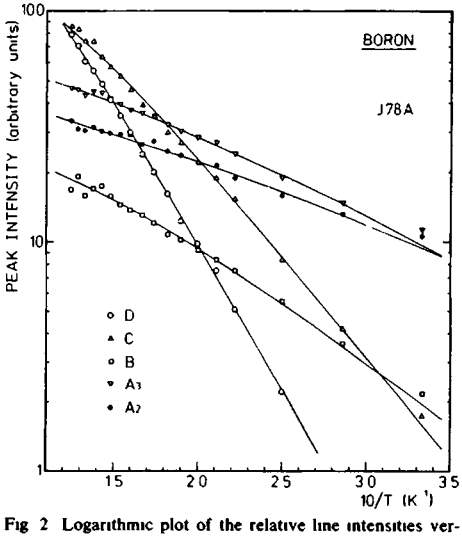

Fig 2 Logarithmic plot of the relative line intensities versus $10/T$ for several boron lines in sample J78A The solid curves represent computer fits to eq (1)

For each transition observed the sum of ΔE and the energy of the transition E as obtained from the measured spectra yields the energy of the ground state E_{g_s} of the impurity involved In this way we obtain for the ground state energies of aluminium, boron and phosphor the values presented in table I As is shown in this table these values are in excellent agreement with the theoretically deduced values for Al and B of Jones and Fisher [8] and the value for P of Reuszer and Fisher [9]

Table I
The ground state energies of Al B and P in germanium in cm $^{-1}$

	Al	B	P
E_{g_s} (this work)	87 1 ± 0 4	84 5 ± 0 1	102 9 ± 0 5
E_{g_s} (refs 8 and 9)	87 1 ± 0 2	84 5 ± 0 2	102 9 ± 0 3

3. The effect of a magnetic field

In a low magnetic field, in the low field limit, the Zeeman term connected with the magnetic field produces a linear splitting of the $l \neq 0$ levels while the diamagnetic term gives a quadratic correction On the other hand, in the high field limit the impurity potential produces a set of sublevels associated with each Landau level Again we refer to the review of Bassani et al [1]

Experimentally Boyle et al [10] investigated As donors in germanium by measuring the far infrared transmission of samples containing $\sim 1.5 \times 10^{15}$ arcenic atoms/cm^3 in magnetic fields up to 30 kG Horii et al [11] did the same for arsenic and antimony up to 46 kG, while Soepangkat et al [12] studied boron and thallium acceptors in germanium in magnetic fields up to 20 kG using the same method Nisida et al [13] investigated germanium containing antimony and arsenic impurities by measuring the photoconductivity in a varying magnetic field up to 40 kG under the influence of intraband radiation of a laser source

In our experiment we measured the photothermal conductivity response of our high-purity germanium samples as a function of the frequency of the far infrared radiation at several values of the magnetic field up to 20 kG Fig 3

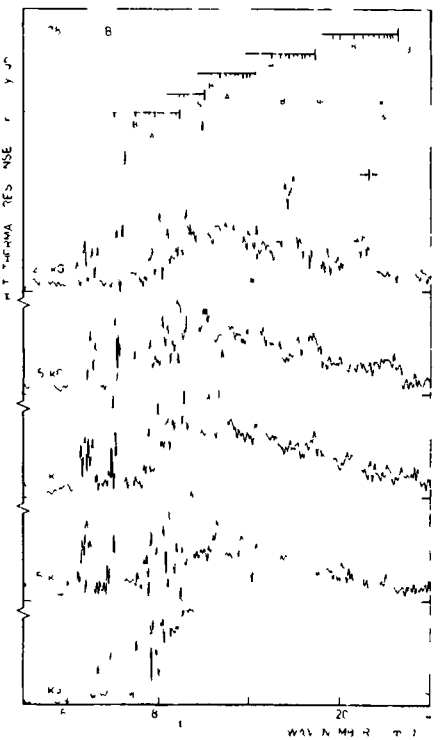

Fig 3 Photoconductivity spectra of sample J78A at 7 5 K for several values of the magnetic field with $B \| [100]$ Impurity concentrations 2×10^{13} at /cm^3 B 4.7×10^{13} at /cm^3 Al 1.9×10^{13} at /cm^3 P The labelling at the top shows the boron spectrum with the Zeeman splitting and the first four Landau levels with their associated sublevels at 15 kG

shows that the general behaviour sketched above manifests itself in these spectra on a very clear and illustrative way After a shift and splitting of the hydrogen like levels lying below the band edge to higher energies in low fields, these levels are forced up to energies higher than the band edge energy in higher fields At these fields the continuum above the band edge changes more and more in a number of peaks the Landau levels with their associated sublevels By plotting the resonance frequencies as function of the magnetic field each line could easily be followed and identified In this way the identification indicated in fig 3 has been performed The notation is that of Jones and Fisher

[8] From the energy differences of the first four Landau levels which can be identified we obtain an effective mass of $m^*/m = 0.08 \pm 0.05$ which has to be compared with the effective mass $m^*/m = 0.04$ of the light hole, cf. Sze [14]. The inaccuracy is caused by the non linearity of the shift of the Landau levels with the magnetic field in this region since the high field limit is not entirely reached. For the lower levels, our results are in accordance with those of the authors mentioned above. However, in contrast to these authors, we obtained also information about the higher levels. More quantitative results about these magnetic data will be published separately [15].

We thank Dr. H.J.A. van Dijk, Philips Research Laboratories, for providing the Ge samples and performing the impurity concentration analysis. This work was performed as part of the research program of the Stichting voor Fundamenteel Onderzoek der Materie (FOM) with financial support from the Nederlandse Organisatie voor Zuiver Wetenschappelijk Onderzoek (ZWO).

References

[1] F. Bassani, G. Iadonisi and B. Preziosi, Rep. Progr. Phys. 37 (1974) 1099.
[2] S. Dana, Seccombe and D.M. Korn, Solid State Commun. 11 (1972) 1539.
[3] P.F. Simmonds, J.M. Chamberlain, R.A. Hoult, R.A. Stradling and C.C. Bradley, J. Phys. C: Solid State Phys. 7 (1974) 4164.
[4] K. Nagasaka and S. Narita, Solid State Commun. 7 (1969) 467.
[5] E.F. Haller and W.L. Hansen, Solid State Commun. 15 (1974) 687.
[6] H.W.H.M. Jongbloets, J.H.M. Stoelinga, M.J.H. Van de Steeg, P. Wyder and H.J.A. van Dijk, to be published.
[7] L. Spenke, Electronic Semiconductors (McGraw Hill Book Company, Inc. 1958) p. 387.
[8] R.L. Jones and P. Fisher, J. Phys. Chem. Solids 26 (1965) 1125.
[9] J.H. Reuszer and P. Fisher, Phys. Rev. 135 (1965) A 1125.
[10] W.S. Boyle and R.E. Howard, J. Phys. Chem. Solids 19 (1961) 181.
[11] K. Horii and Y. Nisida, J. Phys. Soc. Jap. 31 (1971) 783.
[12] H.P. Soepinkat and P. Fisher, Phys. Rev. B8 (1973) 870.
[13] Y. Nisida and K. Muro, Suppl. Progr. Theor. Phys. 57 (1975) 77.
[14] S.M. Sze, Physics of Semiconductor Devices (John Wiley and Sons, Inc. 1969) p. 20.
[15] H.W.H.M. Jongbloets, J.H.M. Stoelinga, M.J.H. Van de Steeg, P. Wyder, to be published.

IV.3 Temperature dependence of the photothermal conductivity of high-purity germanium containing very low concentrations of Al, B, and P

H W H M Jongbloets, J H M Stoelinga, M J H van de Steeg, and P Wyder
Research Institute for Materials University of Nijmegen, Toernooiveld Nijmegen The Netherlands
(Received 7 February 1979)

The temperature dependence of the photothermal conductivity in the far-infrared region (10 to 200 cm^{-1}) is studied in pure germanium containing $\sim 10^{10}$ atoms/cm^3 of Al, B, and P A theoretical expression for the temperature dependence of the intensities is given which is in excellent agreement with the experimental results From these very detailed spectra, reliable values for the ground-state energies of the impurities are obtained and a quantitative chemical analysis of the impurity concentration as a function of the position in a Czochralski-grown single crystal is achieved

I INTRODUCTION

The photothermal conductivity in the far-infrared region of very pure germanium containing residual impurities of very low concentrations ($\simeq 10^{10}$ atoms/cm^3) has been the subject of several studies in the past [1–6] A recent review of this subject was given by Kogan and Lifshits [7] However, surprisingly enough, the temperature dependence of this effect has drawn little attention so far

It is generally believed that, in order to get a photothermal response, the donors or acceptors are ionized through a two-step process First, the electrons (or holes) are excited from their ground state to a higher bound state by irradiation with light in the far-infrared region (10–200 cm^{-1}) Then, a subsequent excitation to the free conduction (or valence) band occurs by interaction with thermal phonons The photoconductivity is measured as a function of the radiation frequency, whereas the sample temperature is held constant, typically between 2 and 10 K At higher temperatures the photoconductivity signal decreases due to the increase of the carrier density in the free band, while lower temperatures provide too few thermal phonons necessary for the second step of the process Although the influence of the temperature on the effect is thus qualitativley well understood, the precise temperature dependence has never been studied in a quantitative way Most authors assume a temperature dependence typically of the form $\exp(-\Delta E/kT)$, where ΔE is the energy difference between the excited level and the conduction (or valence) band edge [2 3 6 8] However, the agreement with experimental results is rather poor, and estimates for the binding energy of the impurities yield values which are about 3 cm^{-1} too low [3]

In this paper, we will concentrate upon this aspect In Sec II the experimental details will be described, while in Sec III the results will be presented and analyzed It will be shown that the measurements are in very good agreement with our calculations of the temperature dependence of the photothermal response Finally, a qualitative and a quantitative chemical analysis of the samples will be given, based on the photoconductivity data This analysis will be compared with results based on Hall-effect measurements on the same ingot from which the samples were obtained Preliminary results of these investigations have been published before [9]

II SAMPLE PREPARATION AND EXPERIMENTAL DETAILS

All our germanium samples were cut from the same boule These ultrapure samples were kindly supplied by Dr H J A van Dijk of the Philips Research Laboratories, who also performed Hall-effect measurements to determine the residual impurity concentration The polycrystalline samples, R78*A* and R78*B*, were obtained from both of the ends of the high-purity zone-refined ingot Then, from the remaining ingot, a single crystal was grown with the Czochralski method Again from both ends of this crystal two monocrystalline samples J78*A* and J78*B* were cut Figure 1 shows the variation of the impurity concentration along this single crystal as calculated from Hall-effect measurements, assuming aluminum, boron, and phosphorus as the main impurities and using the known segregation properties of these elements

The samples used for the photoconductivity measurements were cubes with dimensions of $\sim 1 \times 1 \times 1$ cm^3 The cubes were polished and etched, and then electrical contacts were produced by wetting with a mixture of In-Hg (50 50) Although these contacts were not entirely ohmic, we found no evidence that the contacts had any effect on the data

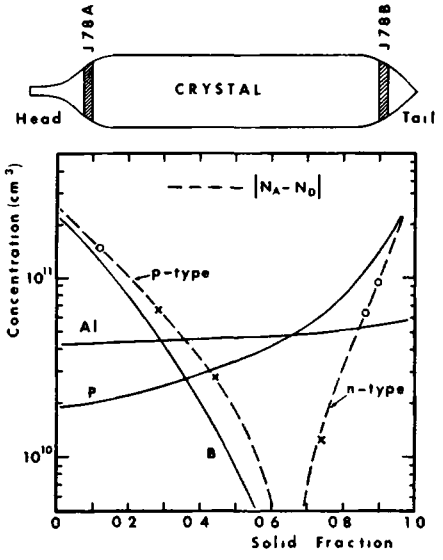

FIG 1 Distribution of phosphorus, boron and aluminum impurities along a germanium single crystal, calculated from Hall-effect measurements (Segregation coefficients used P $k_P = 0.1$ B $k_B = 5.7$ Al $k_{Al} = 0.9$) N_A and N_D are the concentrations of the acceptors and donors, respectively

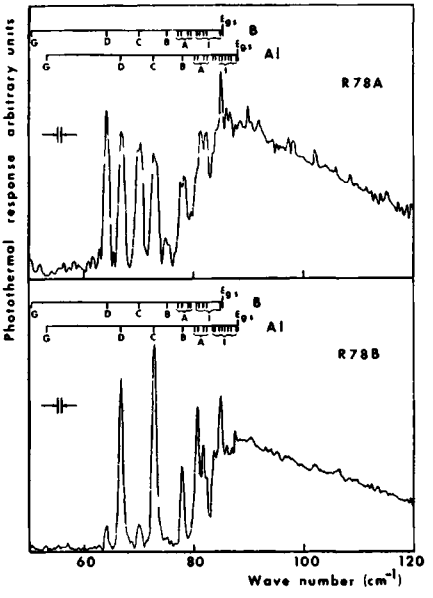

FIG 2 Photoconductivity spectra of the polycrystalline germanium samples R78*A* and R78*B* containing boron and aluminum impurities The spectra at the top are from Refs 4 and 5

The samples were positioned in a semispherical cavity wherein the chopped far-infrared radiation entered through a conical light pipe Thermal contact was made by clamping the sample onto the base of the cavity The clamp and the sample could be heated above the temperature of the surrounding helium bath with an electronically controlled heater system The temperature of the sample was stabilized within 0 1 K An Allen-Bradley carbon resistor was used as a thermometer

Using standard lock-in techniques, the photoconductivity was measured as a function of the wave number of the incident radiation produced by a Grubb-Parson Michelson interferometer operating with phase modulation at 90 Hz The data were punched on tape, and subsequently handled and analyzed on a PDP-12 laboratory computer linked to a plotter All spectra were corrected for the varying spectral background of the interferometer by dividing through a spectrum obtained by replacing the Ge sample with a Si bolometer

III RESULTS AND DISCUSSION

Figure 2 shows the photothermal response as a function of the wave number of the incident radiation for the polycrystalline samples R78*A* and R78*B* at a temperature of 7 5 K Indicated are also the expected transitions for boron and aluminum known from the literature [4 5] From these spectra one can conclude that R78*A* contains B and Al in about equal amounts, while in sample R78*B* the Al concentration exceeds the B concentration as is expected in a zone-refined ingot Figure 3 shows similar data for the monocrystalline samples, J78*A* contains both B and Al, with B having the highest concentration, while in sample J78*B*, apart from phosphorus, some lithium is present as well [3 5] In addition, indicated by an asterisk in the figure, in J78*B* some other transitions, with an origin not entirely known, are found, these transitions may be due to a LiO complex [10] The wave numbers where the transitions are observed agree within 0 2 cm^{-1} with the expected ones from the literature[3–5], however, due to the limited resolution, the *A* and *I* transitions of aluminum and boron are not fully resolved in these spectra The continuum in the spectra is caused by direct optical transitions from the ground state into the valence (or conduction) band In this context, it is interesting to note that with the method of photothermal ionization both donor and acceptor impurities can be seen simultaneously in one sample

The strength of a spectral line is proportional to the thermal ionization probability of the excited states

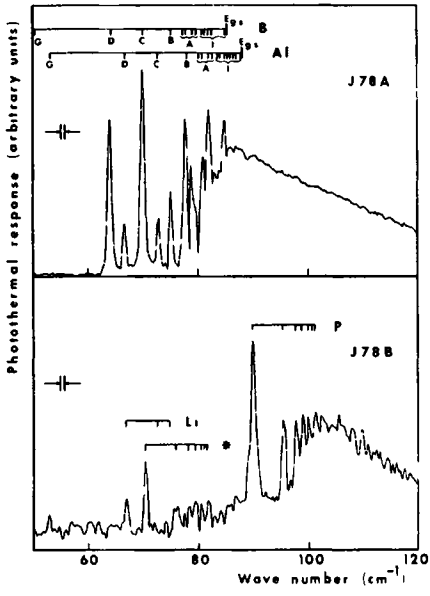

FIG 3 Photoconductivity spectra at $T = 7.5$ K of the monocrystalline germanium samples J78*A*, containing boron and aluminum, and J78*B*, containing phosporus, lithium, and probably a LiO complex The spectra at the top are from Refs 3, 4, 5, and 10

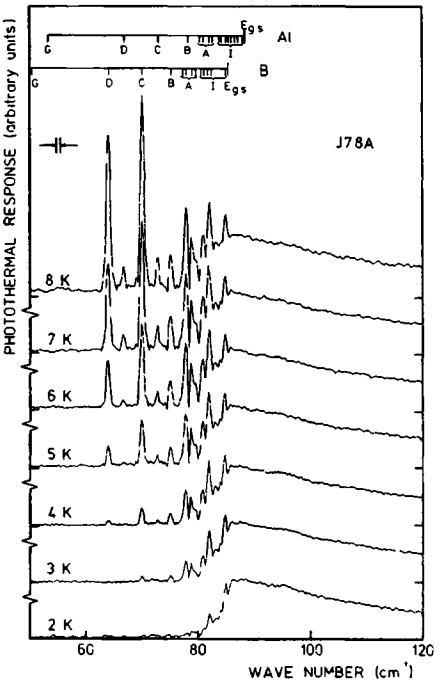

FIG 4 Photoconductivity spectra at several temperatures of the monocrystalline germanium sample J78*A* Impurity concentration B 2.1×10^{11} atoms/cm^3, Al 4.3×10^{10} atoms/cm^3

and this can be studied by comparing the line intensities at various temperatures with the height of the continuum [2] Figure 4 shows the spectrum of sample J78*A*, containing aluminum and boron, at different temperatures All these spectra are corrected for the spectral background of the interferometer and are normalized to the same continuum height Similar measurements were also performed on a sample containing phosphorus

From the voltage drop across the sample, the current through the sample and the measured change in voltage in a typical experiment, it is possible to get a rough estimate of the number of carriers involved Typical data yield for the number n of the free carriers in the band $n \sim 10^8$ (cm^{-3}) and the change Δn in carriers due to photothermal ionization $\Delta n \sim 10^5$ (cm^{-3}) This means that n and Δn are small compared with the total number of impurity states Therefore the average number of optical excitations to one of the excited levels may be considered as independent of temperature at very low temperature Since the excited levels are very localized in $\vec{k}$ space,[11] thermal ionization from this level will at low temperatures only take place to the nearest band extremum The average number of ionizations in equilibrium is found in the usual way by optimizing the number of possibilities for ionization at constant total energy Hereby the strong Coulomb interaction of electrons in an excited state has to be taken into account which can be done in a similar way as in considerations regarding donor and acceptor ionization probabilities [12] In this manner the line intensity I, which is proportional to the average number of ionizations is found to be given by

$$I = A\left[1 + \frac{1}{gg'}\exp\left(\frac{\Delta E}{kT}\right)\right]^{-1} \qquad (1)$$

for both donors and acceptors Here, ΔE is the energy difference between the intermediate level and the band edge, g is the degeneracy of the excited level, and g' is the degeneracy of the band The factor A is proportional to the concentration of the impurity and to the optical transition probability for the spectral line under consideration For donor states, where spin-orbit interaction is small, thermal processes with spin flip may be neglected so that g' is the band de-

generacy apart from spin, thus $g' = 1$ for germanium Although for acceptor states the situation is less obvious, the degeneracy of the valence band in germanium will be taken only as the effective-mass degeneracy at $\vec{k} = 0$, yielding $g' = 2$

Figure 5 shows the relative line intensities for the phosphorus spectrum, plotted on a logarithmic scale, as a function of the inverse temperature The solid curves in this figure represent computer fits of Eq (1) to the experimental data, using ΔE and A as adjustable parameters The degeneracy factors g were deduced from measured level splittings due to magnetic fields Here our own observations[9-13] confirmed the splittings found in the literature for the lower levels of the donors[11] and acceptors,[14,15] and extended the results to higher levels As is shown in Fig 5, the measured temperature dependence of the line intensities is within experimental accuracy in agreement with Eq (1) Similar results were obtained for the Al and B spectra of sample J78A Table I collects the numerical results of the computer fits for the parameters A and ΔE In the fitting procedure also the product gg' was varied by integer values It was not possible however to obtain a reasonable fit for other values of gg' than those quoted which supports the assumption of the neglect of spin in the band degeneracy made above

The energy of the ground state E_{gs} of the impurity involved is now simply the sum of ΔE and the energy of the optical transition E_{trans} (as obtained from the measured spectra) In this way it is possible to obtain the ground-state energies of boron, aluminum and phosphorus as presented in Table II As can be seen

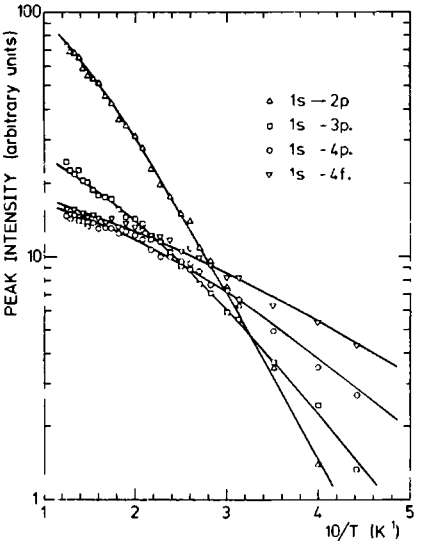

FIG 5 Logarithmic plot of the relative line intensities vs $10/T$ for several phosporus lines The solid curves represent computer fits to Eq (1) (See also Table I)

from this table, these experimentally found values are in excellent agreement with the theoretically deduced values of Jones and Fisher[16] for B and Al and of Reuszer and Fisher[17] for P

As a factor A is proportional to the impurity con-

TABLE I Values of A and ΔE as obtained from a computer fit from the temperature dependence of various lines in the B, Al, and P spectra [see Eq (1)]

Transition		E_{trans}(cm^{-1})	g	A (arb units)	ΔE(cm^{-1})
Boron	D	64 0 ± 0 2	4	450 ± 15	20 5 ± 0 2
	C	70 1	3	265 ± 8	14 4 ± 0 2
(J78A)	B	75 2	2	44 ± 1	9 3 ± 0 2
	A_3	77 9	1	123 ± 3	6 6 ± 0 2
	A_2	78 9	1	78 ± 2	5 6 ± 0 2
Aluminum	D	66 7 ± 0 2	4	70 ± 7	20 5 ± 0 6
	C	72 8	3	41 ± 3	14 1 ± 0 5
(J78A)	I_5	85 0	1	36 ± 2	2 3 ± 0 5
Phosphorus	$1s \rightarrow 2p_{\pm}$	90 0 ± 0 2	4	285 ± 10	12 9 ± 0 2
	$1s \rightarrow 3p_{\pm}$	95 5	4	44 ± 3	7 5 ± 0 2
	$1s \rightarrow 4p_{\pm}$	97 9	4	26 ± 2	5 3 ± 0 3
	$1s \rightarrow 4f_{\pm}$	99 0	2	33 ± 3	4 0 ± 0 3

TABLE II Energies of the ground state of B, Al, and P in germanium, measured in cm^{-1}

	B	Al	P
E_{gs} (experimental, this work)	84 5 ± 0 2	87 1 ± 0 3	103 0 ± 0 2
E_{gs} (theoretical, Refs 16 and 17)	84 5 ± 0 2	87 1 ± 0 2	102 9 ± 0 3

centration, it is in principle possible to get some information on the relative impurity content from a determination of A Assuming the same transition probability for transitions between similar states of different donors or acceptors, the ratio of the A factors for corresponding lines will therefore indicate the ratio of the concentrations of the impurities For sample J78A one finds for the ratio of the A factors for the C and D transitions of boron and of aluminum a value of 6 4 ± 0 5 This value can be compared with the concentrations obtained from Hall-effect measurements as presented in Fig 1 From this figure one concludes that for sample J78A the ratio of the concentrations of B and Al is

$$(2\,1 \times 10^{11}\ \mathrm{cm^{-3}})/(4\,3 \times 10^{10}\ \mathrm{cm^{-3}}) = 5 \pm 1 \quad ,$$

which is in good agreement with the value obtained from the photoconductivity measurements

In conclusion we can remark that we have given a theoretical expression for the temperature dependence of the photoconductive response which is in excellent agreement with our experimental results The values found from these data for the ground-state energies of various impurities confirm theoretical calculations very well In addition, we have shown that the concentration ratios of the impurities as obtained from photoconductive measurements are in reasonable agreement with values obtained from Hall-effect measurements

ACKNOWLEDGMENTS

Part of this work has been supported by the Stichting voor Fundamenteel Onderzoek der Materie (FOM) with financial support from the Nederlandse Organisatie voor Zuiver Wetenschappelijk Onderzoek (ZWO) We thank Dr H J A van Dijk, Philips Research Laboratories, for providing the Ge samples and performing the impurity-concentration analysis

[1]T M Lifshits and F Ya Nad', Sov Phys Dokl 10, 532 (1965)
[2]T M Lifshits, N I Likhtman, and V I Sidorov, Sov Phys Semicond 2, 652 (1968)
[3]S Dana Seccombe and D M Korn, Solid State Commun 11, 1539 (1972)
[4]E E Haller and W L Hansen, Solid State Commun 15, 687 (1974)
[5]M S Skolnick, L Eaves, R A Stradling, J C Portal, and S Askenazy, Solid State Commun 15, 1403 (1974)
[6]E M Bykova, L A Goncharov, T M Lifshits, V I Sidorov, and R N Hall, Sov Phys Semicond 9, 1223 (1976)
[7]S M Kogan and T M Lifshits, Phys Status Solidi A 39, 11 (1977)
[8]P E Simmonds, J M Chamberlain, R A Hoult, R A Stradling, and C C Bradley, J Phys C 7, 4164 (1974)
[9]H W H M Jongbloets, J H M Stoelinga, M J H van de Steeg, and P Wyder, Physica (Utrecht) B 89, 18 (1977)
[10]R L Aggarwal, P Fischer, V Mourzine, and A K Ramdas, Phys Rev 138, A882 (1965)
[11]F Bassani, G Iadonisi, and B Preziosi, Rep Prog Phys 37, 1099 (1974)
[12]E Spenke, *Electronic Semiconductors* (McGraw Hill, New York, 1958), p 387
[13]H W H M Jongbloets, J H M Stoelinga, M J H van de Steeg, and P Wyder (unpublished)
[14]H P Soepangkat and P Fisher, Phys Rev 8, 870 (1973)
[15]E P Kartheuser, S Rodriguez, and P Fisher, Phys Status Solidi B 64, 11 (1974)
[16]R L Jones and P Fisher, J Phys Chem Solids 26, 1125 (1965)
[17]J H Reuszer and P Fisher, Phys Rev 135, A1125 (1965)

IV.4 DETERMINATION OF THE IMPURITY CONCENTRATION PROFILE IN A Ge SINGLE CRYSTAL GROWN WITH THE CZOCHRALSKI METHOD

Figure 1 of the preceding paper (Section IV.3) showed the distribution of the phosphorus, boron and aluminum impurities along the germanium crystal, from which our samples J78A and J78B were cut. In this section it will be shown how this figure was obtained from Hall effect measurements, performed by Dr. H.J.A. van Dijk of Philips Research Laboratories.

The variation of the impurity concentration along a crystal which is grown by the Czochralski method, is caused by the segregation of dissolved impurities during non-equilibrium solidification[1,2]. For low impurity concentrations the ratio of the concentration C_S in the just solidified material and the concentration C_L in the remaining liquid will be a constant K, the so-called segregation coefficient.

If the location in the crystal is denoted by the weight fraction g of the original melt that was solidified at that point, the distribution of every impurity along the crystal can be described by[3]:

$$C_S(g) = C_S(0)(1-g)^{K-1} , \qquad (1)$$

where $C_S(0)$ is the concentration at the head of the crystal (i.e. g=0).

The number of uncompensated holes N_A-N_D is determined by the net impurity concentration

$$[N_A-N_D](g) = \sum_A C_S^A(g) - \sum_D C_S^D(g) , \qquad (2)$$

where A and D denote acceptors and donors respectively. The value of N_A-N_D at various positions in the crystal can be deduced from Hall effect measurements[4].

The photothermal conductivity spectra of samples J78A and J78B (Fig. 3, Section IV.3) reveal that the Al and B acceptors and P donor are the most important residual impurities in our crystal. From the measured values of N_A-N_D for three different locations g, indicated in Fig. 1 by small circles, equations (1) and (2) can be solved for $C_S^{Al}(0)$, $C_S^B(0)$ and $C_S^P(0)$. The concentration profile for Al, B and P can then be calculated with Eq. (1). These

solutions are represented in Fig. 1 (Section IV.3) by the solid curves, whereas the dashed curve shows the calculated profile of $|N_A-N_D|$.

As a check the values of N_A-N_D were also measured for three intermediate positions, indicated in Fig. 1 (Section IV.3) by crosses; they fit very well to the calculated $|N_A-N_D|$ curve.

The segregation coefficient used for these calculations were: $K_P=0.1$, $K_B=5.7$ and $K_{Al}=0.9$. Aluminum has normally a segregation coefficient $K_0=C_S(0)/C_L(0)=0.1$, but when a crystal is grown with the Czochralski method Al shows only a small segregation[5], so that in Eq. (1) we have used $K_{Al}=0.9$.

However, in the zone-refining process[6] used for the purification of the original Ge ingot, one has $K_{Al}=0.1$. We find boron and aluminum in about equal amounts in the region where the zone is started (sample R78A was cut from this region). Near the opposite end the boron concentration is reduced but aluminum is increased (sample R78B).

References.

1. The structure and properties of materials. IV: Electronic properties. Ed. John Wiley & Sons, New York (1966), pp. 146-154.
2. R.N. Hall and T.J. Soltys, IEEE Trans. Nucl. Sci. 18, 160 (1971).
3. E.M. Bykova, L.A. Goncharov, T.M. Lifshits, V.I. Sidorov, and R.N. Hall, Sov. Phys. Semicond. 9, 1223 (1976).
4. C. Kittel; Introduction to solid state physics, 4th edition, John Wiley & Sons, New York (1971), p. 288.
5. H.J.A. van Dijk, private communication.
6. W.G. Pfann; Zone melting, John Wiley & Sons, New York (1958), p. 211.

IV.5 TEMPERATURE DEPENDENCE OF THE PHOTOTHERMAL CONDUCTIVITY OF SEMICONDUCTORS AT LOW TEMPERATURES

ABSTRACT

A careful analysis has been made of the temperature dependence of the signal strength in a photoconductivity experiment in a semiconductor. The temperature dependence of the line intensity in a photothermal conductivity spectrum has been calculated. The results are in excellent agreement with measurements on high purity germanium containing boron, aluminum and phosphorus as residual impurities ($\sim 10^{11}$ atoms/cm^3).

1. Introduction.

Photothermal conductivity spectroscopy is of considerable interest for the study of impurity states in semiconductors (Lifshits and Nad' 1965). It offers the most sensitive method of analysis of impurities at very low concentrations (10^{10}-10^{11} atoms/cm^3) in semiconductors. The method is sensitive enough to investigate subtle features such as the magnetic field dependence of central cell corrections (Stoelinga et al 1978). A lot of work has been done related to this subject. A recent review has been given by Kogan and Lifshits (1977, further referred to as Ref. I).

However, the well known strong temperature dependence of the photothermal conductivity signal has met relatively little attention so far. Frequently a simple exponential behaviour, $\exp(-\Delta E/kT)$, has been assumed for the relative ionization probability of the two-step photothermal conductivity process (Lifshits et al 1968, Seccombe and Korn 1972, Stillman et al 1972, Simmonds et al 1974, Bykova et al 1976, Ref. I). Here ΔE is the energy difference between the band edge and the intermediate level to which optical excitation from the ground state takes place followed by thermal ionization from this level to the band edge. The experimental results do not agree very well with this assumption; this has been tentatively attributed to the effect of clustering of the impurities (Nagasaka and Narita 1969).

In this paper we will analyze the temperature dependence of the photothermal conductivity in semiconductors in detail, and derive a theoretical expression for this temperature dependence which according to our measurements on shallow impurities in high purity germanium is in excellent agreement with the experimental results. This

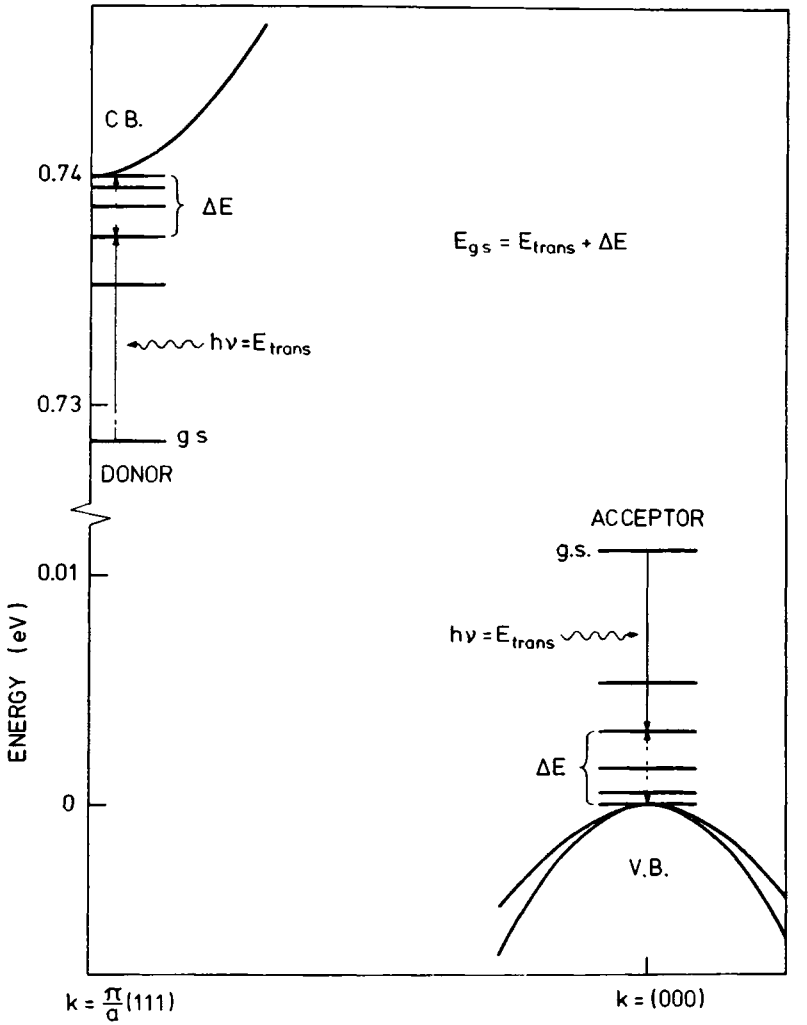

Fig. 1 : Illustration of the mechanism for photothermal ionization. Shown is part of the band structure of germanium along the (111) direction in $\vec{k}$ space, with the conduction band (C.B.), the valence band (V.B.) and some shallow donor and acceptor levels, i.e. the impurity ground state (g.s.) and the excited levels.

expression enables one to determine the ground state levels of the impurities very accurately from photothermal conductivity experiments (Jongbloets et al 1977 and 1979, further referred to as Ref. II and III). In analyzing the experimental data it will become clear why photothermal conductivity spectroscopy is applicable only in a relatively small temperature region (2-10 K).

2. Signal formation in a photoconductivity experiment.

In photothermal conductivity spectroscopy, electrons (or holes) are excited from their ground state with binding energy $E_{g.s.}$ to an excited state by radiation of energy $h\nu$ equal to the transition energy E_{trans}, as illustrated in figure 1. The radiation frequency ν is usually in the far infrared region (10-200 cm^{-1}). While being in such an excited state, the extra energy ΔE needed to overcome the remaining part of the binding energy is gained by interaction with thermal phonons. This ionization can be observed as an increase in the electric conductivity of the sample. The photoconductivity is usually measured as a function of the radiation frequency at constant temperature, typically between 2 and 10 K, yielding characteristic "hydrogen-like" excitation spectra for the various shallow impurities (Refs. I, II and III). In the measured spectra one can distinguish between a continuum, caused by direct photo-ionization from the bound ground state into the free band, and sharp peaks due to the two-step photothermal ionization process via bound intermediate states.

In order to analyze the temperature dependence of the photothermal ionization process, we will treat a typical experiment as an example, the results are of general validity however. In such an

experiment the source for the chopped excitation radiation is usually a Michelson interferometer. The sample is connected to an electric circuit so that a bias current is provided by a battery (V_B) via a load resistor (R_L) in series with the sample. The change in voltage drop across the sample due to the radiation is measured at various temperatures, using standard lock-in techniques.

The electric conductance of a sample of area A and length ℓ is given by $Ae\mu n/\ell$, where n is the free carrier concentration, μ is the mobility and e is the charge of the carrier. Introducing the quantity $\alpha = R_L Ae/\ell$ the d.c. voltage drop V across the sample may be written as

$$V = V_B(1 + \alpha\mu n)^{-1} \quad . \tag{1}$$

Without the chopped excitation radiation the number of ionizations, n, will be determined by the background radiation and by the few phonons of sufficient energy available at low temperature. The chopped radiation causes a change Δn of the free carrier concentration, and thus a change in the conductivity of the sample. Assuming $\Delta n << n$ the photoconductive response will be an a.c. voltage with amplitude

$$\Delta V = V_B \alpha\mu \cdot \Delta n(1 + \alpha\mu n)^{-2} \tag{2}$$

so that ΔV is directly proportional to Δn.

One now has to distinguish between the change in free carrier density Δn_p due to photothermal ionization via an intermediate level and the change Δn_c due to direct photo-ionization. The "continuum" carrier density variation Δn_c is expected to be independent of temperature in the temperature region of present interest. However, it

will be shown below that the "peak" carrier density variation Δn_p is strongly temperature dependent, and that this temperature dependence can be investigated by looking at the ratio $\Delta V_p/\Delta V_c$.

3. Derivation of the temperature dependence of the photothermal ionization process.

As will be shown in section 4 in a typical experiment the free carrier densities n, Δn_c and Δn_p are small compared to the total number of impurity states, so that most of the impurities remain in their ground state. The average number N of optical transitions to one of the excited states may therefore be treated as independent of temperature at the low temperatures at which these experiments are usually carried out, so that only the subsequent thermal ionization needs to be considered. N is directly proportional to the impurity concentration.

In electron-phonon interaction the longitudinal acoustic phonons are most important. At the low thermal energies (< 10 K) where the experiments under consideration take place these phonons have a small wave vector $\vec{k}$. Since the excited states are very localized in $\vec{k}$-space (Bassani et al 1974), ionization by phonons from these levels will only take place to the nearest band extremum. Generally the excited state is g-fold degenerated, so the strong Coulomb interaction of electrons (holes) in such a state has to be taken into account. This can be done by stating that an excited level can be occupied by only one electron (hole) but in g different ways (Spenke 1958). The number of ways, g', in which a particle can be transferred from one of the g degenerate excited states to a band state depends on the degeneracy of the band and on the selection rules for such transitions via a

phonon. The number of ways W in which Δn_p particles can be transferred from the N optical excited levels to a band state is then given by:

$$W = (gg')^{\Delta n_p} \cdot N! \, [\Delta n_p!(N-\Delta n_p)!]^{-1} \quad . \tag{3}$$

The equilibrium state is now easily obtained in the well known manner by demanding that W is maximal under the condition that the energy:

$$U = N \cdot E_{trans} + \Delta n_p \cdot \Delta E$$

is a constant. Maximizing (with respect to Δn_p) of:

$$\ln W + \beta(U - N \cdot E_{trans} - \Delta n_p \cdot \Delta E)$$

using Stirling's formula yields:

$$\Delta n_p = N \left[1 + \left(\frac{1}{gg'}\right) \exp(\beta \cdot \Delta E) \right]^{-1} \quad , \tag{4}$$

where $\beta = 1/kT$. The intensity I of a line in the photothermal conductivity spectrum relative to that of the continuum is now given by:

$$I = \Delta V_p / \Delta V_c = \Delta n_p / \Delta n_c$$

$$= A \left[1 + \left(\frac{1}{gg'}\right) \exp(\Delta E/kT) \right]^{-1} \quad , \tag{5}$$

where equation (2) has been used. Here A contains the optical transition probability of the line under consideration.

Since both Δn_p and Δn_c are proportional to the impurity concentration the intensity I is independent of the latter. If a sample contains several impurities the various Δn_c's add up in forming one continuum band in the spectrum. The ratios of the intensities of corresponding peaks, all compared with the intensity of the combined continuum band, yield a measure of the ratios of the concentrations

of these impurities in the sample, cf. the experimental work of Ref. III.

As argued above, in equation (5) g is the degeneracy of the excited bound state while g' is partly determined by the selection rules for transitions via phonons from this state to the nearest band extremum. For donor states in germanium and silicon, where the spin-orbit interaction is small, thermal processes in which spin flips occur may be neglected and the selection rule simply converts to that of spin conservation. In this case g' is the band degeneracy apart from spin, thus g' = 1 for germanium and silicon. Although for acceptor states, where spin-orbit interaction is not negligible, the situation is less obvious the degeneracy of the valence band at $\vec{k} = 0$ will be taken in analogy only as the effective mass degeneracy, yielding g' = 2 for germanium and silicon.

4. Comparison with experimental results.

In this section the analysis of the previous sections will be compared with experimental results obtained on high purity germanium samples. These samples contained aluminum, boron and phosphorus as residual impurities in concentrations of 10^{10}-10^{11} atoms/cm^3 (Refs. II and III). The dimensions of the cube-shaped samples were 1x1x1 cm^3. The bias voltage V_B was provided by a 12.6 Volt mercury battery over a load resistor R_L of 5 MΩ in series with the sample. The quantity α introduced in section 2 has thus a value of $8\text{x}10^{-13}$[V·cm·s].

The photoconductive signal strength ΔV_p and ΔV_c, corresponding with the change in carrier density Δn_p and Δn_c respectively, can be deduced from the measured spectra by taking the area of a peak and of

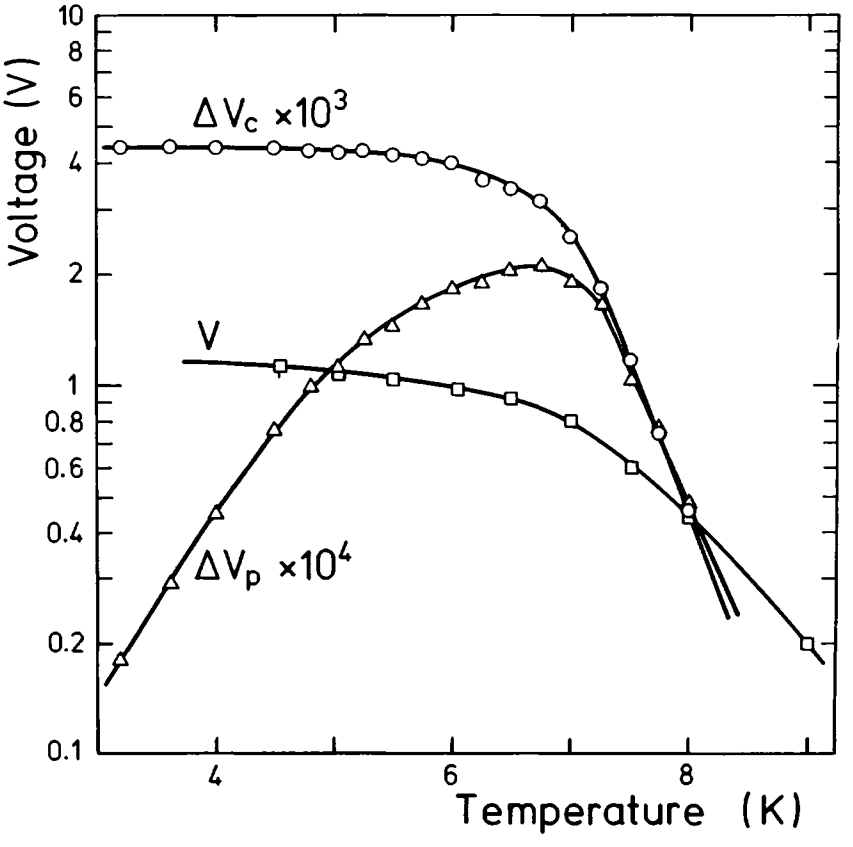

Fig. 2 : For a germanium sample with impurity concentration 2.1x10^{11} atoms/cm^3 are shown as a function of temperature: the voltage drop V across the sample, the contribution ΔV_c of the continuum to the photoconductive signal, and the contribution ΔV_p of the peak belonging to the C-transition of the boron spectrum.

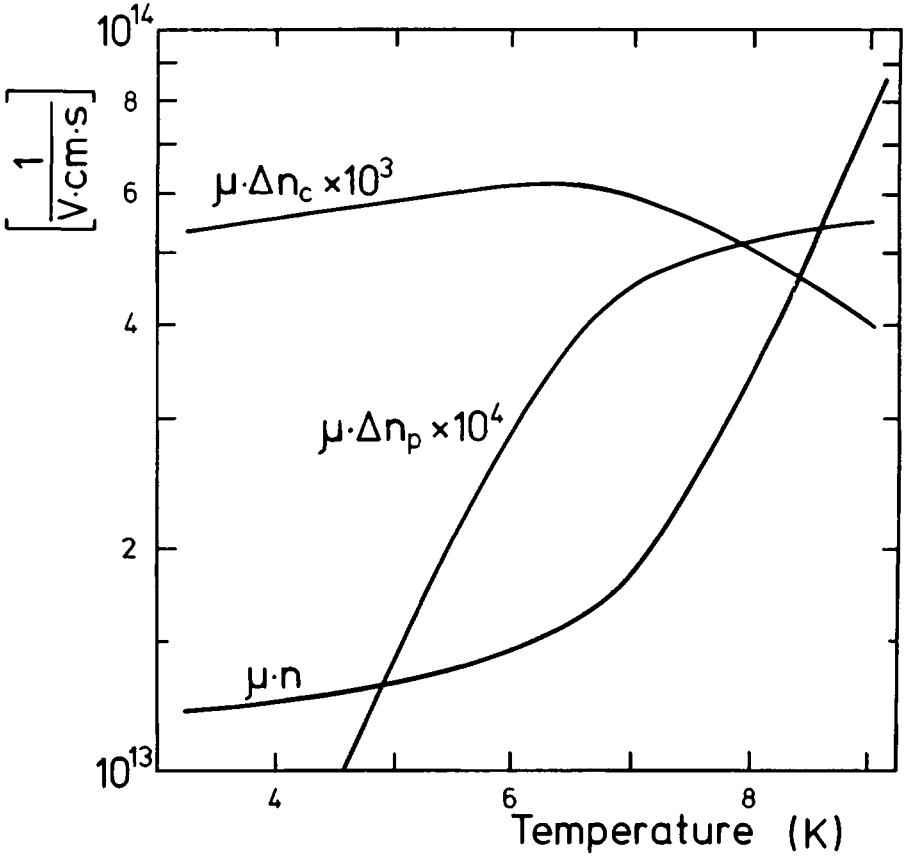

Fig. 3 : The values for μn, $\mu \cdot \Delta n_c$ and $\mu \cdot \Delta n_p$ as a function of temperatu calculated from figure 2 with equations (1) and (2). Here μ is the carrier mobility, n the carrier concentration, Δn_p the variation of the latter by photothermal ionization vi an excited state and Δn_c its variation by direct photo-ioniza

the continuum. In figure 2 this is shown as a function of temperature for the C-transition peak and continuum of the boron spectrum from a sample with impurity concentration 2.1×10^{11} atoms/cm^3. Also shown in figure 2 is the d.c. voltage-drop V across the sample. It is seen that ΔV_c decreases very rapidly above 7 K whereas V decreases more slowly. The peak strength ΔV_p increases with temperature as expected, but above 7 K ΔV_p decreases along with ΔV_c.

The values for μn, $\mu \cdot \Delta n_c$ and $\mu \cdot \Delta n_p$ can now be calculated from the measured V, ΔV_c and ΔV_p with equations (1) and (2); the results are presented in figure 3. The precise temperature dependence of μ is not known but according to Debye and Conwell (1954) typical values for μ lie between 10^5-10^6[cm^2/V·s] in this temperature range and for this impurity concentration. As the "continuum" carrier density variation Δn_c is expected to be independent of temperature, the shape of the $\mu \cdot \Delta n_c$ curve in figure 3 will reflect the temperature dependence of μ.

We thus conclude from figure 3 that $\Delta n_c \approx 10^5$[cm^{-3}] and that the strongly temperature dependent value of Δn_p is of the order of 10^4[cm^{-3}]. The mean free carrier concentration n approaches an assymptotic value for low temperatures, probably due to ionization by background radiation. For temperatures above 7 K n increases because of thermal ionization. In the considered temperature region the value of n is of the order of 10^8[cm^{-3}]. We may conclude from all this that although Δn_c does not change with temperature, the photoconductive signal (i.e. ΔV_c and ΔV_p) decreases very rapidly above 7 K due to the increase of n, according to equation (2). Furthermore we see that n, Δn_c and Δn_p are very small compared with the impurity concentration (2.1×10^{11} atoms/cm^3), so that practically

most impurities remain in their ground states. The temperature dependence of the photothermal ionization process can now be studied by comparing the measured peak strength ΔV_p at various temperatures with the area of the continuum ΔV_c, so by studying:

$$I = \Delta V_p / \Delta V_c = \Delta n_p / \Delta n_c \ .$$

In references II and III where equation (5) was already propounded, it was shown that experimental results on boron, aluminum and phosphorus dopes in high purity germanium were in excellent agreement with this equation. This is illustrated in figure 4 for two lines of the phosphorus spectrum. These results justify the assumption made about g' in section 3. The line intensities were taken from spectra which were normalized to the same continuum area. The solid curves in this figure represent least square computer fits of equation (5) to the experimental data, using ΔE and A as adjustable parameters. The degeneracy g of the intermediate levels was deduced from measured level splittings due to a magnetic field (Bassani et al 1974). The numerical results of these fits for ΔE are presented in table 1, together with the ground state energies ($E_{g.s.}$) calculated as:

$$E_{g.s.} = E_{trans} + \Delta E \ . \qquad (6)$$

The values for $E_{g.s.}$ found in this way from the various spectral lines are consistent with each other within experimental accuracy and, as is shown in reference III, agree with data obtained by other means. As an illustration that the simple exponential behaviour

$$I \propto \exp(-\Delta E/kT) \ , \qquad (7)$$

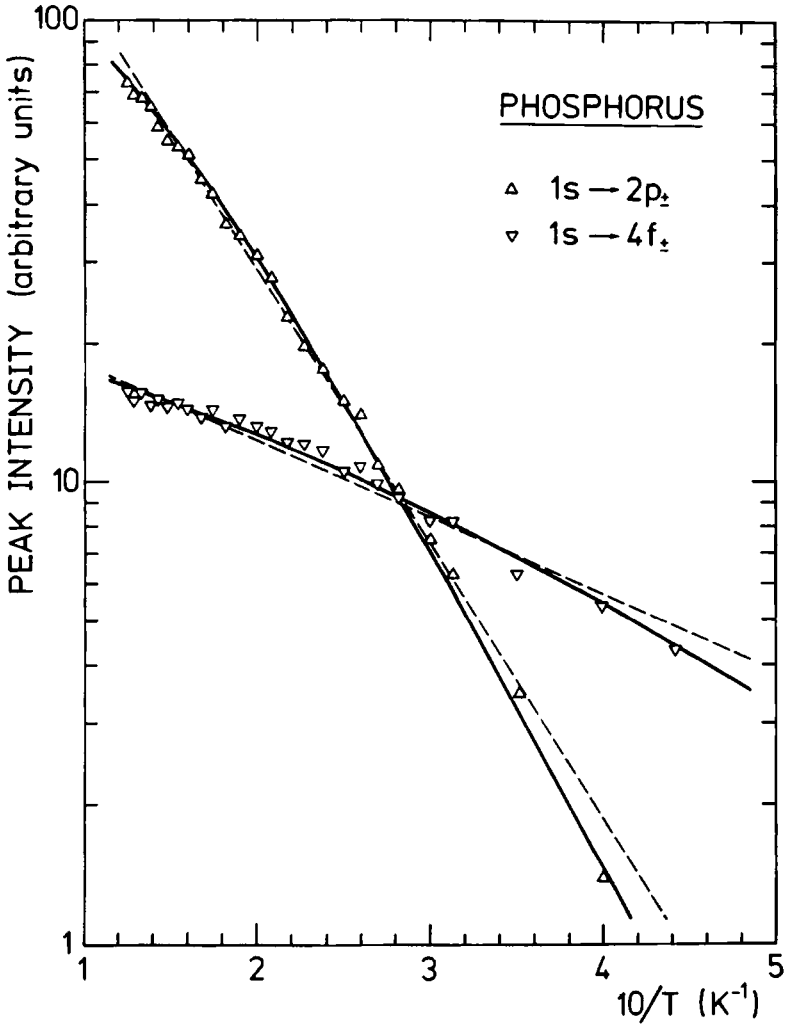

Fig. 4 : Logarithmic plot of the relative line intensities versus 10/T for two phosphorus lines. The solid curves represent least square computer fits to equation (5), the dotted lines those to equation (7). (See also table 1.)

Table 1 : Values of ΔE and $E_{g.s.}$ as obtained from computer fits of equations (5) and (7) from the temperature dependence of two lines of the phosphorus spectrum.

			With Eq. (5)		With Eq. (7)	
transition	$E_{trans}(cm^{-1})$	g	$\Delta E(cm^{-1})$	$E_{g.s.}(cm^{-1})$	$\Delta E(cm^{-1})$	$E_{g.s.}(cm^{-1})$
$1s \rightarrow 2p_{\pm}$	90.0 ± 0.2	4	12.9 ± 0.2	102.9 ± 0.2	9.5 ± 0.4	99.5 ± 0.4
$1s \rightarrow 4f_{\pm}$	99.0 ± 0.2	2	4.0 ± 0.3	103.0 ± 0.3	2.6 ± 0.5	101.6 ± 0.5

frequently assumed ad hoc in the literature, does not yield very reliable results equation (7) was also fitted to the experimental data. The results are shown in figure 4 (dotted lines) and in table 1. As can be seen from figure 4 the fit is not as good as with equation (5) and the calculated values for $E_{g.s.}$ are not consistent with each other.

Summarizing we may conclude that the theory about the line intensity in a photoconductivity spectrum, as outlined above, is in excellent agreement with the experimental results.

References.

Bassani F, Iadonisi G and Preciosi B 1974 Rep. Prog. Phys. 37 1099-210

Bykova E M, Goncharov L A, Lifshits T M, Sidorov V I and Hall R N 1976 Sov. Phys. - Semicond. 9 1223-7

Debye P P and Conwell E M 1954 Phys. Rev. 93 693-706

Jongbloets H W H M, Stoelinga J H M, Steeg M J H van de and Wyder P 1977 Physica 89B 18-21

—— 1979 Phys. Rev. 20 3328-32

Kogan S M and Lifshits T M 1977 Phys. Stat. Solidi 39 11-39

Lifshits T M and Nad' F Ya 1965 Sov. Phys. - Doklady 10 532-3

Lifshits T M, Likhtman N I and Sidorov V I 1968 Sov. Phys. - Semicond. 2 652-5

Nagasaka K and Narita S 1969 Solid St. Commun. 7 467-70

Seccombe S D and Korn D M 1972 Solid St. Commun. 11 1539-45

Simmonds P E, Chamberlain J M, Hoult R A, Stradling R A and Bradley C C 1974 J. Phys. C: Solid St. Phys. 7 4164-84

Spenke E 1958 Electronic Semiconductors (McGraw-Hill Book Company, Inc.) p 387

Stillman G E, Wolfe C M and Korn D M 1972 Proc. XI Int. Conf. Semicond. Phys. (Warsaw) p 863

Stoelinga J H M, Larsen D M, Walukiewicz W, Aggarwal R L and Bozler C O 1978 J. Phys. Chem. Solids 39 873-7

IV.6 MAGNETIC FIELD DEPENDENCE OF PHOTOTHERMAL CONDUCTIVITY SPECTRA IN THE FAR INFRARED OF THE BORON ACCEPTOR IN GERMANIUM

ABSTRACT

Photothermal conductivity spectra in the far infrared (10 - 200 cm^{-1}) of boron doped germanium (dopant concentration $\sim 10^{10}$ atoms/cm^3) have been obtained in magnetic fields B up to 2 T ($\vec{B}$//[001]) at a temperature of T = 7.5 K. The coefficients of the linear and quadratic field dependence of the Zeeman splittings and the resulting g values of the associated levels have been determined for the well known D and C transitions, and for the B and several A and I transitions as well. Moreover the field dependence has been studied of transitions to final states which could be identified as I_6 like states associated with light-hole Landau levels. The results are discussed in terms of existing theories.

1. Introduction.

From a theoretical point of view, transitions between impurity states of semiconductors like GaAs and InSb are easier to discuss than those in Ge and Si because of the less complicated band structure of the former materials. However, in Ge and Si interactions between the impurity states are easier to avoid since impurity concentrations of $\sim 10^{10}$ atoms/cm^3 can be achieved, while the lowest impurity concentration in a material like GaAs is of the order of 10^{14} atoms/cm^3, where interactions cannot be excluded (Larsen 1976, Stoelinga et al. 1978).

Impurity states have been studied mostly by measuring the transmission in the far infrared region (see the review article by Bassani et al. 1974). Soepangkat and Fisher (1973, further referred to as SF) employed this technique to investigate the Zeeman effect of lower levels of the boron and thallium impurities in germanium. For this type of measurements, relatively high impurity concentrations are needed.

By measuring the photothermal conductivity, samples of much higher purity can be used, yielding very narrow line widths of the spectra. This method was used by Lifshits and Nad (1965) for the first time and a recent review of this subject was given by Kogan and Lifshits (1977).

In a set of previous papers (Jongbloets et al. 1977, 1979 and 1980, further referred to as I, II and III) it has been shown how very accurate values for the ground state energies of the impurities can be deduced from the temperature dependence of the peaks in the spectra, obtained with the technique of photothermal ionization spectroscopy. Broeckx et al. (1979, further referred to as BCSV)

used this technique to investigate the Zeeman effect of the D and C transitions of the aluminum acceptor in germanium. Here, experimental results will be presented, not only for the D and C transitions, but also for the B and several A and I transitions of the boron acceptor in germanium. The labeling of the transitions is the same as used by Haller and Hansen (1974).

The Zeeman term connected with the magnetic field produces a linear splitting of the levels, whereas the diamagnetic term gives a quadratic correction. In addition, the impurity potential produces a set of sublevels associated with each Landau level (for detailed references, see the review article of Bassani et al. 1974).

In this paper, the splitting of one of the zero-field levels into sublevels associated with Landau levels is studied. Taking into account the magnetic field dependence of this zero-field level, values of the magnetic field dependence of the light-hole Landau levels are obtained. This dependence is in excellent agreement with theoretical considerations.

2. Experimental details.

The measurements were performed on a germanium sample containing 2.1×10^{11} atoms/cm^3 boron and 4.3×10^{10} atoms/cm^3 aluminum. The photothermal conductivity spectrum of the sample was measured as function of the wave number of the far infrared excitation radiation, using a Grubb Parsons Cube interferometer. The position of the peaks in the spectra were determined with an accuracy of 0.2 cm^{-1}. A magnetic field of up to 2 Tesla could be applied with a superconducting solenoid (Oxford Instruments). Most of the experimental details were given in reference II.

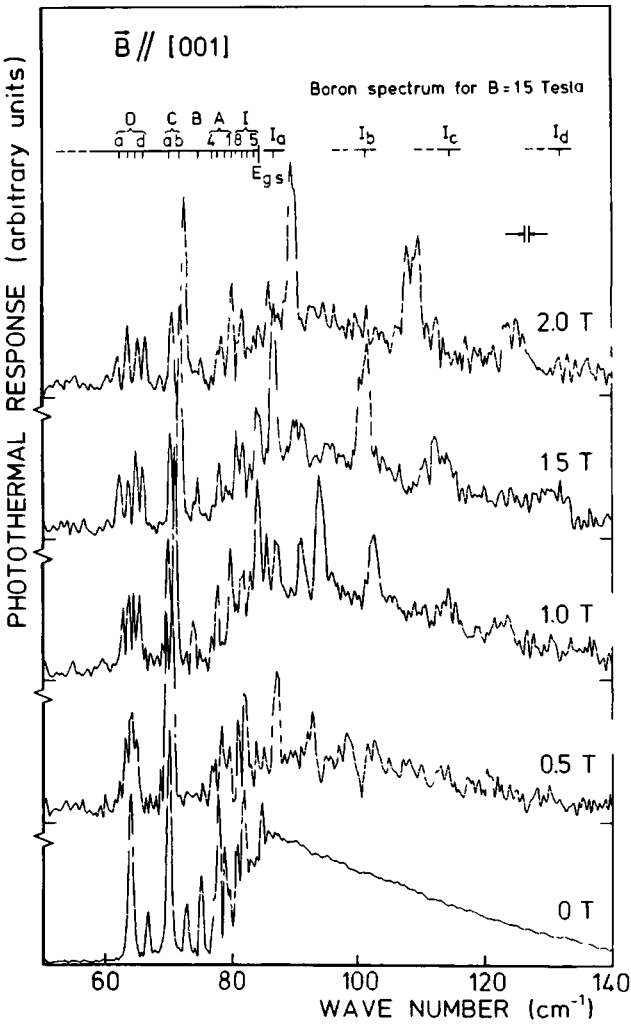

Fig. 1 : Photothermal conductivity spectra at 7.5 K of shallow acceptors in germanium for several values of the magnetic field $\vec{B}$ // [001]. Impurity concentrations: 2.1×10^{11} at./cm^3 B, 4.3×10^{10} at./cm^3 Al. The labelling at the top shows the boron spectrum at 1.5 Tesla including the Zeeman splitting and four satellite peaks of the I_6 transition associated with Landau levels.

Figure 1 shows some of the measured spectra for several values of the magnetic field with $\vec{B}$//[001]. The sample was held at a temperature of 7.5 K. The labeling of the lines of the boron spectrum at 1.5 Tesla is shown in the upper part of figure 1. The zero-field band edge corresponds with the ground state binding energy $E_{g.s.}$, as determined by the method outlined in references II and III. The continuum above $E_{g.s.}$ in the zero-field spectrum is due to direct photo-ionization from the impurity ground state into the free band, whereas the peaks below $E_{g.s.}$ are caused by the two-step photothermal ionization process. It is clearly visible in figure 1 that on applying a magnetic field the spectra not only exhibit a splitting or shift of the peaks below $E_{g.s.}$, but also develop a set of peaks in the continuum. These two types of peaks will be discussed separately in the following sections.

3. Field dependence of the peaks below $E_{g.s.}$

In figure 2 the transition energies of the peaks with wave numbers below the continuum onset $E_{g.s.}$ are plotted as a function of the magnetic field. As a linear and a quadratic Zeeman term is expected for each transition, a quadratic polynomial

$$E(B) = E(0) + aB + bB^2 \qquad (1)$$

was fitted to the experimental data. The solid curves in figure 2 calculated in this way, show an excellent fit to the data. The parameters a and b for the various spectral lines are summarized in table 1.

A similar procedure was applied by SF to the D and C lines of boron, and by BCSV to the D and C lines of aluminum. BCSV used

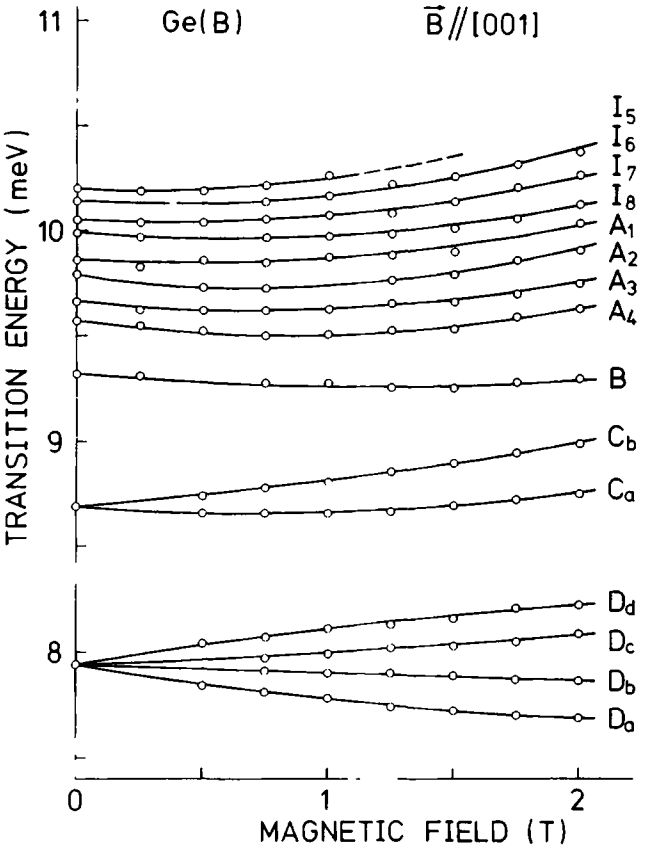

Fig. 2 : Zeeman effect in the photothermal conductivity spectrum of the boron acceptor in germanium with $\vec{B}$ // [001]. The curves are least square fits of a quadratic polynomial to the experimental data. (See also table 1.)

Table 1 : Linear and quadratic Zeeman parameters for the spectral lines of the boron impurity in germanium with $\vec{B}$ // [001] as determined from figure 2.

Transition	a (meV/T)	b (meV/T^2)
D_a	-0.205 ± 0.005	0.031 ± 0.004
D_b	-0.041 ± 0.005	0.003 ± 0.002
D_c	0.050 ± 0.005	0.020 ± 0.004
D_d	0.198 ± 0.009	-0.027 ± 0.006
C_a	-0.081 ± 0.005	0.061 ± 0.004
C_b	0.094 ± 0.003	0.032 ± 0.001
B	-0.094 ± 0.009	0.042 ± 0.006
A_4	-0.17 ± 0.01	0.103 ± 0.006
A_3	-0.117 ± 0.007	0.086 ± 0.006
A_2	-0.175 ± 0.005	0.124 ± 0.004
A_1	-0.07 ± 0.01	0.08 ± 0.01
I_8	-0.09 ± 0.01	0.082 ± 0.007
I_7	-0.057 ± 0.007	0.084 ± 0.005
I_6	-0.079 ± 0.007	0.108 ± 0.006
I_5	-0.07 ± 0.01	0.12 ± 0.01

polarized radiation in the Faraday configuration with the polarization vector $\vec{E} \perp \vec{B}$, SF used the Voigt configuration with $\vec{E} \perp \vec{B}$ and $\vec{E}//\vec{B}$. So the relative intensities of the peaks within one multiplet could be used for the identification of the transitions (see Bhattacharjee and Rodriguez, 1972). The experimental results of SF and BCSV for $\vec{B}//[001]$ are collected in table 2. The corresponding notations for the transitions, used by BCSV and SF, and in the present paper are also given there.

In this experiment the sample was mounted inside a semispherical integrating cavity; therefore it was not possible to use polarized radiation. This was not a serious problem, however, because the only lines seen to be splitting into multiplets with $\vec{B}//[001]$ are the D and C transitions, for which the identification was already given by BCSV. Comparing table 1 and 2 a good agreement can be seen between the present values for the linear and quadratic Zeeman terms for the D and C transitions, and those of SF and BCSV.

For the higher transitions (i.e. B, A and I lines) no comparable experimental values are available from the literature. Comparison with theory is also not possible because, as can be seen from figure 2, the theoretical assumption (Bhattacharjee and Rodriguez, 1972) that the unperturbed states at $B = 0$ are sufficiently well separated to treat the splitting of each state separately, does not hold for the higher lines any longer. The violence of this assumption for the A and I-lines can be seen from the nearly similar values for b, which is a consequence of the mutual repulsion of these lines because of their narrow spacing. A common feature of the B, A and I lines is the negative sign for the values of a.

Table 2 : Linear and quadratic Zeeman parameters a and b with $\vec{B}$ // [001] for the D and C transition of the Al acceptor in Ge, as determined by BCSV (Faraday configuration, $\vec{E} \perp \vec{B}$), together with the values for the B acceptor in Ge, as determined by SF (Voigt configuration, $\vec{E} \perp \vec{B}$ and $\vec{E}$ // $\vec{B}$).

This work	BCSV values for Ge(Al)			SF values for Ge(B)		
Trans.	Trans.	a (meV/T)	b (meV/T^2)	Trans.	a (meV/T)	b (meV/T^2)
D_a	D_4	-0.208	0.028	D_1	-0.176	0.015
				D_2	-0.163	0.014
D_b	D_3	-0.054	0.009	D_3	-0.045	0.005
				D_4	-0.030	0.002
D_c	D_2	0.055	0.017	D_6	0.057	0.019
				D_5	0.046	0.021
D_d	D_1	0.219	-0.030	D_8	0.185	-0.017
				D_7	0.187	-0.020
C_a	$C_{4,3}$	-0.066	0.062	C_2	-0.048	0.052
				C_1	-0.064	0.055
C_b	$C_{2,1}$	0.120	0.033	C_3	0.095	0.038
				C_4	0.107	0.037

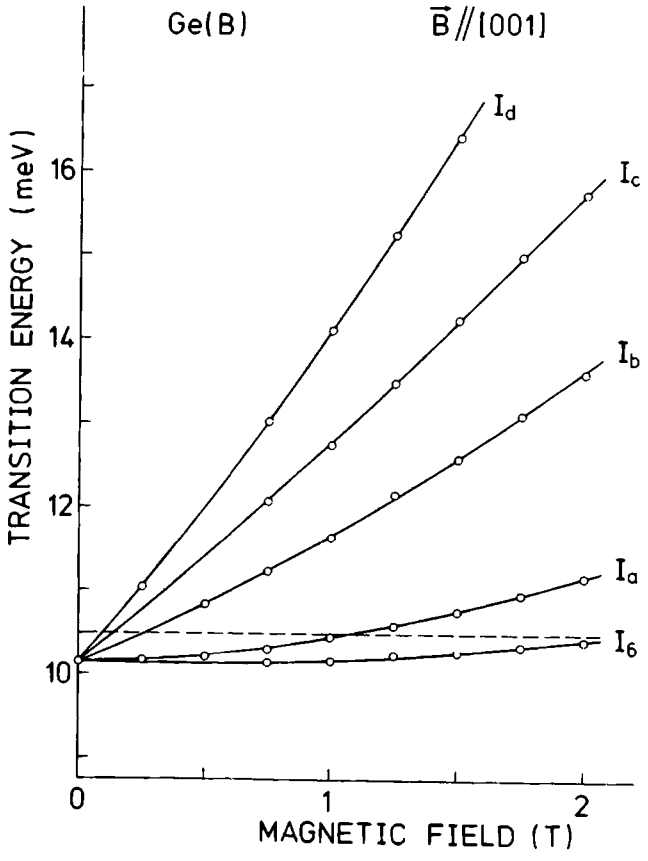

Fig. 3 : Magnetic field dependence in the photoconductivity spectra of the I_6 transition and four satellite transitions to bound states associated with Landau levels. The dashed line indicates the zero-field band edge. The curves are least square fits of a quadratic polynomial to the experimental data. (See table 3.)

4. Field dependence of the peaks in the continuum.

Apart from the peaks below the band edge, the photoconductivity spectra (figure 1) show a great number of peaks in the continuum that are almost impossible to identify unambiguously. However, some very pronounced peaks appear (labelled I_a, I_b, I_c and I_d) that can easily be recognized in every spectrum. The magnetic field dependence of these peaks is shown in figure 3, together with the I_6 transition. Again a quadratic polynomial was fitted to the experimental points, i.e.

$$E_n(B) = E_n(0) + p_n B + q_n B^2 \quad , \quad n = a,b,c,d \quad . \tag{2}$$

A very good fit can be obtained if the zero-field energy intercepts $E_n(0)$ of the curves coincide with the zero-field I_6 transition energy; this has been plotted in figure 3. The parameters p_n and q_n of these fits are summarized in table 3.

This allows the conclusion that the I_a, I_b, I_c and I_d transitions are of the same type as I_6, i.e. transitions from the impurity ground state to impurity excited states rather than valence band levels. Kaplan (1968) observed similar features in transmission spectra of boron in germanium and attributed the excited states tentatively to light-hole Landau states. The present very accurate experimental data support this conclusion (section 6).

5. Zeeman effect.

Soepangkat and Fisher (1973) interpreted their absorption spectra of the boron impurity in germanium under the assumption that the Zeeman splitting of the ground level is of the same order of magnitude as that of the final state of the D transition. However,

Table 3 : Linear and quadratic fit parameters for the magnetic field dependence of the I_a, I_b, I_c and I_d transitions of the boron impurity in germanium with $\vec{B}$ // [001] (see figure 3). Also listed are the differences between these parameters and those of the I_6 transition.

Transition	p_n (meV/T)	q_n (meV/T^2)	$p_n - a(I_6)$ (meV/T)	$q_n - b(I_6)$ (meV/T^2)
I_a	0.11 ± 0.01	0.20 ± 0.01	0.19 ± 0.02	0.09 ± 0.01
I_b	1.28 ± 0.03	0.24 ± 0.03	1.35 ± 0.03	0.13 ± 0.03
I_c	2.46 ± 0.04	0.16 ± 0.03	2.53 ± 0.04	0.05 ± 0.03
I_d	3.47 ± 0.04	0.47 ± 0.04	3.55 ± 0.04	0.36 ± 0.04

Table 4 : Calculated parameters for the linear Zeeman effect of the final state of the D and C transitions with $\vec{B}$ // [001] for Ge(B). Also shown are the values of BCSV for Ge(Al).

		$g'_{1/2}$	$g'_{3/2}$	r	g'_1
D	this work	7.0 ± 0.2	-0.52 ± 0.04	-0.120 ± 0.005	7.9 ± 0.2
	BCSV	7.4 ± 0.2	-0.63 ± 0.07	-0.119 ± 0.006	8.4 ± 0.2
C	this work	3.0 ± 0.1	1.01 ± 0.04	-0.077 ± 0.004	3.3 ± 0.1
	BCSV	3.2 ± 0.2	1.07 ± 0.07	- 1/13	3.5 ± 0.2

Tokumoto and Ishiguro (1977) concluded from magnetoacoustic resonance attenuation measurements on Ga-doped Ge that the splitting of the ground state of shallow acceptors in Ge is much smaller than previously assumed. BCSV pointed out that the ground state splitting is in fact so small that the observed line-splittings in photothermal conductivity spectra would reflect the splittings in the final state of the transitions only. This simplifies greatly the interpretation of the spectra, BCSV proposed the assignment of both the D and C lines to $\Gamma_8^+ \rightarrow \Gamma_8^-$ transition. We will proceed along the same line and compare our results for the Zeeman effect of the D and C transitions of boron in germanium with $\vec{B}//[001]$ with the results of BCSV for aluminum.

Using symmetry considerations Bhattacharjee and Rodriguez (1972) have shown that with $\vec{B}//[001]$ the energy shifts of the Zeeman levels of a Γ_8 state are given by

$$\Delta E_\mu = \mu_B(g_1'\mu + g_2'\mu^3)B + [q_1 + (q_2 + q_3)\mu^2]B^2 , \qquad (3)$$

where $\mu = 3/2, 1/2, -1/2, -3/2$, and μ_B is the Bohr magneton. Introducing the parameter $r = g_2'/4g_1'$ which measures the cubic anisotropy, and the principal g-factors $g_{1/2}'$ and $g_{3/2}'$ defined by

$$\begin{aligned} g_{1/2}' &= g_1' (1 + r) , \\ g_{3/2}' &= g_1' (1 + 9r) , \end{aligned} \qquad (4)$$

the linear part of equation (3) can be written as:

$$\begin{aligned} \Delta E_{\pm 1/2} &= \pm 1/2\ g_{1/2}'\mu_B B \\ \Delta E_{\pm 3/2} &= \pm 3/2\ g_{3/2}'\mu_B B . \end{aligned} \qquad (5)$$

So the splitting of a Γ_8 level will be symmetrical relative to the zero-field energy for $\mu = -1/2, +1/2$ and $\mu = -3/2, +3/2$.

BCSV assign to the D multiplet with $\vec{B}//[001]$ the transitions: $D_a = \Gamma_8 \rightarrow -1/2$, $D_b = \Gamma_8 \rightarrow +3/2$, $D_c = \Gamma_8 \rightarrow -3/2$ and $D_d = \Gamma_8 \rightarrow +1/2$. With this assignment the principal g-factors $g'_{1/2}$ and $g'_{3/2}$ can be deduced from the measured parameters a with equation (5), and from this g'_1 and r can be calculated with equation (4). The results are shown in table 4, together with the results of BCSV. For the C multiplet BCSV give the assignment $C_a = \Gamma_8 \rightarrow -3/2, -1/2$ and $C_b = \Gamma_8 \rightarrow +3/2, +1/2$. This leads to the g-factors for the C-final state which are also summarized in table 4. As can be seen from table 4 there is a good agreement between our values and those of BCSV.

6. Landau levels.

In a uniform magnetic field $\vec{B}$ the continuum of states in the energy band coalesces into a set of discrete quantum states, the Landau levels. Usually these Landau levels form a "ladder" of equidistant energies with spacing $\hbar\omega_c$ defined by the classical cyclotron frequency $\omega_c = eB/m^*$, m^* being the effective mass of the charge carrier. However, for degenerate bands such as the valence band edge in Ge the situation is more complex. Using the quantum-mechanical effective mass formalism Luttinger (1956) predicted that the lowest Landau levels would have irregular spacings, while the higher levels tend to uniform intervals. Numerical values for the Landau energy levels in Ge were derived by Evtuhov (1962) from second order perturbation theory.

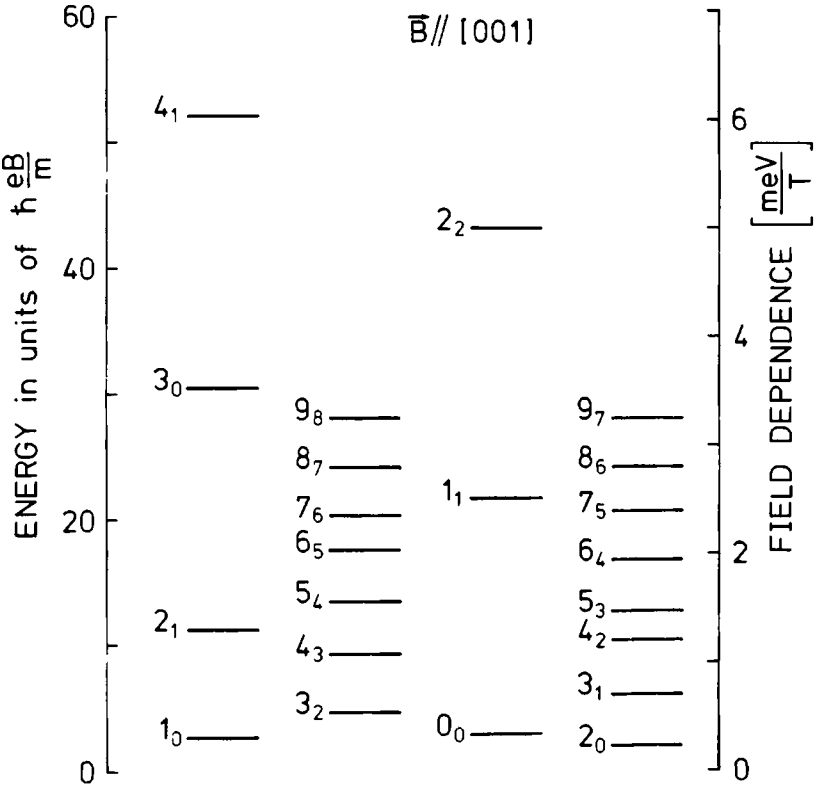

Fig. 4 : Valence-band Landau levels in germanium with $\vec{B}$ // [001], as calculated by Hensel and Suzuki (1974).

Very extensive calculations have been carried out by Hensel and Suzuki (1974) who applied uniaxial stress to the Ge crystal as a means to uncouple the valence bands in order to decipher the complicated quantum spectra. They found a separate Landau ladder for every value of the magnetic quantum number M_J, i.e. two heavy hole ladders ($M_J = \pm 1/2$) and two light hole ladders ($M_J = \pm 3/2$). Their results for $\vec{B}//[001]$ are plotted in figure 4.

Boyle and Howard (1961) and Horii and Nisida (1971) have shown that in Zeeman transmission spectra of Ge donors every bound state with energy E(B) has a set of satellite states associated with conduction band Landau levels. The energy $E_n(B)$ of these satellite states is given by

$$E_n(B) = E(B) + L_n(B) ,$$

where $L_n(B)$ is the energy of the n-th Landau level relative to the zero-field band edge. Applying the same idea to acceptor spectra, the valence band Landau levels can be deduced from the experimental data of figure 3 and table 2 by subtracting the linear and quadratic fit parameters of the I_6 transition from those of the I_a, I_b, I_c and I_d transition i.e.

$$L_n(B) = [p_n - a(I_6)]\cdot B + [q_n - b(I_6)]\cdot B^2 \qquad n = a,b,c,d .$$

The results are listed in table 3. A comparison of the values of the linear field dependence with the calculations of Hensel and Suzuki (figure 4), yields that the value of $(p_a - a(I_6))$ for L_a has a fair agreement with Landau levels 1_0 and 0_0, whereas the corresponding values for L_b, L_c and L_d agree excellently with the Landau levels

2_1, 1_1 and 3_0 respectively. So apparently the spectral lines I_a, I_b, I_c and I_d can be assigned to transitions from the boron ground state to I_6-like final states associated with light-hole Landau levels.

In conclusion it should be emphasized that the technique of photothermal ionization spectroscopy not only provides an excellent method for the study of the Zeeman effect of shallow impurities in germanium, but also for the analysis of the Landau level structure of the energy bands. It is shown that the results obtained with this technique are in excellent agreement with existing theories.

References.

Bassani F, Iadonisi G and Preciosi B 1974 Rep. Prog. Phys. 37 1099-210

Bhattacharjee A K and Rodriguez S 1972 Phys. Rev. B6 3836-56

Boyle W S and Howard R E 1961 J. Phys. Chem. Solids 19 181-8

Broeckx J, Clauws P, Van den Steen K and Vennik J 1979 J. Phys. C: Solid St. Phys. 12 4061-79

Evtuhov V 1962 Phys. Rev. 125 1869-79

Haller E E and Hansen W L 1974 Solid St. Commun. 15 687-92

Hensel J C and Suzuki K 1974 Phys. Rev. B9 4219-57

Horii K and Nisida Y 1971 J. Phys. Soc. Jap. 31 783-91

Jongbloets H W H M, Stoelinga J H M, Steeg M J H van de and Wyder P 1977 Physica 89B 18-21

Jongbloets H W H M, Stoelinga J H M, Steeg M J H van de and Wyder P 1979 Phys. Rev. B20 3328-32

Jongbloets H W H M, Steeg M J H van de, Stoelinga J H M and Wyder P 1980 accepted for publication in J. Phys. C: Solid St. Phys.

Kaplan R 1968 Phys. Rev. Letters 20 329-31

Kogan S M and Lifshits T M 1977 Phys. Stat. Solidi 39 11-39

Larsen D M 1976 Phys. Rev. B13 1681-91

Lifshits T M and Nad' F Ya 1965 Sov. Phys. - Doklady 10 532-3

Luttinger J M 1956 Phys. Rev. 102 1030-41

Soepangkat H P and Fisher P 1973 Phys. Rev. B8 870-93

Stoelinga J H M, Larsen D M, Walukiewicz W, Aggarwal R L and Bozler C O 1978 J. Phys. Chem. Solids 39 873-7

Tokumoto H and Ishiguro T 1977 Phys. Rev. B15 2099-117

APPENDIX COMPUTER PROGRAM "PHASE2"

This appendix shows the computer program, that has been developed for the processing of the data from the interferometer equipment, described in Chapter II. It is intended for handling phase-modulated interferograms, but only minor modifications are necessary for amplitude-modulation. The program is written in assembler language for a PDP-12 (DEC) laboratory computer. But it is also suited for a PDP-8 system; only the instructions for reading and writing of magnetic tapes have to be adapted.

The program is divided into two parts:

1. The main program "PHASE2", the structure of which is shown in Fig. A.1.
2. "FIRUTIL", a series of utily subroutines, such as:
   - a software floating point system,
   - a subroutine to type text strings,
   - an incremental plotter subroutine,
   - a subroutine to plot alphanumeric characters,
   - a subroutine to read papertapes and convert codes,
   - a subroutine to read or write magnetic tapes.

The program "PHASE2" reads interferograms, which are punched on papertape. "PHASE2" can handle a single interferogram, or a combination of a sample- and background-interferogram. These sample- and background-interferograms can be registered as separate measurements, but also simultaneously with a two-channel system. "PHASE2" has also the possibility to transform a series of interferograms and average the resulting spectra.

Each interferogram is preceded by control data, such as step length and number of channels used, and a series of 30 BCD characters defined by the operator with thumbwheel switches on the scanner-control unit. These 30 characters are used to provide the program with an identification number for the spectrum, and information about the sensitivity of the detection system. This last information is necessary to calculate the correct average and ratio of spectra.

The maximum number of interferometric data points that can be transformed is N = 1024. The interferogram should ideally be double sided with approximately an equal number of data points on either side of zero path. However, there is no need to have exactly the correct amount as the program is arranged to either truncate or pad the data as necessary.

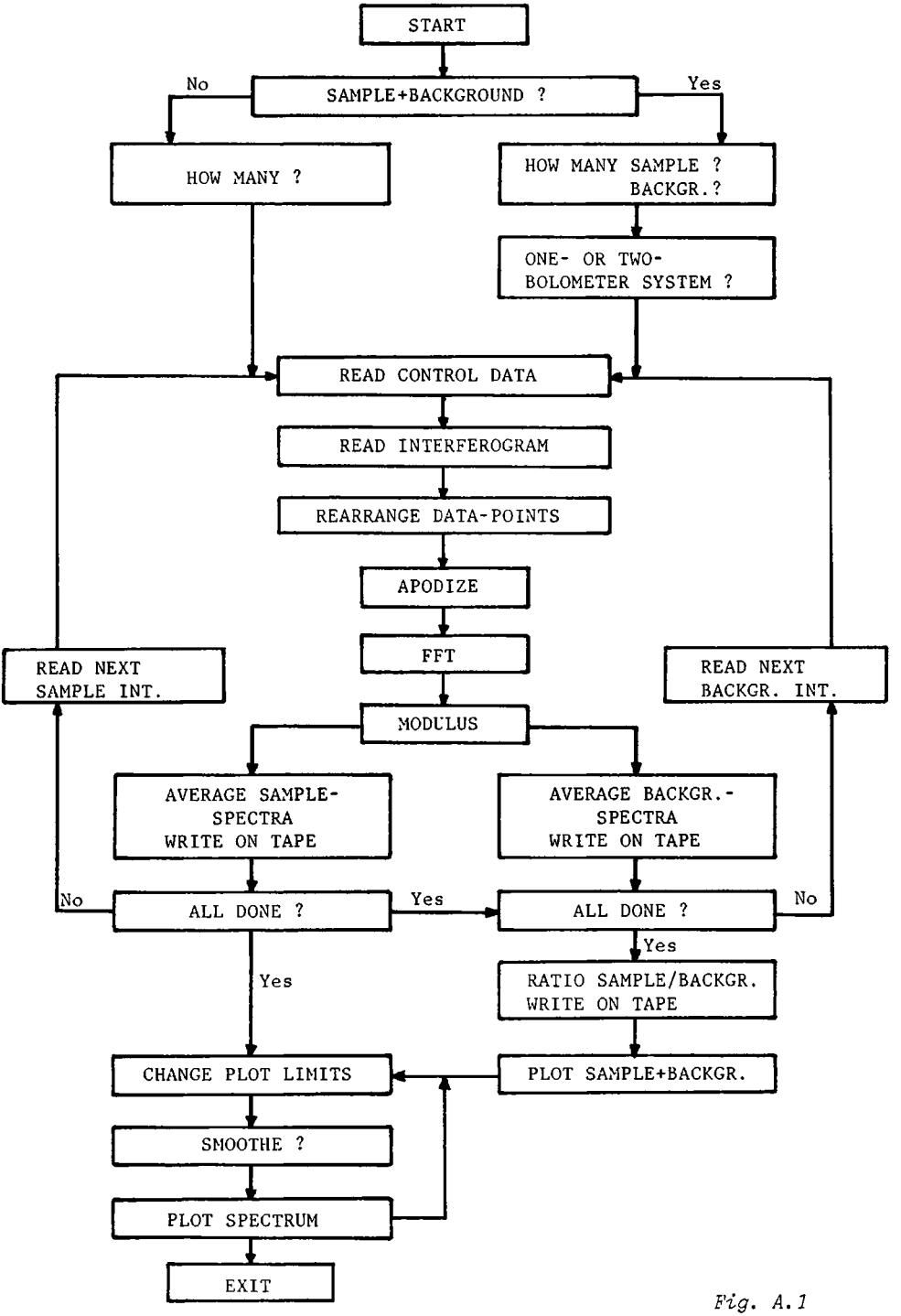
START
SAMPLE+BACKGROUND ?
No
Yes
HOW MANY ?
HOW MANY SAMPLE ?
BACKGR.?
ONE- OR TWO-
BOLOMETER SYSTEM ?
READ CONTROL DATA
READ INTERFEROGRAM
REARRANGE DATA-POINTS
APODIZE
FFT
MODULUS
READ NEXT
SAMPLE INT.
READ NEXT
BACKGR. INT.
AVERAGE SAMPLE-
SPECTRA
WRITE ON TAPE
AVERAGE BACKGR.-
SPECTRA
WRITE ON TAPE
No
ALL DONE ?
Yes
ALL DONE ?
No
Yes
Yes
RATIO SAMPLE/BACKGR.
WRITE ON TAPE
CHANGE PLOT LIMITS
PLOT SAMPLE+BACKGR.
SMOOTHE ?
PLOT SPECTRUM
EXIT

Fig. A.1

After reading the entire interferogram the maximum positive and negative values of the data are located, and the data point in between is attributed to zero path difference. The average value of the entire data array is subtracted from every data point to remove a possible D.C. offset present in the interferogram. The data array is then padded out to the maximum size of N = 1024 (if necessary) with zero's and then re-located such that the order is undisturbed but zero path is in the first location. The data array is then apodized from both ends towards the middle with a "cosine squared" function, after which the program calls for the "Fast Fourier Transform" (FFT). The FFT subroutine is based on a program written by P.L. Walton[1], which employs a modification of the Cooley-Tukey fast Fourier transform algorithm[2]. The FFT program calculates the complex spectrum

$$P(n\cdot\Delta\sigma) = \frac{1}{N}\sum_{m=0}^{N-1} I(m\cdot\Delta x)\cdot\exp(-\frac{2\pi i}{N}\cdot n\cdot m) \quad , \qquad n = 0,1,\ldots,N/2 \ .$$

The spectrum points are equidistant with a frequency-interval $\Delta\sigma = (N\cdot\Delta x)^{-1}$, where Δx is the sampling interval of the interferogram points. Then the modulus-spectrum is calculated as

$$|P(n\cdot\Delta\sigma)| = \sqrt{[\,\mathrm{Re}(P)\,]^2 + [\,\mathrm{Im}(P)\,]^2} \ ,$$

and stored on magnetic tape.

If a number of spectra must be averaged, the relevant interferograms are now read one by one, transformed and averaged with the already stored spectrum. The same procedure is then repeated for possible background-spectra, and the ratio of the (averaged) sample- and background-spectrum is calculated. Finally the resultant spectrum is plotted on an incremental plotter, within wave number limits chosen by the operator. Noisy spectra can be improved somewhat (at the cost of resolution) by a mathematical smoothing procedure, and then plotted again.

References.

1. P.L. Walton, "TOFAST-Fast Direct and Inverse Discrete Fourier Transform Routines.". DECUS Program Library: 8-260 (1970).
2. J.W. Cooley and J.W. Tukey, "An Algorithm for the Machine Calculation of Fourier Series.", Math. of Computers, 19, 297-301 (1965).

```
                *0
                /*PHASE.* (FOR INFRA RED INTERFEROMETER
                /(PHASE MODULATION)
                /(SCANNER TYPE 2)
                /        -       --          - -
                /THIS PROGRAM READS A SERIES OF INTERFEROGRAMS
                /(SAMPLE AND BACKGROUND) FROM TAPE1TAPE,
                /EXTENDS THEM WITH ZEROS TO 1024 POINTS,
                /PERFORMS A FOURIER TRANSFORM (FFT METHOD),
                /AVERAGES THE RESULTING SPECTRA, CALCULATES
                /THE RATIO SPECTRUM, PLOTS THE RESULTS
                /AND SMOOTHES THE SPECTRUM, IF DESIRED.
                /
                /MUST BE COMBINED WITH *FIRUTIL*.
                /ASSEMBLING  SEQUENCE (WITH TIME MS):
                /AS CLEARSYM (CLEARS THE SYMBOL TABLE)
                /AS FIRUTIL  (COMMON PART IS SAVED)
                /SR FIRUTIL, ZE
                /AS PHASE2 +AR FIRUTIL +SR PHASE2
                /
                /TO PUT ON *FIR DATA* TAPE:
                /DIAL MS TAPE(CONTAINING *PHASE**) ON UNIT 0
                /*FIR DATA* TAPE ON UNIT 1+REMOTE+WRITE ENABLE
                /START DIAL MS
                /LINK FIRU, LO PHASE2+0
                /LSW 4000, STOP, F MODE, I/O RESET
                /START LS
                /
                /CALLING SEQUENCE: VIA *FIR*
                /WRITE ENABLE
                /
                        FODSYM
                        FMODE
                        *20
0020  0011    START,  .START          /USED BY *FIR*
0021  4000    ISTORE, 4000            /FREQ. ARRAY
0022  0000    KUN,    0               /SAM. & BACKG.-1
0023  0000    NR,     0               /NO.OF BACKGROUNDS
0024  0000    NI,     0               /SAMPBACKG.2
0025  0000    NNR,    0               /NO. OF BACKGR.
0026  0000    N SPCTR, 0              /COUNTER FOR SPECTRA
0027  0000    FSPCTR, 0               /NO. O  SPECTRA
0030  0000    FLOW,   0               /LOWEST FREQUENCY
0031  0000            0
0032  0000            0
0033  0000    FH GH,  0               /HIGHEST FREQUENCY
0034  0000            0
0035  0000            0
0036  0000    MAX,    0               /MAXIMUM
0037  0000            0
0040  0000            0
0041  0000    DELF,   0               /FREQUENCY  N ERVAL
0042  0000            0
0043  0000            0
0044  0000    SENS,   0               /SENSITIVITY
0045  0000            0
0046  0000            0
0047  0000    RES,    0               /RESOLUTION
0050  0000            0
0051  0000            0
0052  0016    C10000, 00 6             10000
0053  0349            1349
0054  0000            0000
0055  0000    TORE,   0
0056  04n0    IFERST, 460             /FIRST FAR BLOCK
0057  7443    ANL,    7443            / IBM NL
0060  7447    MINYES, 7447            / YES
0061  7270    MINO,   7270            / 0
0062  0173    SAMP,   SAMPLE
0063  0471    BCKGR,  BACK
0064  0054    FFT,    FFT
0065  3400    RESNR,  NRRES
0066  3570    SPECTR, SPECOT
0067  3017    SPECT,  SPECO1
0070  3340    LIM1,   LIM
0071  3423    MAXIL,  MAXI
0072  3400    NORMI,  NORM
0073  3700    SMITH,  SMOOTH
0074  0000    MAXLOC, 0               /LOCATION OF MAXIMUM
0075  0000    MINLOC, 0               /LOCATION OF MINIMUM
0076  3456    INITL,  INIT
0077  3466    LAST,   LST
0100  0001    FF,     0001            /FF
0101  3110            3110
0102  3755            3755
0103  1703    INDEXL, INDEX
0104  0777    FILL,   777             /FILL
0105  1000    FILL,   1000            /FILL
0106  0000    I,      0
0107  0000    K,      0
0110  0000    AJL,    0
0111  0000    ANFJL,  0
0112  0000    ANI,    0
0113  0000    ANFNL,  0
0114  0000    N,      0
0115  0000    C,      0
0116  0000            0
0117  0000            0
0120  0000    S,      0
0121  0000            0
0122  0000            0
0123  0000    F,      0
0124  0000            0
0125  0000            0
0126  0000    V,      0
0127  0000            0
0130  0300            0
                        *700
0700  7775    TENTH,  7775            /0.1
0701  3146            3146
0702  3147            3147
0703  0003    FIVE,   0003
0704  2400            400
```

```
0705  0000            0000
0706  1444    FNR,    NR
0707  0641    STEPS,  STEPS
0710  1641    HNDRD,  HNDR            /0.01
                /START OF PROGRAM *PHASE2*.
0711  7300    START,  CLA CLL
0712  3152            DCA TYPFLT      /SET TYPE FLAG
0713  3534            DCA I FLAGTF    /FIELD=1
0714  6046            TLS             /INITIALIZE TTY
0715  6014            RFC             /AND TAPE READER
0716  4746            JMS I PCRLF     /CR LF
0717  4404            WRITE
0720  3404            ME%62           /*SAM & BACKGR?*
0721  4417            JMS I ANSWER
0722  1140            TAD ANSWR
0723  1060            TAD MINYES
0724  7650            SNA CLA
0725  7001            IAC             /YES: NI=2
0726  7001            IAC             /NO, NI=1
0727  3024            DCA NI
0730  4404            WRITE
0731  3661            ME%619          /*HOW MANY SPECTRA ?*
0732  7344            STA CLL RAL
0733  1024            TAD NI          /NI 2 ?
0734  7640            SZA CLA
0735  5250            JMP SPECTR
0736  4404            WRITE           /YES
0737  3653            ME%69           /*SAMPLE:*
0740  4541             JMS I SIGNV    /NO. OF SAMPLES
0741  3055            DCA STORE
0742  4404            WRITE
0743  3660            MESG10          /*BACKGR:*
0744  4541            JMS I SIGNV
0745  3025            DCA NNR         /BNR NO.OF BACKGROUNDS
0746  1055            TAD STORE
0747  7351            JMP .+2
0750  4541    SPECTR, JMS I SIGNV     /NO. OF SPECTRA
0751  3027            DCA FSPCTR
0752  1027            TAD FSPCTR
0753  7041            CIA
0754  1026            TCA NSPCTR      /NSPCTR -PSPCTR
0755  4404            WRITE           /*INTERFEROMETER*
0756  3467            ME%61
0757  4406            READ            /READ TRAILER TILL
0760  1057            TAD MNL         /FIRST *NEW LINE*.
0761  7640            SZA CLA
0762  5757            JMP .-3
0763  4406            READ            /READ NR
0764  1043            TCA NR
0765  7344            STA CLL RAL
0766  1023            TAD NR          /NR-1 OR 2 ?
0767  7740            SMA SZA C A
0770  4545            JMS I BUG
0771  7240            STA
0772  1023            TAD NR
0773  7640            SZA CLA
0774  5300            JMP .+4
0775  4404            WRITE
0776  3617            ME%64           /*ONE*
0777  5303            JMP .+3
0300  4404            WRITE
0301  3621            ME%66           /*NR*
0302  4404            WRITE
0303  3674            ME%66           /*-BELOW HERE :SYSTEM
0304  4406            READ            /SAMPLING INTERVAL*
0305  4407            FENTER
0306  0006            FCDF0
0307  0011            INPUT           /READ STEPS
0310  0002            2
0311  6607            FFUT I STFP
0312  5206            FMPY FIVE       /1  TEF=5 MICRON
0313  6047            FFUT %ES
0314  0017            OUTPUT          /PRINT
0315  0050            50
0316  5052            FGET C10000
0317  4047            FDIV RES
0320  6047            FPUT RES        /RES=10000/#STEPS
0321  0000            FEXT
0322  7332            CLA STL RTR     /1024
0323  4541            JMS I FLOAT
0324  4407            FENTER
0325  6162            FPUT FFAL
0326  5047            FGET RES
0327  4162            FDIV FFAL1
0330  6041            FPUT DELF       /DELF 10000/5*STEPS*1024
0331  0000            FEXT
0332  4404            WRITE
0333  3646            ME%68           /*MICRON*
0334  4406            READ
0335  4404            WRITE
0336  3765            ME%632          /*MODULATION AMPLITUDE*
0337  4407            FENTER
0340  0011            INPUT           /READ NR
0341  0005            5
0342  6115            FFUT C
0343  3610            FMPY I HNDRD
0344  6606            FPUT I FNR
0345  0000            FEXT
0346  4406            READ
0347  4407            FENTER
0350  0011            INPUT           /READ MODAMP IN
0351  0004            4               /0.1 MICRONS.
0352  5200            FMPY TENTH
0353  0012            OUTPUT          /PRINT
0354  0041            41
0355  0007            FCDF1           /SET F1.0,F.-1
0356  0000            FEXT
0357  4406            READ
0360  4404            WRITE
0361  3646            ME%68           /*MICRON*
0362  1024            TAD NI
0363  7041            CIA
0364  3 2             DCA RUN
```

```
0365 5374          JMP SAMPLE+1
                   #4/2
0372 0607 CHECK1, CHECK
                   /READ SAMPLE INTERFEROGRAM.
0373 4772 SAMPLE, JMS I CHECK1      /READ NB, STEP
0374 1036          TAD IFIRST
0375 3533          DCA I BLNTF      /FIRST IFEEDBACK
0376 4404          WRITE
0377 3553          MESG9            /*SAMPLE1*
0400 4605          JMS I LOCK       /READ SENS
0401 4210          JMS SKP9
0402 4406          READ
0403 4406          READ
0404 7213          JMP DATA         /READ DATA
0405 0000 LOCK,    LOCKIN
0406 1003 CONTR1,  CONTR
0407 7622 NLC,     7622             /-ITEM LC
0410 0000 SKP9,    0                /SKIP 9 CHAR.
0411 1217          TAD M9
0412 3156          DCA COUNT
0413 4406          READ
0414 2156          ISZ COUNT
0415 5213          JMP .-2
0416 5610          HLT I SKP9
0417 7767 M9,      7767             / 9
0420 0607 CHECK,   CHECK
                   /READ BACKGROUND INTERFEROGRAM.
0421 7344 BKGR,    SZA CLL RAL
0422 1023          TAD NR
0423 7640          SZA CLA          /IF NR > 0 WIND TAPE
0424 5244          JMP BACKGR
0425 4544          JMS I REWRD
0426 4406          READ
0427 1055 REWIND,  TAD STORE
0430 3136          DCA STOR1
0431 4406          READ
0432 3046          DCA STORE
0433 1055          TAD STORE
0434 1207          TAD M          /LOOK FOR *LOWER CASE*
0435 7640          SZA   A
0436 5237          JMP REWIND
0437 1136          TAD STOR1        /FOUND?  PREVIOUS
0440 1057          TAD MNL          /CHAR. *NEW LINE*
0441 7640          SZA CLA
0442 5237          JMP REWIND
0443 4545          JMS I FRWRD      /YES, FORWARD
0444 4620 BACKGR,  JMS I CHECK2
0445 4710          JMS SKP9
0446 4406          READ
0447 4406          READ
0450 4404          WRITE
0451 3 60          MESG10           /*BACKGR*
0452 4605          JMS I LOCK       /READ SENS
                   /READ INTERFEROGRAM.
0453 7332 DATA,    CLA STL RTR      /INITIALIZE MAX, MIN
0454 3123          DCA F            /AND AVERAGE
0455 7333          CLA IAC STL RTR
0456 3124          DCA FH           /MAX  0.5**2 1024
0457 7332          CLA STL RTR
0460 3120          DCA S
0461 7337          CLA STL RTR
0462 3121          DCA V41          /MIN 0.5**2 1024
0463 3126          DCA V
0464 3127          DCA V41
0465 3130          DCA V42          /AVER 0
0466 3106          DCA J
0467 4606 DATA1,   JMS I CONTR1     /MORE DATA ?
0470 1106          TAD J
0471 4503          JMS I INDEXL     /FIND FLOATING ADDRESS
0472 3110          DCA AJL
0473 1023          TAD NR           /IF NR > AND RUN  1
0474 1037          TAD RUN          /SKIP SAM., READ BACKG.
0475 7740          SMA SZA CLA
0476 4210          JMS SKP9
0477 4407          FENTER
0500 0044          INPUT            /READ DATA
0501 0005          5                /(5 DIGITS)
0502 0000          FEXT
0503 4406          READ
0504 7041          CIA
0505 7001          IAC
0506 7640          SZA CLA          /OVERLOAD ?
0507 5314          JMP .+5
0510 4407          FENTER           /YES
0511 6053          FLET C10000      /SET 10000
0512 1052          FADD C10000
0513 0000          FEXT
0514 4406          READ
0515 7041          CIA
0516 7001          IAC
0517 7640          SZA CLA          /DATA NEGATIVE ?
0520 5324          JMP .+4
0521 4407          FENTER           /YES, NEGATE
0522 0010          NEGATE
0523 0000          FEXT
0524 4406          READ
0525 4407          FENTER
0526 4052          FDIV C10000
0527 3044          FMPY SENS
0530 6510          FFUT I AJL       /A(J)=DATA(N)/10000
0531 1176          FADD V           /V+A(J)
0532 6126          FFUT V
0533 5510          FGET I AJL       /A(J) T ?
0534 7123          FSUB T
0535 0000          FEXT
0536 1160          TAD HORD
0537 7750          SPA SNA CLA      / 0 ?
0540 5347          JMP .+7          /NO
0541 4407          FENTER           /YES, T A( )
0542 5510          FGET I AJL
0543 6123          FFUT T
0544 0000          FEXT
0545 1106          TAD J

0546 3074          DCA MAXLOC       /LOCATION OF MAX NUM
0547 4407          FENTER
0550 5120          FGET T
0551 7510          FSUB I AJL       /S A(J)
0552 0000          FEXT
0553 1160          TAD HORD
0554 7750          SPA SNA CLA      / 0 ?
0555 5364          JMP .+7          /NO
0556 4407          FENTER
0557 5510          FGET I AJL
0560 6170          FFUT S           /YES, S A(J)
0561 0000          FEXT
0562 1106          TAD J
0563 3075          DCA MINLOC       /LOCATION OF MINIMUM
0564 7740          SMA
0565 1023          TAD NR           /IF NR 1 OR RUN  0
0566 7450          SNA              /SKIP BACKGR.
0567 5373          JMP .+4
0570 1037          TAD RUN
0571 7640          SZA CLA
0572 4210          JMS SKP9
0573 2136          ISZ J
0574 7554          CLA CLL CMA SNL
0575 1006          TAD J
0576 7640          SZA CLA          / IF 0
0577 5267          JMP DATA1        /NO, CONTINUE
0600 4406          READ             /YES  NOW READ
0601 1 05            AD END
0602 7640          SZA CLA
0603 5 00          JMP . 3
0604 5606          JMP I CALC1
0605 7620 END,     160
0606 1075 CALC1,   CALC
                   /READ AND CHECK NC AN. STEP.
0607 0000 CHECK,   0
0610 4406          READ             /READ IN HEIGHT TEST
0611 1057          TAD MNL          /TEST *NEW LINE*
0612 7640          SZA CLA
0613 5213          JMP .-5
0614 4404          WRITE
0615 7041          CIA
0616 1023          TAD NR           /READ AND CHECK NC
0617 7640          SZA CLA
0620 4435          JMS I BIG
0621 4404          WRITE
0622 4407          FENTER
0623 0011          INPUT            /READ AND CHECK  TEP
0624 0002          2
0625 5245          FSUB TEPS
0626 0000          FEXT
0627 1160          TAD HORD
0630 7640          SZA CLA
0631 4545          JMS I BIG
0632 4406          READ
0633 4407          FENTER
0634 0011          INPUT            /READ NU
0635 0005          5
0636 6115          FFUT C
0637 0011          INPUT            /SKIP 6 CHAR
0640 0006          6
0641 0000          FEXT
0642 4406          READ
0643 7300          CLA CLL
0644 5607          JMP I CHECK
0645 0000 STEPS,   0
0646 0000          0
0647 0000          0
                   /LOCK IN AMPLIFIER SETTINGS.
0650 0000 LOCKIN,  0
0651 4404          WRITE
0652 3544          MESG8            /*NR*
0653 4407          FENTER
0654 5115          FGET C
0655 0012          OUTPUT           /PRINT NR
0656 0050          50
0657 0000          FEXT
0660 4404          WRITE
0661 3612          MESG12           /*SENSITIVITY*
0662 1027          TAD F FLTR
0663 4543          JMS I FLOAT
0664 4407          FENTER
0665 6167          FFUT FRACT
0666 0011          INPUT            /SENSITIVITY
0667 0003          3
0670 6120          FFLT S
0671 0012          OUTPUT
0672 0030          30
0673 5170          FGET S
0674 4162          FDIV FRACT
0675 6044          FFUT SENS        /SENS SENS/ SCALE
0676 0000          FEXT
0677 4406          READ             /SENS.SCALE
0700 4547          JMS I CONVRT
0701 3056          DCA STORE
0702 7344          STA CLL RAL      / 2
0703 1055          TAD STORE
0704 7500          SMA              /SCALE < 2
0705 5311          JMP .+4
0706 4404          WRITE            /YES
0707 3623          MESG13           /*NANO*
0710 5310          JMP .+2.0
0711 7440          SZA              /SCA   2 ?
0712 5316          JMP .+4
0713 4404          WRITE            /YES
0714 3626          MESG14           /*MICRO*
0715 5320          JMP .+5
0716 4404          WRITE            /SCALE 1
0717 3632          MESG15           /*MILLI*
0720 4404          WRITE
0721 3636          MESG16           /*VOLT*
0722 1055          TAD STORE
0723 7041          CIA
0724 3156          DCA COUNT
```

```
0725  4407          FENTER
0726  5044          FGE  SEN
0727  3343          FMFY C1000
0730  6044          FFUT SENS       /SENS SENS*(1000 SENSSL)
0731  0000          FEXT
0732  2156          ISZ COUNT
0733  5325          JMP .-6
0734  1346          TAD N7
0735  3156          DCA COUNT
0736  4406          READ
0737  2 56          ISZ COUNT
0740  5336          JMP .-2
0741  7300          CLA CLL
0742  5650          JMP I LOCKIN
0743  0012  C1000,  0012            /1000
0744  3720          3720
0745  0000          0000
0746  7771  N7,     7
      /RATE OF APODISATION,
0747  0000  APOD,   0
0750  1074          TAD MAXLOC
0751  7104          CLL RAL         /*M
0752  7041          CIA
0753  1106          TAD J           /J-2*M
0754  7510          SPA             / =0 ?
0755  7200          CLA             /NO, STORE M
0756  1074          TAD MAXLOC      /YES, STORE J M
0757  7041          CIA
0760  1105          TAD FS 2
0761  7041          CIA             /(M-512) OR (J M 512)
0762  7500          SMA             / 0 ?
0763  7200          CLA             /NO, STORE SL)
0764  1105          TAD FS12        /YES, STORE-M OR   M
0765  3055          DCA STORE
0766  1055          TAD STORE
0767  7104          CLL RAL         /2*STORE
0770  4443          JMS I FLOAT
0771  4407          FENTER
0772  4100          FDIV PI
0773  6123          FFUT F          /T 2*5*ORE/FI
0774  0000          FEXT
0775  5747          JMP I TOD
                    *1000
1000  7746  M/ERO,   0032            /-.RM 0
1001  7652  MENR,    3 0160          /-.RM R
1002  0002  MLC,     160 0156        / IBM,LOWER CASE
      /CONTROL OF DATA, (MORE DATA ? END?, LOW TAPE ?)
1003  0000  CONTR,   0
1004  4406          READ
1005  1200          TAD M/ERO       /ZERO ?
1006  7450          SNA
1007  5603          JMP I CONTR     /YES, EXIT
1010  1701          TAD MEND        /END OF DATA ?
1011  7450          SNA
1012  5225          JMP CALCU       /YES,START CALC.
1013  1702          TAD MLC         /LOWER CASE ?
1014  7640          SZA CLA
1015  4535          JMS I BUG       /NO! ERROR !
1016  4406          READ            /YES, SKIP
1017  1200          TAD MZERO       /TILL NEXT ZERO
1020  7650          SNA CLA
1021  5603          JMP I CONTR
1022  5216          JMP . 4
      /START OF CALCULATIONS,
1023  4406  CALCU,   READ
1024  7300          CLA CLL
1025  1074          TAD MAXLOC      /CALC. LOC. OF CENTRE
1026  1075          TAD MINLOC
1027  7110          CLL RAR         /MAXLOC=
1030  3074          DCA MAXLOC      /(MINLOC+MAXLOC)/2
1031  4404          WRITE
1032  3565          MESG11          /*NO.OF DATA POINTS*
1033  1106          TAD J
1034  4543          JMS I FLOAT
1035  4407          FENTER
1036  6115          FFUT C          /C=FLOAT(J)
1037  0012          OUTPUT          /PRINT
1040  0040          40
1041  5126          FGET V
1042  4115          FDIV C          /AVERAGE=
1043  6126          FFUT V          /V V/FLOAT(J)
1044  0000          FEXT
1045  1024          TAD NI
1046  1022          TAD RUN
1047  7640          SZA CLA
1050  5262          JMP CALC 1
1051  1026          TAD NSPCTR      /FIRST SAMPLE SPECTRUM ?
1052  1027          TAD PSPCTR
1053  7440          SZA CLA
1054  5262          JMP CALC 1      /NO
1055  4407          FENTER          /YES, CALCULATE
1056  5047          FGET RES        /RESOLUTION
1057  4115          FDIV C
1060  6047          FFUT RES        /RES=10000/5*STEPS*J
1061  0000          FEXT
1062  3107          DCA K           /INITIALIZE K
1063  1107  CALC,   TAD K
1064  4503          JMS I INDEXL
1065  3112          DCA AKL
1066  4407          FENTER
1067  5512          FGET I AKL      /SUBTRACT AVERAGE
1070  2126          FSUB V          /A(K)=A(K) V
1071  6512          FFUT I AKL
1072  0000          FEXT
1073  2107          ISZ K
1074  1107          TAD K
1075  7041          CIA
1076  1106          TAD J
1077  7640          SZA CLA         /K J ?
1100  5263          JMP CALC        /NO-CONTINUE
1101  1104          TAD J           /YES
1102  4503          JMS I INDEXL
1103  3055          DCA STORE

1104  6211          CDF  0
1105  3435          DCA I STORE     /CLEAR LOC.
1106  2035          ISZ STORE       /DID  ????
1107  5305          JMP .-2
1110  6201          CDF 00
1111  4736          JMS I AFODI     /PREPARE FOR
1112  7200          CLA             /    APODISATION
      /K ARRANGE DATA SO THAT CENTRE IS AN LOCATION 0
1113  0?            TAD FS12
1114  7041          CIA
1115  0?4           TAD MAXLOC
1116  7450          SNA             MAXLOC 5 2 ?
1117  5364          JMP .+5+3-1     /YES, JUMP
1120  3114          DCA H           /H MAXLOC -512
1121  3107          DCA K
1122  1114  RRNG,   TAD H
1123  7210          SPA  CLA        /H 0 ?
1124  5337          JMP .+RNG1      /NO
1125  1107          TAD K           /YES-SHIF  LEFT H PLACES
 126  4503          JMS I INDEXL
 27   3113          DCA ANL         /AN =A(K)
 30   1107          TAD K
1 31  1114          TAD H
1 32  4503          JMS I INDEX
 33   3110          DCA AJL         /AJ  A(K+MAXLOC-512)
 34   1345          JMP .+RNG2
 35   1?72  FMV,    FLMOV
  6   0747  AFODI,  FOD
 37   1107  RRNG1,  TAD K           /H 0
1140  7041          CIA             /SHIFT RIGHT H PLACES
1141  1074          TAD MAXLOC
1142  1104          TAD FS11
1143  4503          JMS I INDEXL
1144  3110          DCA AJL         /AJ  A(MAXLOC-FS11 K)
1145  7333          CLA STL IAC RTR
1146  1107          TAD K
1147  7001          IAC
1150  7041          CIA
1151  4503          JMS I INDEXL
1152  3112          DCA AKL         /AKL A(1023-K)
1153  4407  RRNG2,  FENTER
1154  5010          FGET I AJL
1155  6512          FFUT I AK       /AKL AJL
1156  0000          FEXT
1157  2107          ISZ K
1160  7333          CLA STL IAC RTR
1161  1107          TAD K
1162  7640          SZA CLA         /K 1024 ?
1163  5427          JMP RRNG        /NO CONTINUE
1164  3107          DCA K           /YES
1165  1107  RRNG3,  TAD K           /INTERCHANGE FFT
1166  1105          TAD FS12        /AND RIGHT HALVES
1167  3106          DCA J
1170  4736          JMS I FLIMV     /SWITCH AC(J) AND AC(K)
1171  2107          ISZ K
1172  1107          TAD K
1173  7041          CIA
1174  1105          TAD FS12
1175  7640          SZA CLA         /K 512 ?
1176  5365          JMP RRNG3       /NO CONTINUE
      /APODIZE WITH COSINE^2 FUNCTION.
1177  3107          DCA K
1200  1107  AFOD,   TAD K
1201  4503          JMS I INDEXL
1202  3112          DCA AKL         /AKL A(K)
1203  7333          CLA STL IAC RTR
1204  1107          TAD K
1205  7041          CIA
1206  4503          JMS I INDEXL
1207  3110          DCA AJL         /AJL A(1023-K)
1210  1107          TAD K
1211  4543          JMS I FLOAT
1212  4407          FENTER
1213  4123          FDIV T
1214  0004          COS
1215  0001          SHRF
1216  6115          FFUT C          /C COS(FLOAT(K)/1?2?
1217  5512          FMFY I AKL
1220  6512          FFUT I AKL      /A(K) A(K)*C
1221  5510          FGET I AJL
1222  5115          FMFY C
1223  6510          FFUT I AJL      /A(1024-K)
1224  0000          FEXT            /   A(1024-K)*C
1225  2107          ISZ K
1226  1107          TAD K
1227  7041          CIA
1230  1055          TAD STORE
1231  7700          SMA CLA
1232  5200          JMP AFOD        /NO CONTINUE
1233  4464          JMS I FFT1      /YES FOURIER TRANSFORM
1234  7200          CLA
1235  3107          DCA K
      /CALC. LENGTH OF COMPLEX VECTOR.
1236  1107  POWER,  TAD K
1237  4503          JMS I INDEXL
1240  3112          DCA AKL
1241  1107          TAD K
1242  1105          TAD FS12
1243  4503          JMS I INDEXL
1244  3113          DCA ANKAL
1245  4407          FENTER
1246  5512          FGET I AKL
1247  6115          FFUT C          /C=A(K), REAL
1250  5513          FGET I ANKAL
1251  6120          FFUT S          /S=A(5124-K), IMAGINARY
1252  0000          FEXT
1253  1107          TAD K
1254  7450          SNA             /K 0 ?
1255  5262          JMP .+5
1256  7041          CIA             /NO
1257  1105          TAD FS12
1260  7440          SZA CLA         /K=512 ?
1261  5264          JMP .+4         /NO JUMP
```

```
1262  4122          DCA S           /K=0 OR 512, SET S 0
1263  3121          DCA S#1
1264  3122          DCA S#2
1265  4407          FENTER
1266  3115          FDLT I
1267  0001          SORF
1270  6113          FFUT T
1271  5140          FGET S
1272  0001          SORE
1273  1113          FADD T
1274  0002          SORRT           /MODULUS
1275  6512          FFUT I ANI      /A(K)=SQROOT(I **2 +
1276  0000          FEXT
1277  4477          JMS I LAST      /K=512, ?
1300  5236          JMP POWER       /NO, CONTINUE
1301  1037          TAD FSPCTR      /FIRST SPECTRUM ?
1302  1036          TAD NSPCTR
1303  7650          SNA CLA
1304  5333          JMP NEXT        /YES, WRITE ON L TAPE
1305  3107          DCA K           /NO, MOVE DATA
1306  4476  MOVE,   JMS I INITL
1307  4407          FENTER
1310  5512          FGET I ANI
1311  6510          FFUT I ADJ      /A(K)=FSTORE) A(K)
1312  0000          FEXT
1313  4477          JMS I LAST      /K 512 ?
1314  5306          JMP MOVE        /NO, CONTINUE
1315  1061          TAD MIN8        /YES, READ PREVIOUS
1316  4532          JMS I RDTAPE    /SUM FROM L TAPE
1317  1061          TAD MIN8
1320  4533          TAD I BLNTP
1321  3533          DCA I BLNTP     /TPBLK-8
1322  3107          DCA K
1323  4476  ADD,    JMS I INITL
1324  4407          FENTER
1325  5512          FGET I ANI
1326  1510          FADD I ADJ
1327  6511          FFUT I ANI      /A(K) A(K)+SUM(K)
1330  0000          FEXT
1331  4477          JMS I LAST      /K 512 ?
1332  5323          JMP ADD         /NO, CONTINUE
1333  7001  NEXT,   CLA IAC
1334  1036          TAD NSPCTR      /NSPCTR  1 ?
1335  7640          SZA CLA
1336  5343          JMP .+5         /NO
1337  7344          STA CLL RAL     /YES
1340  1024          TAD NI          /NI-2 ?
1341  7640          SZA CLA
1342  5760          JMP I RATIO1    /NO, CALCULATE FREQ,
1343  1061          TAD MIN8        /YES, WRITI
1344  4531          JMS I WRTAPE    /ON L TAPE
1345  7344          STA CLL RAL
1346  1023          TAD NB          /NB-2 ?
1347  7640          SZA CLA
1350  5362          JMP NXT         /NO
1351  2022          ISZ RUN         /YES, READ AND
1352  5463          JMP I BCKGR     /TRANSFORM BACKGR
1353  7344          STA CLL RAL
1354  3022          DCA RUN         /RUN  2
1355  1036          TAD NSPCTR      /LAST SPECTRUM ?
1356  5462          JMP I SAME      /NO,READ NEXT SAMPLE
1357  5761          JMP I NXTS      /CALCULATE RATIO
1360  1412  RATIO1, RATIO 1
1361  1404  NXT3,   NXT
1362  1024  NXT,    TAD NI
1363  1022          TAD RUN         /RUN  NI ?
1364  7640          SZA CLA
1365  5377          JMP NXT1
1366  1036          TAD NSPCTR      /YES, LAST SAMPLE ?
1367  5462          JMP I SAME      /NO, CONTINUE
1370  1035          TAD BNK         /YES
1371  3037          DCA FSPCTR      /FSPCTR=BNK
1372  1027          TAD FSPCTR
1373  7041          CIA
1374  3036          DCA NSPCTR      /NSPCTR -PSPCTR
1375  2022          ISZ RUN
1376  5463          JMP I BCKGR     /READ FIRST BACKGR
1377  1061  NXT1,   TAD MIN8
1400  1533          TAD I BLNTP
1401  3533          DCA I BLNTP     /TPBLK=TPBLK-8
1402  1036          TAD NSPCTR      /LAST BACKGR ?
1403  5463          JMP I BCKGR     /NO,CONTINUE
 404  0036  NXT2,   TAD TPFRST
1405  1533          TCA I BLNTP
1406  1061          TAD MIN8
1407  7104          CLL RAL
1410  4532          JMS I RDTAPE    /READ SAMPLE AND BACKGR,
1411  7700          CLA
1412  3107          DCA K
1413  4476  RATIO,  JMS I INITL
1414  7344          STA CLL RAL
1415  1024          TAD NI          /IF NI=1, CALCULATE
1416  7640          SZA CLA         /FREQUENCY
1417  5235          JMP FREQ
1420  4407          FENTER
1421  5512          FGET I ANI      /CALCULATE RATIO
1422  6510          FDIV I ADJ      /A(K)=
1423  6512          FFUT I ANI      /A(K)/A(K+FSTORE)
1424  0000          FEXT
1425  1107  FREQ,   TAD K          /CALCULATE FREQUENCY
1426  4543          JMS I FLOAT
1427  4407          FENTER
1430  3041          FMFY DELF
1431  6510          FFUT I ADJ      /A(K+FSTORE)=DELF*FLOAT(K)
1432  0000          FEXT
1433  4477          JMS I LAST      /K 512 ?
1434  5213          JMP RATIO       /NO, CONTINUE
1435  7344          STA CLL RAL
1436  1024          TAD NI
1437  7640          SZA CLA         /IF NI-2, WRITE RATIO
1440  5443          JMP .+3         /ON L-TAPE
1441  1061          TAD MIN8
1442  4531          JMS I WRTAPE

1443  4407          FENTER
1444  5047          FGET RES
1445  1047          FADD RES        /CALCULATE
1446  1047          FADD RES        /RESOLUTION,
1447  6047          FFUT RES        /RES-3*RES
1450  6030          FPUT FLOW       /FLOW-RES
1451  0000          FEXT
1452  1105          TAD P512
1453  4543          JMS I FLOAT
1454  4407          FENTER
1455  3041          FMPY DELF
1456  6033          FPUT FHIGH      /FHIGH 512*DELF
1457  0000          FEXT
1460  7344          STA CLL RAL
1461  1024          TAD NI
1462  7640          SZA CLA         /NI-2 ?
1463  5330          JMP DIRCT
1464  4404          WRITE           /YES
1465  3373          MES623          /PLOT
1466  4404          WRITE           /SAMPLE AND
1467  3504          MES62           /BACKGROUND ?
1470  4537          JMS I ANSWER
1471  1140          TAD ANSWR
1472  1060          TAD MINYES
1473  7640          SZA CLA
1474  5312          JMP DIRECT      /NO-PLOT RATIO
1475  1056          TAD TPFRST      /YES
1476  3533          DCA I BLNTP
1477  1061          TAD MIN8        /READ SAMPLE
1500  4532          JMS I RDTAPE    /FROM L-TAPE
1501  4472          JMS I NORM1     /NORMALIZE
1502  4466          JMS I SFELT     /PLOT SCALES
1503  4467          JMS I SFELT     /PLOT SAMPLE
1504  1061          TAD MIN8
1505  4531          JMS I RDTAPE    /READ BACKGROUND
1506  4472          JMS I NORM1     /NORMALIZE
1507  4467          JMS I SFELT     /PLOT
1510  1061          TAD MIN8        /READ RATIO SPECTRUM
1511  4532          JMS I RDTAPE    /FROM L TAPE
1512  4471  DIRECT, JMS I MAX11    /FIND MAXIMUM
1513  5321          JMP DIRCT+1
1514  0007  HNDRD,  0007           /100
1515  3100          3100
1516  0000          0000
1517  1601  PLOTS1, PLOTS2
1520  4472  DIRCT,  JMS I NORM1     /IF NI-1, NORMALIZE
1521  4404          WRITE
1522  3732          MFSG28          /*FLOW*
1523  4407          FENTER
1524  5030          FGET FLOW
1525  0012          OUTPUT
1526  0040          40              /PRINT FLOW
1527  0000          FEXT
1530  4404          WRITE
1531  3736          MESG29          /*FHIGH*
1532  4407          FENTER
1533  5033          FGET FHIGH
1534  0012          OUTPUT
1535  0040          40              /PRINT FHIGH
1536  0000          FEXT
1537  4404          WRITE
1540  3652          MESG18          /*MAXIMUM(IN %):*
1541  4407          FENTER
1542  5036          FGET MAX
1543  3314          FMFY HNDRD
1544  0012          OUTPUT
1545  0030          30              /PRINT MAX
1546  0000          FEXT
1547  4546          JMS I FCRLF
1550  7201          CLA IAC
1551  3022  PLOTS,  DCA RUN
1552  4404          WRITE           /NEW FREQ.LIMITS ?
1553  3715          MES627
1554  4537          JMS I ANSWER
1555  1140          TAD ANSWR
1556  1060          TAD MINYES
1557  7640          SZA CLA
1560  5717          JMP I PLOTS1    /NO
1561  4404          WRITE           /YES
1562  3732          MFSG28          /*FLOW*
1563  4541          JMS I SIGNV     /INPUT
1564  4543          JMS I FLOAT
1565  4407          FENTER
1566  6030          FFUT FLOW
1567  0000          FEXT
1570  4404          WRITE           /*FHIGH*
1571  3736          MES629
1572  4541          JMS I SIGNV     /INPUT
1573  4543          JMS I FLOAT
1574  4407          FENTER
1575  6033          FFUT FHIGH
1576  0000          FEXT
1577  4546          JMS I FCRLF
1600  2022          ISZ RUN
1601  4404  PLOTS2, WRITE           /*NEW MAXIMUM ?*
1602  3641          MES617
1603  4537          JMS I ANSWER
1604  1140          TAD ANSWR
1605  1060          TAD MINYES
1606  7640          SZA CLA
1607  5222          JMP SM          /NO
1610  4404          WRITE           /YES
1611  3652          MESG18          /*MAXIMUM(IN %):*
1612  4541          JMS I SIGNV     /INPUT
1613  4543          JMS I FLOAT
1614  4407          FENTER
1615  3243          FMFY HNDR
1616  6036          FFUT MAX
1617  0000          FEXT
1620  4546          JMS I FCRLF
1621  2022          ISZ RUN
1622  4404  SM,     WRITE           /*SMOOTHE ?*
1623  3743          MESG30
```

```
1634  4537          JMS I ANSWER
1635  1140          TAD ANSWR
1636  1040          TAD MINYES
1637  7640          SZA CLA
1640  5235          JMP .+3             /NO, START PLOT
1641  4473          JMS I SMTH1         /YES! SMOOTHE
1642  2032          ISZ RUN
1643  1032          TAD RUN
1644  7650          SNA CLA
1645  5646          JMP I BEGN
1646  4466          JMS I SCALE         /PLOT SCALES
1647  4465          JMS I RESNR         /PLOT NR AND RES
1650  4467          JMS I SPECT         /PLOT SPECTRUM
1651  5642          JMP I .+1
1652  1551          FLOTS
1653  7777  HNDR,   7772                /0.01
1654  2436          2436
1655  5605          5605
1656  3361  BEGN,   BEGIN
                    #1634
                /FAST FOURIER TRANSFORM.
1657  0000  FFT,    0
1660  4312          JMS FLTFMT          /PERMUTE TO COMPLEX
1661  4462          JMS I MAINR         /DO FFT
1662  4461          JMS I UNSCRL        /UNSCRAMBLE
1663  5657          JMP I FFT           /EXIT
1664  7700  UNSCRL, UNSCRM
1665  7000  MAINR,  MAIN
                /SUBROUTINE TO FIND FLOATING ADDRESSES OF
                /A(J),A(512+J),A(K), AND A(512+K)
1666  0000  SETLOC, 0
1667  1106          TAD J
1670  4303          JMS INDEX
1671  3110          DCA AJL             /ADDRESS OF A(J)
1672  1102          TAD P512
1673  1106          TAD J
1674  4303          JMS INDEX
1675  3111          DCA AJHL            /ADDRESS OF A(512+J)
1676  1107          TAD K
1677  4303          JMS INDEX
1700  3112          DCA AKHL            /ADDRESS OF A(512+K)
1701  5665          JMP I SETLOC        /EXIT
                /SUBROUTINE TO FIND FLOATING ADDRESS OF A(C(AC))
1702  0000  INDEX,  0
1703  4311          DCA INXSTR
1704  1311          TAD INXSTR
1705  7104          CLL RAL
1706  1311          TAD INXSTR
1707  5703          JMP I INDEX
1710  0000  INXSTR, 0
                /SUBROUTINE TO BIT REVERSE PERMUTE 1024
                /FLOATING DATA
1711  0000  FLTFMT, 0
1712  7345          CLA STL IAC RTR
1713  7001          IAC
1714  7001          IAC
1715  7001          IAC                 /1022 DATA
1716  3372          DCA CTR1            / NO.OF DATA
1717  7401          CLA IAC
1720  3106          DCA J
1721  1106  FMTNXT, TAD J
1722  3350          DCA FLP1
1723  1377          TAD F10
1724  7041          CIA
1725  3373          DCA CTR2            /10 BITS TO BE REV.
1726  3351  FLFLOP, DCA FLP2
1727  1350          TAD FLP1
1730  7110          CLL RAR             /READ J FROM K TO L
1731  3350          DCA FLP1
1732  1351          TAD FLP2
1733  7004          RAL                 /BUILD K FROM L TO R
1734  2373          ISZ CTR2            /HAVE ALL BITS BEEN REV.
1735  5326          JMP FLFLOP          /NO-NEXT
1736  3107          DCA K               /K BIT REVERSED J
1737  1107          TAD K
1740  7041          CIA
1741  1106          TAD J
1742  7210          SZA CLA             /IS K J ?
1743  4352          JMS FLTMOV          /YES SWITCH DATA J,K
1744  2106          ISZ J               /NEXT J
1745  2372          ISZ CTR1            /HAVE ALL DATA BEEN DONE
1746  5321          JMP FMTNXT          /NO NEXT
1747  5712          JMP I FLTFMT        /EXIT
1750  0000  FLP1,   0
1751  0000  FLP2,   0
                /SUBROUTINE TO SWITCH DATA A(J) AND A(K)
1752  0000  FLTMOV, 0
1753  1106          TAD J
1754  4303          JMS I INDEXI
1755  3110          DCA AJL             /ADDRESS OF A(J)
1756  1107          TAD K
1757  4303          JMS I INDEXL
1760  3113          DCA AKL             /ADDRESS OF A(K)
1761  4407          FENTER
1762  5512          FGET I AKL
1763  6374          FFUT T3             /T3=A(K)
1764  5510          FGET I AJL
1765  6512          FFUT I AKL          /A(K)=A(J)
1766  5374          FGET T3
1767  6510          FFUT I AJL          /A(J)=T3
1770  0000          FEXT
1771  5752          JMP I FLTMOV        /EXIT
1772  0000  CTR1,   0
1773  0000  CTR2,   0
1774  0000  I3,     0
1775  0000          0
1776  0000          0
1777  0012  F10,    12
                    #2000
                /SUBROUTINE TO TRANSFORM 512 FLOATING-POINT
                /COMPLEX DATA.
2000  0000  MAIN,   0
2001  7201          CLA IAC
2002  3366          DCA DJ              /START WITH DJ=1
2003  1275          TAD P9
2004  7041          CIA
2005  3367          DCA MINF            /9 INTERMEDIATE TRANS.
2006  4304  PLOOP,  JMS LOOP1          /SET UP FOR INT. TRANS.
2007  3370          DCA L               /L=0
2010  1114          TAD H
2011  7041          CIA
2012  3371          DCA MINL            /H PART./INT.
2013  1370  LLOOP,  TAD L
2014  3106          DCA J               /J=L
2015  1106  JLOOP,  TAD J
2016  1114          TAD H
2017  3107          DCA K               /K=J+H
2020  4674          JMS I SETLOP        /GET ADDRESSES
2021  4407          FENTER
2022  5513          FGET I ANFNL
2023  3120          FMFY S
2024  6276          FFUT D1
2025  5512          FGET I AKL
2026  3115          FMFY C
2027  1276          FADD D1
2030  6276          FFUT D1             /D1=C*A(K)+S*A(512+K)
2031  5512          FGET I AKL
2032  3120          FMPY S
2033  6301          FFUT E1
2034  5513          FGET I ANFNL
2035  3115          FMFY C
2036  2301          FSUB E1
2037  6301          FFUT E1             /E1=C*A(512+K)-S*A(K)
2040  5510          FGET I AJL
2041  2276          FSUB D1
2042  6512          FFUT I AKL          /A(K)=A(J)-D1
2043  5511          FGET I ANFJL
2044  2301          FSUB E1
2045  6513          FFUT I ANFKL        /A(512+K)=A(512+J)-E1
2046  5510          FGET I AJL
2047  1276          FADD D1
2050  6510          FFUT I AJL          /A(J)=A(J)+D1
2051  5511          FGET I ANFJL
2052  1301          FADD E1
2053  6511          FFUT I ANFJL        /A(512+J)=A(512+J)+E1
2054  0000          FEXT
2055  1106          TAD J
2056  1366          TAD DJ
2057  3106          DCA J               /J=J+DJ
2060  1106          TAD J
2061  7041          CIA
2062  1104          TAD P511
2063  7700          SMA CLA             /IS J 511 ?
2064  5215          JMP JLOOP           /NO-NEXT PASS OF PART.
2065  2371          ISZ MINL            /YES-ARE ALL PART.S DONE
2066  5272          JMP MOREL           /NO-NEXT PARTIAL
2067  2367          ISZ MINF            /YES-ARE ALL INT.S DONE
2070  5206          JMP FLOOP           /NO NEXT INTERMEDIATE
2071  5600          JMP I MAIN          /YES-EXIT
2072  4340  MOREL,  JMS SETUPL          /SET UP FOR NEXT PARTIAL
2073  5213          JMP LLOOP
2074  1663  SETLOP, SETLOC
2075  0011  F9,     11
2076  0000  D1,     0
2077  0000          0
2100  0000          0
2101  0000  E1,     0
2102  0000          0
2103  0000          0
                /SUBROUTINE TO SET UP FOR INTERMEDIATE TRANSFORM
2104  0000  LOOP1,  0
2105  1366          TAD DJ
2106  3114          DCA H               /H=DJ
2107  1366          TAD DJ
2110  7104          CLL RAL
2111  3366          DCA DJ              /DJ=2*DJ
2112  1114          TAD H
2113  4543          JMS I FLOAT
2114  4407          FENTER
2115  6372          FPUT R4
2116  5100          FGET PI
2117  4372          FDIV R4
2120  6372          FFUT R4             /R4=PI/H
2121  0004          COS
2122  6123          FFUT T              /T=COS(R4)
2123  5372          FGET R4
2124  0003          SIN
2125  6126          FFUT V              /V=SIN(R4)
2126  0000          FEXT
2127  7201          CLA IAC
2130  3115          DCA C
2131  7132          STL RTR
2132  3116          DCA C+1
2133  3117          DCA C+2             /C=1
2134  3120          DCA S
2135  3121          DCA S+1
2136  3122          DCA S+2
2137  5704          JMP I LOOP1         /EXIT
                /SUBROUTINE TO SET UP FOR INTERMEDIATE PARTIAL
                /TRANSFORM EXCEPT FOR FIRST ONE
2140  0000  SETUPL, 0
2141  4407          FENTER
2142  5115          FGET C
2143  6371          FFUT R4             /R4=C
2144  5120          FGET S
2145  3126          FMFY V
2146  6115          FFUT C
2147  5372          FGET R4
2150  3123          FMFY T
2151  2115          FSUB C
2152  6115          FFUT C              /C=R4*T-S*V
2153  5120          FGET S
2154  3123          FMFY T
```

```
2155  6120          FPUT S
2156  5372          FGET R4
2157  4746          FMFY V
2160  1120          FADD S
2161  6120          FPUT S              /S=S*T+R4*V
2162  0000          FEXT
2163  2370          ISZ L               /L=L+1
2164  7000          NOP
2165  5740          JMP I SETUPL        /EXIT
2166  0000  DJ,     0
2167  0000  MINP,   0
2170  0000  L,      0
2171  0000  MINL,   0
2172  0000  R4,     0
2173  0000          0
2174  0000          0
                    *2200
              /SUBROUTINE TO UN-SCRAMBLE COEFFICIENTS
2200  0000  UNSCRM, 0
2201  4730          JMS SETUFF          /DO A(0),A(512)
2202  1105          TAD P512            /SET UP REST
2203  7110          CLL RAR
2204  7041          CIA
2205  7001          IAC
2206  3114          DCA N               /255 ITERATIONS
2207  7201          CLA IAC
2210  3106          DCA J               /START WITH J 1
2211  4771  UNLOOP, JMS LOOP4          /UN-SCRAMBLE
2212  2106          ISZ J               /NEXT J
2213  2114          ISZ N               /IS SCRAMBLING DONE
2214  5211          JMP UNLOOP          /NO NEXT
2215  2361          ISZ FN              /YES DO A(256),A(768)
2216  4773          JMS I SETLOL
2217  4407          FENTER
2220  5510          FGET I AJL
2221  7361          FMFY FN
2222  6510          FPUT I AJL
2223  5511          FGET  ANFJL
2224  7361          FMFY FN
2225  6511          FPUT I ANFJL
2226  0000          FEXT
2227  5600          JMP I UNSCRM        /EXIT
              /SUBROUTINE TO UN-SCRAMBLE A(0),A(512), AND
              /SET UP FOR REST
2230  0000  SETUFF, 0
2231  1105          TAD P512
2232  4543          JMS I INDEXL
2233  3112          DCA ANL             /ADDRESS OF A(512)
2234  3555          DCA STORE
2235  1105          TAD P512
2236  4543          JMS I FLOAT
2237  4407          FENTER
2240  6161          FPUT FN             /FN=512
2241  5455          FGET I STOKE
2242  6173          FPUT T              /T A(0)
2243  1512          FADD I ANL
2244  4361          FIDV FN
2245  6455          FPUT I STORE        /A(0)=(A(0)+A(512))/2
2246  5123          FGET T
2247  2512          FSUB I ANL
2250  4361          FIDV FN
2251  6512          FPUT I ANL          /A(512)=(T-A 512))/512
2252  5100          FGET FI
2253  4361          FDIV FN
2254  6373          FPUT FS             /FS=FI/512
2255  0004          COS
2256  6173          FPUT T              /T=COS(FS)
2257  6115          FPUT C              /C=T
2260  5372          FGET FS
2261  0003          SIN
2262  6126          FPUT V              /V=SIN(FS)
2263  6120          FPUT S              /S=V
2264  5351          FGET ZPS
2265  4361          FDIV FN
2266  6361          FPUT FN             /FN=1/1024
2267  0000          FEXT
2270  7630          JMP I SETUFF        /EXIT
              /SUBROUTINE TO DO ACTUAL UN SCRAMBLING
2271  0000  LOOP4, 0
2272  1106          TAD J
2273  7041          CIA
2274  1105          TAD P512
2275  3107          DCA K               /K=512-J
2276  4755          JMS I SETLOL        /GET ADDRESSES
2277  4407          FENTER
2300  5511          FGET I ANFJL
2301  1513          FADD I ANFKL
2302  6177          FPUT R5
2303  3115          FMFY C
2304  6164          FPUT D5             /D5 C*R5
2305  5375          FGET R5*
2306  7120          FMFY S
2307  6375          FPUT R5             /R5=S*R5
2310  5510          FGET I AJL
2311  2512          FSUB I ANL
2312  6356          FPUT Q              /Q=A(J)-A(K)
2313  3115          FMFY C
2314  1375          FADD R5
2315  6167          FPUT E5             /E5=C*Q+R5
2316  5356          FGET Q
2317  3120          FMFY S
2320  2364          FSUB D5
2321  6356          FPUT Q              /Q=S*Q-D5
2322  5510          FGET I AJL
2323  1512          FADD I ANL
2324  6512          FPUT I ANL          /A(K) A(J)+A(K)
2325  2356          FSUB Q
2326  3361          FMFY FN
2327  6510          FPUT I AJL          /A(J) (A(K) Q)*FN
2330  5512          FGET I ANL
2331  1356          FADD Q
2332  3361          FMFY FN
2333  6512          FPUT I ANL          /A(K)=(A(K)+Q)*FN
2334  5511          FGET I ANFJL
2335  2513          FSUB I ANFKL
2336  6511          FPUT I ANFJL        /A(J)=(A(J)
2337  1367          FADD E5             /   A(J)+E5) A(J+K)
2340  3361          FMFY FN
2341  6513          FPUT I ANFKL        /A(K)=(A(J)-
2342  5367          FGET E5             /   (A(J)+E5))*FN
2343  2511          FSUB I ANFJL
2344  3361          FMFY FN
2345  6511          FPUT I ANFJL        /A(J)=
2346  0000          FEXT                /   (A(J)+A(K))*FN
2347  4754          JMS I SETUFL        /SET UP FOR NEXT GROUP
2350  5671          JMP I LOOP4         /EXIT
2351  0000  P5,     0000
2352  2000          2000
2353  0000          0000
2354  2140  SETULL, SETUFL
2355  1663  SETLOL, SETLOL
2356  0000  Q,      0
2357  0000          0
2360  0000          0
2361  0000  FN,     0
2362  0000          0
2363  0000          0
2364  0000  D5,     0
2365  0000          0
2366  0000          0
2367  0000  E5,     0
2370  0000          0
2371  0000          0
2372  0000  S,      0
2373  0000          0
2374  0000          0
2375  0000  R5,     0
2376  0000          0
2377  0000          0
                    *2400
              /NORMALIZE ALGORITHM.
2400  0000  NORM,   0
2401  4773          JMS I MAXL          /DETERMINE MAX.
2402  3107          DCA K
2403  1107          TAD K
2404  4503          JMS I INDEXL
2405  3112          DCA ANL
2406  4407          FENTER
2407  5512          FGET I ANL
2410  4036          FDIV MAX
2411  6512          FPUT I ANL          /A(K) A(K)/MAX
2412  0000          FEXT
2413  4477          JMS I LAST          /A 512 ?
2414  5205          JMP NORM+3          /NO, CONTINUE
2415  7201          CLA IAC             /YES, MAX 1
2416  3036          DCA MAX
2417  7152          SPA CLA
2420  3037          DCA MAX+1
2421  3040          DCA MAX+2
2422  5600          JMP I NORM
              /DETERMINE MAXIMUM AMPLITUDE
2423  0000  MAXL,   0
2424  7300          CLA
2425  3036          DCA MAX
2426  3037          DCA MAX+1
2427  3040          DCA MAX+2           /SET MAX 0
2430  3107          DCA K
2431  4556  MAX1,   JMS INIT
2432  4407          FENTER
2433  5510          FGET I AJL
2434  0000          FEXT
2435  4477          JMS I LIMIT         /DATA BETWEEN
2436  7440          SZA CLA             /FREQUENCY LIMITS ?
2437  5253          JMP MAX2            /NO GET NEXT
2440  4407          FENTER              /YES
2441  5512          FGET I ANL
2442  4036          FSUB MAX
2443  0000          FEXT
2444    60          TAD HORD            /A(K) MAX
2445  7710          SPA CLA
2446  5253          JMP MAX2            /NO GET NEXT
2447  4407          FENTER
2450  5512          FGET I ANL
2451  6036          FPUT MAX            /MAX A(K)
2452  0000          FEXT
2453  4477  MAX2,   JMS I LAST          /A 512 ?
2454  7751          IMP MAX1            /NO, CONTINUE
2455  5624          JMP I MAX1
              /FIND FLOATING ADDRESS OF A(K) AND A(K+1)STORE)
2456  0000  INIT,   0
2457  1107          TAD K
2460  4503          JMS I INDEXL
2461  3112          DCA ANL
2462  1113          TAD ANL
2463  1071          TAD FSTORE
2464  3110          DCA AJL
2465  5656          JMP I INIT
              /ALL 512 DATA POINTS DONE ?
2466  0000  LST,    0
2467  2107          ISZ K
2470  1107          TAD K
2471  7041          CIA
2472  1105          TAD P512            /A 512 ?
2473  7710          SPA CLA
2474  5266          JMP I LST           /YES
2475  5666          JMP I LST
2476  0002  TWO,    0002                /2
2477  0000          2000
2500  0000          0000
2501  0004  TEN,    0004                /10
2502  2400          2400
2503  0000          0000
2504  0005  TWENTY, 0005                /20
2505  2400          2400
2506  0000          0000
2507  0006  FIFTY,  0006                /50
```

```
                3100
                0000
                /SUBROUTINES TO PLOT THE SPECTRUM.
                /1:PLOT THE SCALES.
0010  4455  MSTART, /455              / S
0011  0006  F45,    0006             /45
0012  2640          2640
0013  0000          0000
0014  3664  DELTA,  DFL
0015  5770          JMP I SCFLOT
0016  0000  SCFLOT, 0
0017  4404          WRITE            /START PLOT ?
0020  3674          MES674
0021  4537           MS I ANSWR
0022  1140           TAD ANSWR
0023  7312           AC MSTART
0024  7640          SZA CLA
0025  5243           JMP   4
0026  4407          FENTER
0027  0006           /DFO
0030  4405          FGF  FHIGH
0031  2030          FSUB FLOW
0032  6116          FFLT  V          /V FHIGH FLOW
0033  0000          FEXT
0034  7240          STA
0035  4405           LOT             /INITIALIZE.
0036  7201           IA IAC
0037  4405          FLOT             /PLOT AXES.
0040  0170          0170
0041  0060          0060
0042  7700          CLA
0043  4405           OT
0044  0120          0120
0045  4620          4620
0046  7700          CLA
0047  4403          PLOT
0050   544          2544
0051  4620          4620
0052  7700          CLA
0053  4405          PLOT
0054   544          2544
0055  0060          0060
0056  7700          CLA
0057  4403          PLOT
0060  0120          0120
0061  0060          0060
0062  7701          CLA IAC          /SET TYPE PLOT FLAG
0063  6134          DCA TYPEPLT      /TO PLOT.
0064  7157          CLL IAC RTL      /4
0065  3163          DCA SIZE         /SET SIZE.
0066  7001          IAC
0067  3154          DCA ORIENT       /SET ORIENTATION
0070  4407          FENTER
0071  0115          FGET E
0072  6115          FPUT V
0073  0000          FEXT
0074  1316          TAD DELTA
0075  30            DCA I STORE      /(STORE) ADDR(TWO)
0076  4407  ILL,    FENTER
0077  0111          FGET C
0100  6116          FPUT V
0101  0000          FEXT
0102  1140          TAD HORD
0103  7210          SZA CLA          /V C /
0104  7411          JMP .+3
0105  1430          TAD I STORE      /YES, INTERVAL C(STORE)
0106  7410          JMP SCALE1
0107  4407          FENTER           /NO
0110  0115          FGET E
0111  5664          FMPY I DEL
0112  6115          FPUT C           /C 2*C
0113  0000          FEXT
0114  0030          ISZ STORE        /(STORE) NEXT ADDRESS
0115  7000          JMP SCI
0116  3114  SCALE1, DCA H            /H INTERVAL
0117  3110          DCA S
0120  3111          DCA SH1
0121  3112          DCA SH2
0122  4407          FENTER           /PLOT FREQUENCY SCALE
0123  0110          FGET S
0124  1314          FADD I H         /ADD INTERVAL
0125  6110          FPUT S
0126  0000          FEXT
0127  4470          JMS I  1M1
0130   640          SZA   A
0131  5301          JMP  5 SCL2
0132  4700          JM  I Y JMP1
0133  3 11          DCA .+4
0134  7001          IAC
0135  4403          PLOT             /PLOT MARK
0136  0170          0170
0137  0000          0000
0140  7200          CLA
0141  1341          TA  . 2
0142  3342          DCA .+3
0143  4303          FLT1
0144  0147          CLL?
0145  0000          0000
0146   100          CLA
0147  1324          TAC F40
0150  3110          DCA ASCIX
0151   124          TAD . 4
0152  1324          TAC F40
0153  3111          DCA ASCIY
0154   440          FENTER
0155  0170          FGET S
0156  0013          OUTPUT           /PLOT NUMBER
0157  0030          30
0160  0000          FEXT
0161  5774          JMP SCALE1+4
0162  0426  DEL,    TWO              /2
0163  0 35          FIVE             /
0164  2501          TEN              /10
0165  0144          TWENTY           /20
0166  2507          FIFTY            /50
0167  0200  DELT,   TENTH            /0.1
0170  1643          HNDR             /0.01
0171  0022  F18,    0022             /18
0172  0050  F40,    0050             /40
0173  1130  P600,   1130             /600
0174  4770  F4770,  4770
0175  3070  XCORD1, XCOORI
0176  3100  YCORD1, YCOORD
0177  4407  SCALE2, FENTER
0200  5043          FGET FHIGH
0201  3170          FSUB S
0202  0000          FEXT
0203  1160          TAD HORD
0204  7700          SMA CLA
0205  5224          JMF SCALE1+4
0206  3150          DCA ASCIX
0207  1225          TAD F600
0210  3151          DCA ASCIY
0211  4404          WRITF            /"FREQUENCY (CM )"
0212  3161          MES025
0213  1150          TAD ASCIX
0214  1273          TAD F18
0215  3150          DCA ASCIX
0216  1151          TAD ASCIY
0217  1274          TAD F40
0220  3151          DCA ASCIY
0221  7105          C   IAC RAL      /2
0222  3153          DCA SIZE
0223  4404          WRITF            /"-1"
0224  3171          MES026
0225  7307          CLA CLL IAC RTL /4
0226  3163          DCA SIZE
0227  3120          DCA S            /PLOT AMPL. SCALE
0230  3121          DCA SH1
0231  3122          DCA SH2
0232  4407          FENTER
0233  5036          FGET MAX
0234  2671          FSUB I DELT
0235  0000          FEXT
0236  1160          TAD HORD
0237  7700          SMA CLA          /MAX 0.1 ?
0240  5245          JMF .+3          /NO
0241  1277          TAD DELT+1       /YES, INTERVAL-0.01
0242  7410          SKP
0243  1 71          TAD DELT         /NO, INTERVAL-0.1
0244  3114          DCA H            /H INTERVAL
0245  4407  SCALE4, FENTER
0246  0110          FGET S
0247  0000          FEXT
0250  4677          JMS I XCORD1
0251  3356          DCA .+3
0252  7001          IAC
0253  4403          PLOT             /PLOT MARK
0254  0000          0000
0255  4606          4606
0256  7200          CLA
0257  1376          TAD F4770
0260  3151          DCA ASCIY
0261  1364          TAD . 5
0262  3150          DCA ASCIX
0263  4407          FENTER
0264  5120          FGET S
0265  0013          OUTPUT           /PLOT NUMBER
0266  0032          32
0267  5130          FGET S
0270  1314          FADD I H         /ADD INTERVAL
0271  6170          FPUT S           /S S+H
0272  2036          FSUB MAX
0273  0000          FEXT
0274  1160          TAD HORD
0275  7750          SPA SNA CLA      /S MAX ?
0276  5614          JMP I SCALE5     /NO-CONTINUE
0277  4407          FENTER           /YES
0300  0007          FCDF1
0301  0000          FEXT
0302  5615          JMF I SCFLT2     /EXIT
0303  7517  SCFLT2, SCPLOT-1
0304   747  SCALE5, SCALE4
                /:PLOT SPECTRUM.
0305  0000  SPFLOF, 0
0306  7700          CLA
0307  3107          DCA A
0310  3114          DCA H
0311  4476  PLTSF,  JMS I INITL
0312  4407          FENTER           /Y-COORDINATE
0313  5510          FGET I ADL
0314  0000          FEXT
0315  4470          JMS I  1M1       /BETWEEN FREQ.LIMITS ?
0316  7640          SZA   A
0317  5357          JMF YCORD+2      /NO, SKIP
0320  4300          JMS YCOORD
0321  3255          DCA Y  ND
0322  4407          FENTER
0323  5036          FGET MAX
0324  7510          FSUB I ANL
0325  0000          FEXT
0326  1160          TAD HORD
0327  7700          SMA CLA          /DATA MAX ?
0330  5243          JMF  +3
0331  3114          DCA H
0332  5357          JMF YCORD+2      /YES, SKIP
0333  4407          FENTER           /X COORDINATE
0334  5511          FGET I ANL
0335  0000          FEXT
0336  4470          JMS XCOORD
```

```
3047  3254           DCA XCOKD
3050  1114           TAD H
3051  7650           SNA CLA
3052  7001           IAC
3053  4403           FLOT
3054  0000  XCOKD,   0
3055  0000  YCOKD,   0
3056  2114           ISZ H
3057  4477           JMS I LAST        /K=512 ?
3060  5221           JMP PLTSP         /NO, CONTINUE
3061  3152           DCA TYPFLT        /SET TYPE-PLOT FLAG
3062  7001           IAC               /TO TYPE
3063  4403           FLOT              /NEW PAGE
3064  4160           4160
3065  0000           0000
3066  7300           CLA CLL
3067  5615           JMP I SPFLOT
3070  0000  XCOORD,  0                 /CALCULATE
3071  4407           FENTER            /X COORDINATE.
3072  4036           FDIV MAX
3073  3320           FMFY C1300
3074  0000           FEXT
3075  4323           JMS INT
3076  1314           TAD F80
3077  5670           JMP I XCOORD
3100  0000  YCOORD,  0                 /CALCULATE
3101  4407           FENTER            /Y COORDINATE.
3102  2030           FSUB FLOW
3103  4176           FDIV V
3104  3315           FMFY C2400
3105  2315           FSUB C2400
3106  0010           NEGATE
3107  0000           FEXT
3110  4323           JMS INT
3111  1313           TAD F48
3112  5700           JMP I YCOORD
3113  0060  F48,     0060
3114  0120  F80,     0120
3115  0014  C2400,   0014              /2400
3116  2260           2260
3117  0000           0000
3120  0013  C1300,   0013              /1300
3121  2424           2424
3122  0000           0000
      /CONVERT FL.PNT. TO UNSIGNED SINGLE-PREC SIGN
      /INTEGER.
3123  0000  INT,     0
3124  1160           TAD HORD
3125  7710           SPA CLA           / 0
3126  5723           JMP I INT         /YES, -0
3127  1161           TAD ORD           /NO
3130  7104           CLL RAL
3131  7200           CLA
3132  1160           TAD HORD
3133  7004           RAL
3134  3160           DCA HORD
3135  1157           TAD EXP
3136  1353           TAD M12           / 4095 ?
3137  7510           SPA
3140  5345           JMP .+5           /YES
3141  7640           SZA CLA           /NO,  4095 ?
3142  5723           JMP I INT         /YES,  0
3143  1160           TAD HORD          /NO,  4095
3144  5723           JMP I INT
3145  3157           DCA EXP
3146  1160           TAD HORD
3147  7110           CLL RAR
3150  2157           ISZ EXP
3151  5347           JMP .-2
3152  5723           JMP I INT
3153  7764  M12,     7764
      /TEXT-STRINGS FOR PLOT-ROUTINES.
3154  4040  MESG20,  4040
3155  2205           2205              /RE
3156  2340           2340              /S
3157  7600           7600              /
3160  7400  MESG21,  7400              /
3161  0622  MESG25,  0622              /FR
3162  0521           0521              /EQ
3163  2505           2505              /UE
3164  1603           1603              /NI
3165  3140           3140              /Y
3166  5003           5003              /(C
3167  1540           1540              /M
3170  5100           5100              /)
3171  5561  MESG26,  5561              / I
3172  0000           0000
                     *3200
      /SUBROUTINE TO SMOOTH THE SPECTRUM.
      /4-POINT SMOOTHING WITH POLYNOMIAL OF DEGREE 3.
3200  0000  SMOOTH,  0
3201  7200           CLA
3202  3107           DCA K
3203  3114           DCA H
3204  2107           ISZ K
3205  1107           TAD K
3206  4503           JMS I INDEXL
3207  3 4            DCA ANFJL
3210  2107           ISZ K
3211  4407           FENTER
3212  5514           FGET I H
3213  6120           FPUT S            /S A(0)
3214  5511           FGET I ANFJL
3215  6133           FPUT T            /T-A(1)
3216  0000           FEXT
3217  1107  SMTH,    TAD K
3220  4503           JMS I INDEXL
3221  3112           DCA AKL
3222  1107           TAD K
3223  7001           IAC
3224  4503           JMS I INDEXL
3225  3110           DCA AJL
3226  7326           CLA STL RTL
3227  1107           TAD K
3230  4503           JMS I INDEXL
3231  3113           DCA ANFKL
3232  4407           FENTER
3233  5120           FGET S
3234  6115           FPUT C
3235  5134           FGET T
3236  6120           FPUT S            /S-T
3237  5132           FGET I AKL
3240  6133           FPUT T            /T-A(K)
3241  2120           FSUB S
3242  2510           FSUB I AJL
3243  6126           FPUT V            /V-T-S A(K+1)
3244  1126           FADD V
3245  1123           FADD T
3246  6126           FPUT V            /V V+V+T
3247  1126           FADD V
3250  1115           FADD C
3251  1513           FADD I ANFKL
3252  6126           FPUT V            /V V+V+(A(K+2)
3253  0000           FEXT
3254  7344           STA CLL RAL
3255  1107           TAD K
3256  7640           SZA CLA           /K=2 ?
3257  5271           JMP SMTH2         /NO
3260  4407           FENTER            /YES
3261  3327           FMFY M1
3262  1115           FADD C
3263  6514           FPUT I H          /A(0)= C +.014285714V
3264  5126           FGET V
3265  3332           FMFY M7
3266  1170           FADD S
3267  6511           FPUT I ANFJL      /A(1)= S+.05714285V
3270  0000           FEXT
3271  4407  SMTH2,   FENTER
3272  5126           FGET V
3273  3335           FMFY M3
3274  1123           FADD T
3275  6511           FPUT I AKL        /A(K-1)=T+.085714285V
3276  0000           FEXT
3277  2107           ISZ K
3300  1104           TAD FS11
3301  7041           CIA
3302  1107           TAD K
3303  7640           SZA CLA           /K=31 ?
3304  5217           JMP SMTH          /NO, CONTINUE
3305  1107           TAD K             /YES
3306  4 03           JMS I INDEXH
3307  3114           DCA H
3310  2107           ISZ K
3311  1107           TAD K
3312  4503           JMS I INDEXH
3313  3111           DCA ANFJL
3314  4407           FENTER
3315  5126           FGET V
3316  3332           FMFY M7
3317  1514           FADD I H
3320  6514           FPUT I H          /A(31) A(31)+
3321  5126           FGET V            /    .05714 V
3322  3337           FMFY M1
3323  1511           FADD I ANFJL
3324  6511           FPUT I ANFJL      /A(30 ) A(31)
3325  0000           FEXT              /    .014285714V
3326  5600           JMP I SMOOTH      /EXIT
3327  7772  M1,      7772              /  .014285
3330  4257           4257
3331  4262           4262
3332  7774  M7,      7774              / .057144 A
3333  5520           5520
3334  5520           5520
3335  7775  M3,      7775              /-.085714
3336  5203           5203
3337  5703           5703
      /DATA BETWEEN FREQUENCY LIMITS ?
3340  0000  LIM,     0
3341  4407           FENTER
3342  6142           FPUT FAC1
3343  2040           FSUB I DM
3344  0000           FEXT
3345  1160           TAD HORD
3346  7510           SPA
3347  5740           JMP I LIM
3350  4407           FENTER
3351  5033           FGET FNTGH
3352  2162           FSUB FPAC1
3353  0000           FEXT
3354  1160           TAD HORD
3355  7510           SPA
3356  5740           JMP I LIM
3357  4407           FENTER
3360  5162           GET FLAG1
3361  0000           FEXT
3362  7740           JMP I LIM
3363  4404  BEGIN,   JWITE          /*MODEL
3364  3751           MES631            /    INTERFEROGRAM  **
3365  4537           JMS I ANSWER
3366  1140           TAD ANSWR
3367  0 60           TAD MINYES
3370  7640           SZA CLA
3371  7402           HLT
3372  5420           JMP I START1
3373  4737  MESG23,  4737
3374  2014           2014              /PL
3375  1724           1724              /OT
3376  4000           4000
                     *3400
      /SUBROUTINE TO PLOT NR AND RESOLUTION.
3400  0000  NRRES,   0
3401  1256           TAD I8
3402  3153           DCA SIZE          /SET SIZE
3403  1 67           TAD I3600         /SET COORDINATE
3404  31 3           DCA ADDIX
3405  1 60           TAD I4060
```

```
4406  3151          DLA ASCII
4407  4407          ENTER
4410  5744          GET NR
4411  0017          OUTPUT          /PLOT NR
4412  0057          52
4413  0000          FEXT
4414  4404          WRITE
4415  3154          MESG30          /*  RES  *
4416  7201          CLA IAC
4417  4403          PLOT
4420  3450          3450            /PLOT MARK
4421  3440          3440
4422  7400          CLA
4423  4403          PLOT
4424  1670          2670
4425  3440  RES1,    3440
4426  4407          ENTER
4427  5047          GET RES
4430  4136          FDIV V
4431  5261          IMFY M2400
4432  0030          FEXT
4433  4547          JMS I FIXR
4434  1052          TAD RES1
4435  1241          DLA .+4
4436  7001          IAC
4437  4403          PLOT
4440  3450          3450
4441  0000          0
4442  7300          CLA
4443  1241          TAD .-?
4444  3247          DLA .+4
4445  4403          PLOT
4446  2670          2670
4447  0000          0
4450  7400          CLA
4451  1247          TAD .-?
4452  3151          DLA ASCII
4453  4404          WRITE
4454  3160          MESG31          /* *
4455  6606          JMP I MARES     /EXIT
4456  0010  FR,     10
4457  2600  F 2600, 2600
4460  4400  F 4400, 4400
4461  0014  M 400,  0014            / 2400
4462  3450          3450
4463  0000          0000
4464  0000  NR,     0               /NR. OF SPECTRUM
4465  0000          0
4466  0000          0
                    /TEXT STRINGS,
4467  3737  MESG1,  3737
4470  3211          3211            / I
4471  1674          1674            /NT
4472  0517          0517            /EA
4473  0605          0605            /EL
4474  1142          1142            /AD
4475  1505          1505            /ME
4476  1405          1405            /IF
4477  1240          1240            /R
4500  0013          0013            /CS
4501  0015          2015            /EM
4502  3137          5137            /)
4503  0000          0000
4504  1501  MESG2,  1501            /SA
4505  1540          1540            /M
4506  4640          4640            /&
4507  0301          0301            /MA
4510  0313          0313            /CL
4511  0722          0722            /GA
4512  4077          4077            / ?
4513  4000          4000
4514  1623  MESG3,  1623            /NR
4515  7340          7 40            /
4516  0000          0000
4517  1716  MESG4,  1716            /ON
4520  0600          0600            /E
4521  2417  MESG5,  2317            /TW
4522  1700          1700            /O
4523  5001  MESG6,  5001            / B
4524  1714          1714            /OU
4525  1715          1715            /OM
4526  0574          0574            /ET
4527  0723          0523            /EA
4530  4013          4013            / S
4531  3123          3123            /YS
4532  1405          1405            /TE
4533  1547          1547            /M
4534  1501          1501            /SA
4535  1570          1570            /MP
4536  1411          1411            /CL
4537  1607          1607            /NG
4540  4011          4011            / I
4541  1674          1674            /NT
4542  0522          0522            /EA
4543  2601          2601            /VA
4544  1477          1477            /L:
4545  0000          0000
4546  4015  MESG8,  4015            / M
4547  1103          1103            /IC
4550  2217          2217            /RO
4551  1647          1647            /N
3552  0030          0000
4553  3723  MESG9,  3723            / S
4554  0115          0115            /AM
4555  2014          2014            /EL
4556  0572          0572            /E:
4557  4000          4000
4560  3702  MESG10,  3702           / B
4561  0103          0103            /AI
4562  1307          1307            /KG
4563  2127          227             /R:
4564  4000          4000
4565  4040  MESG11,  4040
```

```
4566  4040          4040
4567  4040          4040
4570  4040          4040
4571  4040          4040
4572  4040          4040
4573  4040          4040
4574  4040          4040
4575  4040          4040
4576  4040          4040
4577  4040          4040
4600  1617          1617            /NO
4601  5617          5617            /.O
4602  0640          0640            /F
4603  0401          0401            /DA
4604  2401          2401            /TA
4605  4020          4020            / P
4606  1711          1711            /OI
4607  1674          1674            /NT
4610  3737          3737            /S:
4611  0000          0000
4612  4040  MESG12,  4040
4613  4040          4040
4614  2305          2305            /SE
4615  1673          1673            /NS
4616  1124          1124            /IT
4617  1136          1136            /IV
4620  1124          1124            /IT
4621  3172          3172            /Y:
4622  4000          4000
4623  4016  MESG13,  4016            / N
4624  0116          0116            /AN
4625  1700          1700            /O
4626  4015  MESG14,  4015            / M
4627  1103          1103            /IC
4630  2217          2217            /RO
4631  0000          0000
4632  4015  MESG15,  4015            / M
4633  1114          1114            /IL
4634  1411          1411            /LI
4635  0000          0000
4636  2617  MESG16,  2617            /VO
4637  1424          1424            /LT
4640  3700          3700
4641  3716  MESG17,  3716            / N
4642  0527          0527            /EW
4643  4015          4015            / M
4644  0130          0130            /AX
4645  1115          1115            /IM
4646  2715          2715            /UM
4647  4077          4077            / ?
4650  4040          4040
4651  4000          4000
4652  3711  MESG18,  3711            / H
4653  0130          0130            /AX
4654  5011          5011            /(
4655  1640          1640            /N
4656  4541          4541            /X)
4657  7240          7240            /:
4660  4000          4000
4661  3737  MESG19,  3737
4662  1017          1017            /HO
4663  2740          2740            /W
4664  1501          1501            /MA
4665  1631          1631            /NY
4666  4023          4023            / S
4667  2005          2005            /PE
4670  0324          0324            /CT
4671  2201          2201            /RA
4672  7740          7740            /?
4673  4000          4000
4674  3723  MESG24,  3723            / S
4675  0524          0524            /ET
4676  4020          4020            / P
4677  0516          0516            /EN
3700  5440          5440            /,
3701  2410          2410            /TH
3702  0516          0516            /EN
3703  4024          4024            / T
3704  3120          3120            /YP
3705  0540          0540            /E
3706  4023          4023            /*S
3707  4240          4240            /*
3710  2417          2417            /TO
3711  4023          4023            / S
3712  2401          2401            /TA
3713  2324          2324            /RT
3714  7200          7200
3715  3716  MESG27,  3716            / N
3716  0527          0527            /EW
3717  4006          4006            / F
3720  2205          2205            /RL
3721  2125          2175            /OU
3722  0516          0516            /EN
3723  033           0331            /CY
3724  4014          4014            / L
3725  115           1115            /IM
3726  1124          1124            /IT
3727  2340          2340            /S
3730  7740          7740            /?
3731  4000          4000
3732  3706  MESG28,  3706            / F
3733  1417          1417            /LO
3734  2772          2772            /W:
3735  4000          4000
3736  3706  MESG29,  3706            / F
3737  1011          1011            /HI
3740  0710          0710            /GH
3741  7240          7240            /:
3742  0000          0000
3743  3723  MESG30,  3723            / S
3744  1517          1517            /MO
3745  1724          1724            /OT
3746  1005          1005            /HE
```

```
3747  4077          4077            / ?
3750  4000          4000
3751  3715  MESG31, 3715            / M
3752  1722          1722            /OR
3753  0540          0540            /E
3754  1116          1116            /IN
3755  2405          2405            /TE
3756  2206          2206            /RF
3757  0522          0522            /FR
3760  1707          1707            /OG
3761  2201          2201            /RA
3762  1523          1523            /MS
3763  7740          7740            /?
3764  4000          4000
3765  1517  MESG32, 1517            /NO
3766  0425          0425            /DU
3767  1401          1401            /LA
3770  2411          2411            /I
3771  1716          1716            /ON
3772  4001          4001            / A
3773  1520          1520            /MF
3774  1411          1411            /LI
3775  2425          2425            /TU
3776  0405          0405            /NE
3777  7200          7200            /;
                    $4000
                /ROUTINE TO PUT PROGRAM ON *FIR-DATA* TAPE.
4000  7201          CLA IAC
4001  3247          DCA TFFLAG      /FIELD=0
4002  1207          TAD F440        /FIRST TAPE BLOCK
4003  3261          DCA TFBLK
4004  1210          TAD MB
4005  4235          JMS WRITTF      /WRITE 8 BLOCKS ON TAPE
4006  7402          HLT
4007  0440  F440,   440
4010  7770  MB,     7770            /-8
                    TFFLAG 4047     /FIELD TIL
                    TFBLK=4061
                    WRITT= 4035
                / -   -  -----  ------     ---    ----
```

SYMBOL	TABLE
.ADD	1325
ALL	0110
AAL	0117
ANFJE	0111
ANFAL	0113
ANSWER	0137
ANSWER	0140
AFGL	1400
ARG I	1136
ARIX	0 50
AUTY	015
A K	24 5
BACKGR	0444
BENGR	0065
BEGIN	1363
BEGN	1746
BNDA	0421
BNDB	0144
BNTF	0133
BF	0025
BUG	0135
	0111
CALF	1063
CALGO	10 4
CALG1	0606
CHECK	0607
CHECK1	0527
CHECK2	0430
CONTR	1005
CONTR1	1436
CONV1	0147
D	0004
DINT	0154
I	1777
DK1	1773
D 400	0744
D 4000	0332
D 5 40	4140
D 6 40	3115
DATA	0453
DETAIL	0467
DF	7664
DFFI	0041
DFFT	7671
DFFTA	7216
DIRECT	1420
DIRECT	1411
DI	7166
DV1	7407
DI	7076
DZ	7464
END	0605
EXF	0157
EI	7101
ES	7467
ENRS	0004
ENTP	1000
ENTRO	0006
ENTRI	0007
ENTV	4000
ENTER	4407
EXI	0000
FFT	1654
FFTL	0664
FIEF	5000
FFIGH	0033
FIFTY	7507
FIVE	0205
FLD	0142
FLAGTF	0134
FLOAT	0143
FLOW	0030
FFF	1750
FFFA	1751
FFFOR	1726
FFINCV	1752
FFRM	1735
FFSTRT	1717
FGET	4000
G	361
FNIS	7000
FNN	0 006
FRAC1	0163
FRUI	6000
FFTO	1420
FFWRD	0145
FSTORE	0021
FFUP	7000
FXO	7515
FX	7477
H	0114
HNDA	1643
HNDRD	1514
HNDR1	0210
HORD	0160
INDEX	1703
INIEXL	0103
INIT	7456
INITL	0076
INPUT	0011
INT	3123
INXSTR	1711
J	0106
JMOD	2015
K	0107
L	2170
LAST	0077
LIM	3340
LIM1	0070
LLOOF	2013

LOCK	0402
LOCKIN	0650
LOOF1	2104
LOOP4	7241
LORD	0161
LSK	7417
LTT	7466
MAIN	7000
MAINL	1662
MAX	0036
MAXE	7433
MAXII	0071
MAXLOC	0024
MAX1	451
MAX2	453
MENC	1001
MESG1	3467
MESG2	3400
MESG3	3601
MESG4	3623
MESG5	3644
MESG6	3636
MESG7	3611
MESG8	3642
MESG9	3661
MESG10	3504
MESG20	3154
MESG21	3160
MESG23	3373
MESG24	3674
MESG25	3161
MESG26	3171
MESG27	3715
MESG28	3731
MESG29	3736
MESG3	3514
MESG30	3743
MESG31	3751
MESG32	3757
MF	0117
MFGS	1765
MFSG	3623
MFSG0	3643
MFSG1	3646
MIN	2171
MIN A	2227
MIN-	2167
MINUS	0060
MINR	0041
MLC	1002
MNL	0027
MORE1	2077
MOVE	1306
MQA	7501
MQL	7421
MULMUY	7455
MSTART	7512
MUY	7405
M ERO	1000
MJP	4453
M*400	3461
ML	4010
MP	0417
MR	0035
NEGATE	0010
NEXT	1353
NI	0034
NLC	0407
NM1	7411
NORM	2400
NORM1	0077
NR	4464
NRRES	3400
N FCTR	00 6
NXT	1362
NXT1	377
O I	1404
OBES	1361
O	6746
OBIENT	0154
OUTPUT	0011
OVFLF	0146
P1	0100
PLCF	6402
PLDD	6414
PLDR	6411
PLDU	6412
PLODF	2006
PLOT	4405
PLOTS	1741
PLOTS	1717
PLOTS	1601
PLTE	6574
PLTL	6511
PLTR	6511
PLTU	6504
PLSF	6501
PLTSF	3071
PLUD	6552
PLUL	6523
PLUR	6513
PMTNX1	1711
POD	0747
POWER	1236
PRCTR	0027
PTO	777
P18	2673
P_600	3457
P40	3674
P440	4007
P600	3460

P4000	4 4
P36	5 3
PTLL	0124
PTLP	0105
P600	2675
P8	1454
P80	3114
P9	7075
Q	2356
Q1	5337
Q3	5343
Q5	5352
RATIO	1413
RATIO1	1460
RDA	6632
RFS	6631
RDTAPE	0133
READ	4406
RES	0047
RETURN	0065
RESA	3415
REWIND	0427
RFO	6634
RNG	1133
RNG1	1167
RNG2	1143
RNG5	1165
RUN	0031
R4	1
R	5 1
S	5 3
SAM	556
SAMPLE	0425
SCA	7431
SCALE1	7610
SCALE	7201
SCALE4	7247
SA	5014
SCI	600
SCI_OF	7570
SCLT	4066
SCLT	4014
SENS	0044
SETUP	1663
SETUP	7355
SETUP	6 74
SIGN	7346
SIGN	7 6
SINE	7140
SR	7413
SINV	7141
SIN	7005
SIZE	0125
SKIP	0110
SL	1e 7
SMOOTH	530
SMTH	521
SMTHL	06 3
SMTH	5 71
SPACE	7155
SPEED	0 53
SPEED	5015
SPLT	3067
SPF	0601
SRAT	0011
TAPE	0211
TAPE	0070
TEP	0307
STEPS	0645
STORE	0057
STOP1	0136
T	0123
TEN	7401
TENTH	0206
TFLD	4061
TFLAG	4047
TFR I	06 5
THENCY	04
TH	476
TYPE	4405
TYPLT	0152
U	1774
UNLOCK	11
UNTAPE	1661
UNTAPE	6
V	0136
WRITE	4404
WRITTF	4035
WTAPE	0131
XCODE1	30 0
XCODE	5 54
XCODE1	6 7
XCODE	55
XCODE	33
XCODE1	2700
XS	3351

```
                        *20
                        /     *FIRUTIL*
                        /
                        /UTILITY SUBROUTINES FOR  FIX PROGRAMS.
                        /(UPDATED MARCH 25TH, 1976)
                        /
                        /ASSEMBLING SEQUENCE (WITH DIAL-MS):
                        /AS CLEARSYM (CLEARS THE SYMBOL TABLE)
                        /AS FIRUTIL   (COMMON PART IS SAVED)
                        /SR FIRUTIL
                        /AS  PROGRAM
                        /AR FIRUTIL
                        /SR PROGRAM
                        /
                        /
                                PMODE
                                FLOT JMS I 3
                                WRITF-JMS I 4
                                TYPE-JMS I 5
                                READ JMS I 6
                                FENT K JMS I 7   /ENTER FLT. PT.
                                FEXT 0000        /EXIT FLT. PT.
                                SQRE 0001        /SQUARE
                                SQRT 0002        /SQUARE ROOT
                                SIN 0003         /SINE
                                COS 0004         /COSINE
                                FABS 0005        /ABSOLUTE VALUE
                                FSTO 0006        /SET FL.PT. 0
                                FST1 0007        /SET FL. PT.=1
                                NEGATE-0010      /NEGATE
                                INPUT 0011       /INPUT PAPERTAPE
                                OUTPUT 0012      /FLOATING OUTPUT
                                FADD-0000        /ADD
                                FSUB 0000        /SUBTRACT
                                FMPY 0000        /MULTIPLY
                                FDIV 0000        /DIVIDE
                                FSET-5000        /SET FLT.PT.NUMB
                                FLOT 6000        /FLOT FLT.PT.NUMB
                                FNOR-7000        /NORMALIZE
                                RBA 6631         /READER BACKWARD
                                RFO 6634         /READER FORWARD
                                SRS 6631         /SKIP IF PAPERW.
                                PLSK 6501        /SKIP ON PLOTTER FLAG
                                P C 6502         /CLEAR PLOTTER FLAG
                                PLPU 6504        /PLOTTER PEN UP
                                PLPR 6511        /PEN RIGHT
                                PLDD 6512        /DRUM UP
                                PLPD-6514        /DRUM DOWN
                                PLPL 6521        /PEN LEFT
                                PLUD 6522        /DRUM UP
                                PLPD 6524        /PEN DOWN
                                PLUR 6513        /UP RIGHT
                                PLUL 6523        /UP LEFT
                                PLDR 6515        /DOWN RIGHT
                                ASR 7415         /ARITHM. SHIFT RIGHT
                                LSR 7417         /LOGICAL SHIFT RIGHT
                                MQA 7501         /INCLUSIVE OR WITH AC
                                MQL 7421         /AC INTO MQ+CLEAR AC
                                MUY-7405         /MULTIPLY
                                NMI 7411         /NORMALIZE
                                SCA 7441         /READ SC INTO AC
                                SHL 7413         /SHIFT LEFT
                                DVI  407         /DIVIDE
                                MQLMUY 7425
                                *5
0005  0400                    FLOTX
0006  7321                    TYPX
0007  7302                    TYPE1
0010  5200                    READ
0011  6600                    FENT
                                *135
0135  4045   WRTAPE,  WRITTP          /WRITE ON LINCTAPE
0136  4117   RDTAPE,  READTP          /READ FROM LINCTAPE
0137  4041   BLNTP,   TPBLK
0140  4047   FLAGTP,  TPFLAG
0141  4367   BUG,     BUG1            /ERROR
0142  0000   * OKEY,  0
0143  4207   ANSWER,  ANS1            /TELETYPE INPUT
0144  0000   ANSWR,   0               /SUBROUTINE
0145  4176   SILONV,  SILONV          /INTERR INPUT
0146  4157   FIXR,    FIX             /FIX F.P. A CU
0147  4550   FLOAT,   FLOA            /FLOAT WORD
0150  5206   BKWRD,   BCKWRD          /READER BACKWARD
0151  5217   FRWRD,   FORWRD          /READER  FORWARD
0152  5365   FCRLF,   CRLF            /CARRIAGE+LINE FEED
0153  5230   CONVRT,  CONV            /IBM TO BINARY
0154  0000   ASCIX,   0               /COORDINATES FOR
0155  0000   ASCIY,   0               /A.S.C.I.I PLOT
0156  0000   TYPFLT,  0               /0 TYPE=1 PLOT
0157  0000   SIZE,    0               /SIZE OF CHAR.
0160  0000   ORIENT,  0               /ORIENTATION.
0161  0240   SPACE,   0240
0162  0000   COUNT,   0
0163  0000   EXP,     0               /FLOATING ACCUMULATOR
0164  0000   MQRD,    0
0165  0000   LORD,    0
0166  0000   FRACT,   0
0167  0000            0
0170  0000            0
                      SAVSYM 1
                      *10
0010  0000   INDEX,   0
0011  0000   INDEXC,  0
                      *165
0165  6646   BUI,     BUG
0166  0000   FORMAT,  0               /TOTAL DIGITS
0167  0000   FORM,    0               /DIGITS BEHIND
0170  0000   EXI,     0               /OPERAND STORE
0171  0000   ACIH,    0
0172  0000   ACII,    0
0173  0000   OVERI,   0
0174  0000   OVER2,   0
0175  0000   EXPI,    0

0176  0000   QUOL,    0
0177  0000   FLAG,    0               /AR.ERROR FLAG
                      *4035
                      /WRITE ON LINC-TAPE.
4035  0000   WRITTP,  0
4036  3356             DCA BLOCKN
4037  1356             TAD BLOCKN      /NUMBER OF BLOCKS.
4040  3354             DCA TFCNT
4041  3244   WRTTP,    DCA MEMO
4042  6141             LINC
                       LMODE
                       SEGMNT 2
                       *43
0043  1020             LDA I
0044  0000   MEMO,     0
0045  0023             TMA
0046  1020             LDA I
0047  0000   TFFLAG,   0
0050  0450             AZE             /TFFLAG=0 ?
0051  6055             JMP .+4
0052  1020             LDA I           /YES, FIELD-1
0053  1020             1020
0054  6057             JMP .+3
0055  1020             LDA I           /NO: FIELD-0
0056  0020             0020
0057  0001             AXO
0060  0736             WRI I U         /WRITE ONE BLOCK
0061  0000   TPBLK,    0               /ON LINCTAPE
0062  0002             PDF
                       PMODE
4063  2261              SZ TPBLK
4064  7300             CLA CLL
4065  1244             TAD MEMO
4066  1355             TAD BLOCK
4067  2354             ISZ TFCNT       /ALL BLOCKS WRITTEN ?
4070  5241             JMP WRTTP       /NO, CONTINUE
4071  7200             CLA             /YES, CHECK.
4072  1356             TAD BLOCKN
4073  3354             DCA TFCNT
4074  1261   WRTTP1,   TAD TPBLK
4075  1354             TAD TFCNT
4076  3301             DCA .+3
4077  6141             LINC
                       LMODE
0100  0717             CHK U           /CHECK ONE BLOCK
0101  0000             0
0102  0002             PDF
                       PMODE
4103  7001             IAC
4104  7640             SZA CLA
4105  5311             JMP .+4         /ERROR!
4106  2354             ISZ TFCNT       /ALL BLOCKS CHECKED ?
4107  5274             JMP WRTTP1      /NO, CONTINUE
4110  5635             JMP I WRITTP    /YES, EXIT
4111  1261             TAD TPBLK       /WRITE AGAIN
4112  1356             TAD BLOCKN
4113  3261             DCA TPBLK
4114  5236             JMP WRITTP+1
                       /READ FROM LINC-TAPE.
4115  0000   READTP,   0
4116  3314             DCA TFCNT
4117  3244   RDTP,     DCA MEMO
4120  6141             LINC
                       LMODE
0121  1000             LDA
0122  0044             MEMO
0123  0023             TMA
0124  1000             LDA
0125  0047             TFFLAG
0126  0450             AZE             /TPFLAG=0 ?
0127  6133             JMP .+4
0130  1020             LDA I           /YES, FIELD=1
0131  1020             1020
0132  6135             JMP .+3
0133  1020             LDA I           /NO, FIELD=0
0134  0020             0020
0135  0001             AXO
0136  1000             LDA
0137  0061             TPBLK
0140  4142             STC .+2
0141  0710             RDL U
0142  0000             0
0143  0002             PDF
                       PMODE
4144  2261             ISZ TPBLK
4145  7300             CLA CLL
4146  1244             TAD MEMO
4147  1355             TAD BLOCK
4150  2354             ISZ TFCNT
4151  5317             JMP RDTP
4152  7300             CLA CLL
4153  5715             JMP I READTP
4154  0000   TFCNT,    0
4155  0400   BLOCK,    0400
4156  0000   BLOCKN,   0               /-NO.OF BLOCKS
                       /FIX FLOATING ACCU.
4157  0000   FIX,      0
4160  1157             TAD EXP
4161  7540             SMA SZA
4162  5365             JMP .+3
4163  7200             CLA
4164  5757             JMP I FIX
4165  1376             TAD M13
4166  3157             DCA EXP
4167  1157             TAD EXP
4170  7700             SMA CLA
4171  5374             JMP .+3
4172  4777             JMS I DV1
4173  5367             JMP .-4
4174  1160             TAD MQRD
4175  5757             JMP I FIX
4176  7765   M13,      -13
4177  7200   DV1,      DIV1            /INTERPRETER
```

```
                        #4_00
                /TELETYPE INPUT SUBROUTINE.
4200  0000  KKBX,   0
4201  6032          KCC
4202  6031          KSF
4203  5202          JMP .-1
4204  6036          KRB
4205  5600          JMP I KKBX
4206  0000  ANS1,   0
4207  4200          JMS KKBX        /READ ANSWER
4210  3140          DCA ANSWR
4211  1140          TAD ANSWR
4212  4405          TYPE
4213  4200  ANS,    JMS KKBX
4214  3232          DCA RETRN
4215  1232          TAD RETRN       /RETURN?
4216  1233          TAD MRTRN
4217  7650          SNA CLA
4220  5230          JMP .+10        /YES
4221  1232          TAD RETRN       /NO
4222  1234          TAD MRUB        /RUB OUT?
4223  7640          SZA CLA
4224  5713          JMP ANS         /NO
4225  1235          TAD BCKSL       /YES
4226  4405          TYPE
4227  5207          JMP ANS1+1      /READ AGAIN
4230  4546          JMS I FLRLF
4231  5606          JMP I ANS1
4232  0000  RETRN,  0
4233  7563  MRTRN,  -215           /-RETURN
4234  7401  MRUB,   377            /-RUB-OUT
4235  0334  BCKSL,  334            /BACKSLASH
                /INTEGER INPUT AND CONVERSION.
4236  0000  SICONV, 0
4237  7300          CLA CLL
4240  1305          TAD HOLD
4241  5263          JMP SINPUT      /READ CHARACTER
4242  3136          DCA STOR1
4243  1136          TAD STOR1
4244  1303          TAD M260        /  260 (IE.'0') ?
4245  7510          SPA
4246  5270          JMP SICTRL      /YES
4247  1304          TAD SIM271      /NO,  271 (IE.'9') ?
4250  7440          SMA SZA CLA
4251  5270          JMP SICTRL      /YES
4252  1305          TAD HOLD        /NO, DECIMAL DIGIT
4253  7106          CLL RTL
4254  1305          TAD HOLD
4255  7004          RAL
4256  3305          DCA HOLD        /HOLD=HOLD*10
4257  1136          TAD STOR1
4260  0307          AND SIMASK
4261  1305          TAD HOLD        /ADD DIGIT
4262  3305          DCA HOLD
4263  6031  SINPUT, KSF
4264  5263          JMP  -1
4265  6036          KRB             /READ
4266  6046          TLS             /WRITE
4267  5242          JMP SICONV+4
4270  7200  SICTRL, CLA
4271  1136          TAD STOR1
4272  1233          TAD MRTRN       /RETURN ?
4273  7650          SNA CLA
4274  5300          JMP  +4
4275  1235          TAD BCKSL       /NO, RUB-OUT
4276  4405          TYPE
4277  5237          JMP SICONV+1    /REINITIALIZE
4300  1305          TAD HOLD        /YES
4301  5636          JMP I SICONV    /EXIT
4302  0017  SIMASK, 17
4303  7520  M260,   -260
4304  7767  SIM271, -11
4305  0000  HOLD,   0
                /FATCH FOR FL.PNT. INTERPRETER.
                /ALL INDIRECT COMMANDS TO FIELD DEFINED BY FLDF
4306  0000  FDF0,   0
4307  7300          CLA CLL         /SET FL DF=0
4310  1344          TAD DF0
4311  3321          DCA INDIR+1
4312  5706          JMP I FDF0
4313  0000  FDF1,   0
4314  7300          CLA CLL         /SET FL.DF=1
4315  1345          TAD DF1
4316  3321          DCA INDIR+1
4317  5713          JMP I FDF1
4320  0000  INDIR,  0
4321  0000          0
4322  1321          TAD  1
4323  3332          DCA STORE1+1
4324  5720          JMP I INDIR
4325  0000  RESET,  0
4326  7006          RTL             /SETS DF=0 AFTER
4327  6201          CDF 0           /LOADING FAC.
4330  5725          JMP I RESET
4331  0000  STORE1, 0
4332  0000          0               /SETS DF FOR FPUT
4333  5731          JMP I STORE1
4334  0000  NEXT1,  0
4335  7300          CLA CLL         /SETS DF=0 BEFORE
4336  6201          CDF 0           /GETTING NEXT
4337  5734          JMP I NEXT1     /INSTRUCTION
4340  1344  DIR,    TAD DF0         /SETS DF=0 FOR
4341  3332          DCA STORE1+1    /STORAGE
4342  5743          JMP I  +1
4343  6630          LOOP01
4344  6201  DF0,    CDF 0
4345  6211  DF1,    CDF 10
4346  0000  PATCH,  0               /FATCH FOR UNORM
4347  1161          TAD LOKD        /CHECK FOR LARGEST
4350  7640          SZA CLA         /NEGATIVE MANTISSA
4351  5746          JMP I PATCH
4352  1160          TAD HORD
4353  7510          SPA
4354  7041          CIA
4355  7700          SMA CLA
4356  5746          JMP I PATCH
4357  2157          ISZ EXP
4360  7000          NOP
4361  1160          TAD HORD
4362  7130          CLL RAR
4363  3160          DCA HORD
4364  5746          JMP I PATCH
                /ERROR SUBROUTINE.
4365  0000  BUG,    0
4366  4404          WRITE
4367  4373          MESG
4370  1365          TAD BUG1        /HALT WITH LOCATION
4371  7402          HLT             /IN ACCU
4372  5765          JMP I BUG1
4373  3705  MESG,   3705           / E
4374  2222          2222            /RR
4375  1722          1722            /OR
4376  3700          3700
                #4400
                /SUBROUTINE TO FLOT ASCII CHARACTERS.
4400  0000  FLTASC, 0
4401  0314          AND MASK77
4402  1334          TAD ASCII
4403  3315          DCA ASC
4404  1150          TAD ASCIX
4405  3317          DCA  15
4406  1151          TAD ASCIY
4407  3214          DCA  +4
4410  7001          IAC
4411  4403          FLOT
4412  0000          0
4413  0000          0
4414  7300          CLA CLL
4415  1715          TAD I ASC
4416  3315          DCA ASC
4417  1315          TAD ASC
4420  0316          AND MSKNUM      /NUMBER OF
4421  7106          CLL RTL         /STORAGE WORDS
4422  7006          RTL
4423  7041          CIA
4424  3317          DCA FLCNT
4425  7040          CMA
4426  1315          TAD ASC
4427  0320          AND MSKADR      /STORAGE ADDR. &
4430  1321          TAD CHAR
4431  3011          DCA INDEXC
4432  1411  FLASC1, TAD I INDEXC
4433  3322          DCA MATRIX
4434  7344          STA CLL RAL     /-2
4435  3323          DCA MTRXN
4436  1322          TAD MATRIX
4437  7012          RTR
4440  7012          RTR
4441  7012          RTR
4442  0314  FLASC2, AND MASK7
4443  3324          DCA MATRX
4444  1324          TAD MATRX
4445  0326          AND MASKX       /MATRIX COLUMN
4446  7110          CLL RAR
4447  7017          RTR
4450  3731          DCA I XCRD1
4451  1324          TAD MATRX
4452  0325          AND MASKY       /MATRIX ROW
4453  3731          DCA I YCRD1
4454  4733          JMS I FSIZE1    /SIZE
4455  1731          TAD I XCRD1     /ORIENTATION
4456  1150          TAD ASCIX
4457  3270          DCA  +11
4460  1732          TAD I YCRD1
4461  1151          TAD ASCIY
4462  3271          DCA  +7
4463  1324          TAD MATRX
4464  0327          AND MSKFEN      /FEN UP OR DOWN?
4465  7640          SZA CLA
4466  7001          IAC
4467  4403          FLOT
4470  0000          0
4471  0000          0
4472  1322          TAD MATRIX
4473  7333          ISZ MTRXN
4474  5242          JMP FLASC2
4475  7300          CLA CLL
4476  2317          ISZ FLCNT
4477  5233          JMP FLASC1
4500  6604          FLFU
4501  1330          TAD NEXT        /SET FOR NEXT
4502  3731          DCA I XCRD1     /CHARACTER
4503  3732          DCA I YCRD1
4504  4733          JMS I FSIZE1
4505  1731          TAD I XCRD1
4506  1150          TAD ASCIX
4507  3150          DCA ASCIX
4510  1732          TAD I YCRD1
4511  1151          TAD ASCIY
4512  3151          DCA ASCIY
4513  5600          JMP I FLTASC
4514  0077  MASK77, 0077
4515  0000  ASC,    0
4516  7000  MSKNUM, 7000
4517  0000  FLCNT,  0
4520  0777  MSKADR, 0777
4521  4721  CHAR,   CHARAC
4522  0000  MATRIX, 0
4523  0000  MTRXN,  0
4524  0000  MATRX,  0
4525  0007  MASKY,  0007
4526  0030  MASKX,  0030
4527  0040  MSKFEN, 0040
4530  0005  NEXT,   0005
4531  4717  XCRD,   XCRD
4532  4720  YCRD1,  YCRD
```

```
4634 4635 FSIZF1, SIZF1
4634 4636 ASCII, .+1
4635 1000          1000          /0,
4636 4001          4001          /1,A
4637 5005          5005          /2,B
4640 4012          4012          /3,C
4641 3016          3016          /4,D
4642 3021          3021          /5,E
4643 2024          2024          /6,F
4644 6026          6026          /7,G
4645 3034          3034          /10,H
4646 3037          3037          /11,I
4647 3042          3042          /12,J
4650 3045          3045          /13,K
4651 2050          2050          /14,L
4652 3052          3052          /15,M
4653 3054          3054          /16,N
4654 6056          6056          /17,O
4655 3064          3064          /20,P
4656 6067          6067          /21,Q
4657 4075          4075          /22,R
4660 6101          6101          /23,S
4661 7107          7107          /24,T
4662 3111          3111          /25,U
4663 2114          2114          /26,V
4664 5116          5116          /27,W
4665 2121          2121          /30,X
4666 5123          5123          /31,Y
4667 2130          2130          /32,Z
4670 1000          1000          /33,
4671 1000          1000          /34,
4672 1000          1000          /35,
4673 1000          1000          /36,^
4674 1000          1000          /37,
4675 1211          1211          /40,SPACE
4676 2240          2240          /41,!
4677 2242          2242          /42,"
4700 1000          1000          /43,
4701 1000          1000          /44,$
4702 6212          6212          /45,%
4703 1000          1000          /46,&
4704  000          1000          /47,
4705 2220          2220          /50,(
4706 2222          2222          /51,)
4707 1000          1000          /52,*
4710 1174          1174          /53,+
4711 1226          1226          /54,,
4712 1227          1227          /55,-
4713 1230          1230          /56,.
4714 1231          1231          /57,/
4715 5132          5132          /60,0
4716 5137          5137          /61,1
4717 4142          4142          /62,2
4720 6146          6146          /63,3
4721 3154          3154          /64,4
4722 5157          5157          /65,5
4723 6164          6164          /66,6
4724 2172          2172          /67,7
4725 7174          7174          /70,8
4726 6203          6203          /71,9
4727 2232          2232          /72,:
4730 2234          2234          /73,;
4731 2244          2244          /74,<
4732 2246          2246          /75,=
4733 2250          2250          /76,>
4734 0000 SIZE1,   0             /SIZE OF CHARAC-
4735 1317          TAD XCRD      /FIX AND
4736 4304          JMS SIZE?     /ORIENTATION.
4737 3317          DCA XCRD
4740 1320          TAD YCRD
4741 4304          JMS SIZE?
4742 3320          DCA YCRD
4743 1154          TAD ORIENT    /ORIENTATION
4744 7450          SNA
4745 5635          JMP I SIZE1
4746 7700          SMA CLA
4747 5760          JMP .+10
4750 1317          TAD XCRD
4751 7041          CIA
4752 3317          DCA XCRD
4753 1320          TAD YCRD
4754 7041          CIA
4755 3320          DCA YCRD
4756 5635          JMP I SIZF1
4757 7040          CMA
4760 1154          TAD ORIENT
4761 7640          SZA CLA
4762 5274          JMP .+11
4763 1320          TAD YCRD
4764 3315          DCA SIZE3
4765 1317          TAD XCRD
4766 3320          DCA YCRD
4767 3317          DCA XCRD
4770 5635          JMP I SIZF1
4771 1317          TAD XCRD
4772 3315          DCA SIZE3
4773 1320          TAD YCRD
4774 7041          CIA
4775 3317          DCA XCRD
4776 1315          TAD SIZE3
4777 3320          DCA YCRD
5000 5635          JMP I SIZE1
5001 0000 SIZE2,   0
5002 3315          DCA SIZE3
5003 1153          TAD SIZE      /SIZE
5004 7041          CIA
5005 3316          DCA SZECNT
5006 1315          TAD SIZE3
5007 2316          ISZ SZECNT
5010 5311          JMP   2
5011 5704          JMP I SIZE2
5012 0000 SIZE3,   0
5013 0000 SZECNT,  0
5014 0000 XCRD,    0
5015 0000 YCRD,    0
5016 4040 CHARAC,  4040
5017 0215          0215          /A
5020 2532          2532
5021 3042          3042
5022 3272          3272
5023 0525          0525          /B
5024 3423          3423
5025 0363          0363
5026 3231          3231
5027 2000          2000
5030 7120          7120          /C
5031 1001          1001
5032 0415          0415
5033 2534          2534
5034 0525          0525          /D
5035 3431          3431
5036 2000          2000
5037 7000          7000          /F
5040 0535          0535
5041 4323          4323
5042 0535          0535          /F
5043 4323          4323
5044 7120          7120          /G
5045 1001          1001
5046 0415          0415
5047 2534          2534
5050 6232          6232
5051 3070          3070
5052 0543          0543          /H
5053 3375          3375
5054 3070          3070
5055 5030          5030          /I
5056 6025          6025
5057 5535          5535
5060 4110          4110          /J
5061 2031          2031
5062 3575          3575
5063 0575          0575          /K
5064 0253          0253
5065 3070          3070
5066 4500          4500          /L
5067 3070          3070
5070 0513          0513          /M
5071 3530          3530
5072 0532          0532          /N
5073 7530          7530
5074 5001          5001          /O
5075 0415          0415
5076 2534          2534
5077 3120          3120
5100 1064          1064
5101 3575          3575
5102 0525          0525          /P
5103 3433          3433
5104 2202          2202
5105 6230          6230
5106 4110          4110          /S
5107 2031          2031
5110 3223          3223
5111 1304          1304
5112 1525          1525
5113 3474          3474
5114 6025          6025          /T
5115 4535          4535
5116 4501          4501          /U
5117 1020          1020
5120 3135          3135
5121 4510          4510          /V
5122 3575          3575
5123 4500          4500          /W
5124 1320          1320
5125 3575          3575
5126 3545          3545          /X
5127 3070          3070
5130 4110          4110          /Y
5131 2031          2031
5132 3543          3543
5133 0312          0312
5134 2233          2233
5135 4535          4535          /Z
5136 0030          0030
5137 5001          5001          /0
5140 0415          0415
5141 2534          2534
5142 3120          3120
5143 1064          1064
5144 3575          3575
5145 0525          0525          /P
5146 3433          3433
5147 2202          2202
5150 5001          5001          /Q
5151 0415          0415
5152 2534          2534
5153 3120          3120
5154 1061          1061
5155 3070          3070
5156 0525          0525          /R
5157 3433          3433
5160 2202          2202
5161 6230          6230
5162 4110          4110          /S
5163 2031          2031
5164 3223          3223
5165 1304          1304
5166 1525          1525
5167 3474          3474
5170 6025          6025          /T
5171 4535          4535
5172 4501          4501          /U
5173 1020          1020
5174 3135          3135
5175 4510          4510          /V
5176 3575          3575
5177 4500          4500          /W
5200 1320          1320
5201 3575          3575
5202 3545          3545          /X
5203 3070          3070
5204 4110          4110          /Y
5205 2031          2031
5206 3543          3543
5207 0312          0312
5210 2233          2233
5211 4535          4535          /Z
5212 0030          0030
5213 5001          5001          /0
5214 0415          0415
5215 2534          2534
5216 3120          3120
5217 1001          1001
```

```
5075  6502            6502            /4
5076  3275            3275
5077  3070            3070
5100  4110            4110            /5
5101  2031            2031
5102  3223            3223
5103  0305            0305
5104  3575            3575
5105  7425            7425            /6
5106  1504            1504
5107  0110            0110
5110  2031            2031
5111  3223            3223
5112  1402            1402
5113  4535            4535            //
5114  1050            1050
5115  5302            5302            /8
5116  0110            0110
5117  2031            2031
5120  3223            3223
5121  1304            1304
5122  1525            1525
5123  3423            3423
5124  4110            4110            /9
5125  2031            2031
5126  3425            3425
5127  1504            1504
5130  0312            0312
5131  2233            2233
5132  7070            7070            /SPACE
5133  3555            3555            /%
5134  0504            0504
5135  1415            1415
5136  6131            6131
5137  3020            3020
5140  2161            2161
5141  6011            6011            /(
5142  1425            1425
5143  5021            5021            /)
5144  2415            2415
5145  4232            4232            /+
5146  6024            6024
5147  5021            5021            /,
5150  4232            4232            /-
5151  6020            6020            /.
5152  3575            3575            //
5153  6020            6020            /:
5154  6424            6424
5155  5021            5021            /;
5156  6424            6424
5157  4131            4131            /=
5160  7303            7303
5161  6521            6521            /?
5162  6020            6020
5163  5425            5425            /*
5164  6435            6435
5165  7302            7302            /^
5166  3171            3171
5167  4332            4332            /
5170  0141            0141
5171  4304            4304            /?
5172  1525            1525
5173  3433            3433
5174  2221            2221
5175  6020            6020
                      *5200
                /READ CHARACTER FROM PAPERTAPE.
5200  0000  READ1,    0
5201  7200            CLA
5202  6011            RSF
5203  5202            JMP .-1
5204  6016            RRB RFC
5205  5600            JMP I READ1
                /READER BACKWARD.
5206  0000  BCKWRD,   0
5207  6011            RSF
5210  5207            JMP .-1
5211  6632            RBA
5212  4406            READ
5213  4406            READ
5214  4406            READ
5215  7200            CLA
5216  5606            JMP I BCKWRD
                /READER FORWARD.
5217  0000  FORWRD,   0
5220  6011            RSF
5221  5220            JMP .-1
5222  6634            RFO
5223  4406            READ
5224  4406            READ
5225  4406            READ
5226  7200            CLA
5227  5617            JMP I FORWRD
                /CHECK DIGIT AND CONVERT IBM-CODE TO BINARY.
5230  0000  CONV,     0
5231  3136            DCA STOR1
5232  7240            STA
5233  3263            DCA FLAG2
5234  1301            TAD MIN10
5235  3264            DCA DIGIT
5236  1264  CONV1,    TAD DIGIT
5237  1266            TAD IBMTBL
5240  3265            DCA IBM
5241  1136            TAD STOR1
5242  1665            TAD I IBM       /LOOK FOR DIGIT
5243  7640            SZA CLA         /IN TABLE
5244  5251            JMP .+5
5245  7001            IAC
5246  1264            TAD DIGIT
5247  7041            CIA
5250  5630            JMP I CONV
5251  2264            ISZ DIGIT
5252  5236            JMP CONV1

5253  1263            TAD FLAG2       /NOT FOUND
5254  4515            JMS I BUG
5255  4206            JMP BCKWRD      /READ AGAIN
5256  4406            READ
5257  4217            JMS FORWRD
5260  4406            READ
5261  3136            DCA STOR1
5262  7034            JMP CONV1 ?
5263  0000  FLAG2,    0
5264  0000  DIGIT,    0
5265  0000  IBM,      0
5266  5301  IBMTBL,   .+13
5267  7747            7747            /IBM 9
5270  7770            7770            / 8
5271  7771            7771            /-7
5272  7752            7752            / 6
5273  7753            7753            / 5
5274  7774            7774            / 4
5275  7755            7755            /-3
5276  7776            7776            / 2
5277  7777            7777            /-1
5300  7746            7746            / 0
5301  7766  MIN10,    7766
                /SUBROUTINE TO TYPE OR FLOT ASCII
                /CHARACTERS.
5302  0000  TYPEIT,   0
5303  3136            DCA STOR1
5304    52            TAD TYPFLT      /* FOR OR FLOT?
5305  7640            SZA CLA
5306  5315            JMP .+7         /FLOT
5307  1136            TAD STOR1       /TYPE
5310  6041            TSF
5311  5310            JMP .-1
5312  6046            TLS
5313  7300            CLA CLL
5314  5702            JMP I TYPE1
5315  1136            TAD STOR1
5316  4720            JMS I FLOTSC
5317  5702            JMP I TYPE1
5320  4400  FLOTSC,   FLTASC
                /SUBROUTINE TO TYPE OR FLOT TEXT.
5321  0000  TYPX,     0
5322  7300            CLA CLL
5323  1721            TAD I TYPX      /GET POINTER
5324  3337            DCA TYPNT       /AND SAVE IT SO ALLY
5325  2321            ISZ TYPX
5326  1737            TAD I TYPNT     /GET LEFT HAND
5327  7012            RTR             /CHARACTER.
5330  7012            RTR
5331  7012            RTR
5332  4340            JMS TYPY        /CONVERT AND TYPE
5333  1737            TAD I TYPNT      RIGHT HAND CHAR.
5334  2337            ISZ TYPNT       /POINT TO NEXT WORD
5335  4340            JMS TYPY        /CONVERT AND TYPE
5336  5326            JMP .-10        /CONTINUE UNTIL DONE
5337  0000  TYPNT,    0               /POINTER TO STRING
5340  0000  TYPY,     0
5341  0357            AND TK77        /MASK OFF CHARACTER
5342  7440            SNA             /TEST FOR TERMINATOR
5343  5721            JMP I TYPX      /EXIT IF TERMINATOR
5344  1360            TAD TKM37
5345  7440            SZA             /TEST FOR CR LF
5346  5351            JMP .+4         /NOT A 37
5347  1361            TAD TK215       /TYPE A CR
5350  4405            TYPE
5351  1362            TAD TKM125      /CONVERTS TO A  LF
5352  7510            SPA             /TEST RANGE
5353  1363            TAD TK100       /RANGE IS 301 336
5354  1364            TAD TK237       /RANGE IS 140 177
5355  4405            TYPE            /TYPE CHARACTER
5356  5740            JMP I TYPY
5357  0077  TK77,     77              /MASK FOR ASC II
5360  7741  TKM37,    -37
5361  0215  TK215,    215
5362  7653  TKM125,   -125
5363  0100  TK100,    100
5364  0237  TK237,    237
                /CARRIAGE RETURN  LINE FEED.
5365  0000  CRLF,     0
5366  7300            CLA CLL
5367  1361            TAD TK215
5370  4405            TYPE
5371  1374            TAD LF
5372  4405            TYPE
5373  5765            JMP I CRLF
5374  0212  LF,       212             /LINE FEED
                      *5400
                /INCREMENTAL PLOTTER SUBROUTINE.
5400  0000  PLOTX,    0
5401  7510            SPA             /MOVE THE PEN
5402  5410            JMP PLOTA       /NOTCONTINUE
5403  1364            TAD PLOTEN      /AND PEN STATUS
5404  7112            CLL RTR
5405  7710            SPA CLA         /ANY CHANGE?
5406  5227            JMP F OT1       /NOTCON INUE
5407  7650            SNL CLA
5410  6214            JMP .+4         /LOWER THE PEN
5411  3364            D A PLOT N      /RAISE THE PEN
5412  6504            PLEJ
5413  5215            JMP .+5
5414  1364            ISZ PLOTPN      /LOWER  HE PEN
5415  6524            PLFD
5416  4373            JMS PLOTWT      /WAIT FOR FLAG
5417  5227            JMP PLOT1       / ONTINUE
5420  7300  PLOTA,    CLA
5421  6504            PLFU            /RAISE THE PEN
5422  3364            DCA PLOTPN
5423  3365            DCA PLOTNX      /0 TO X CO ORD.
5424  3366            DCA PLOTNY      /0 TO Y CO-ORD.
5425  4373            JMS PLOTWT
5426  5600            JMP I PLOTX
5427  1465  PLOT1,    TAD PLOTNX      /FETCH PREVIOUS
5430  7141            CIA CLL         /X CO-ORDINATE.
```

```
5431  1600          TAD I FLOTX     /FORM NX-NFX
5432  7420          SNL             /L=0: NX NFX
5433  7041          CIA             /ABSOLUTE VALUE
5434  3367          DCA FLOTDX      /DF DIFFERENCE.
5435  7004          RAL
5436  3370          DCA FLOTMV      /SAVE SIGN BIT
5437  1600          TAD I FLOTX     /SET NEW
5440  3365          DCA FLOTNX      /PREVIOUS X
5441  2200          ISZ FLOTX       /INCREM.POINTER
5442  1366          TAD FLOTNY      /FETCH PREVIOUS
5443  7141          CIA CLL         /Y CO ORDINATE.
5444  1600          TAD I FLOTX     /FORM NY-NPY
5445  7420          SNL             / =01 NPY NY
5446  7041          CIA             /ABSOLUTE VALUE
5447  3370          DCA FLOTDY      /DF DIFFERENCE.
5450  1372          TAD FLOTMV      /SAVE SIGN BIT
5451  7004          RAL
5452  3372          DCA FLOTMV
5453  1600          TAD I FLOTX     /SET NEW
5454  3366          DCA FLOTNY      /PREVIOUS Y
5455  2200          ISZ FLOTX       /INCREM.POINTER
5456  1367          TAD FLOTDX
5457  7141          CIA CLL
5460  1370          TAD FLOTDY      /L=01
5461  7670          SNL CLA         /DELTA Y DELTA X
5462  5275          JMP FLOT2
5463  1367          TAD FLOTDX      /REVERSE NUMBERS
5464  3371          DCA FLOTNA
5465  1370          TAD FLOTDY
5466  3367          DCA FLOTDX
5467  1371          TAD FLOTNA
5470  3370          DCA FLOTDY
5471  7001          IAC             /SET MAJOR MOT
5472  0372          AND FLOTMV      /ION INSTRUCTION
5473  1345          TAD FLOTT1
5474  5100          JMP .+4
5475  1372  FLOT2,  TAD FLOTMV
5476  7110          CLL RAR
5477  1350          TAD FLOTT2
5500  3371          DCA FLOTNA
5501  1771          TAD I FLOTNA
5502  3343          DCA FLOT4
5503  1372          TAD FLOTMV      /SET COMB.MOTION
5504  1353          TAD FLOTT3
5505  3372          DCA FLOTMV
5506  1772          TAD I FLOTMV
5507  3334          DCA FLOTDB
5510  1367          TAD FLOTDX      /INITIALIZE PLOTNA
5511  7110          CLL RAR
5512  3371          DCA FLOTNA
5513  1367          TAD FLOTDX      /SET STEP COUNTER
5514  7040          CMA
5515  3372          DCA FLOTMV
5516  2372  FLOT3,  ISZ FLOTMV      /PLOT ALGORITHM
5517  7410          SKP
5520  5600          JMP I FLOTX     /ALL DONE
5521  7100          CLL
5522  1371          TAD FLOTNA
5523  1370          TAD FLOTDY
5524  3371          DCA FLOTNA
5525  7430          SZL             /PLOTNA 10000?
5526  5334          JMP FLOTDB      /YES
5527  1371          TAD FLOTNA      /NO
5530  7140          CMA CLL
5531  1367          TAD FLOTDX
5532  7630          SZL CLA
5533  5343          JMP FLOT4       /SINGLE MOTION
5534  0000  FLOTMM, 0               /COMB.MOTION
5535  1367          TAD FLOTDX
5536  7041          CIA
5537  1371          TAD FLOTNA
5540  3371          DCA FLOTNA
5541  4373          JMS FLOTWT
5542  5316          JMP FLOT3
5543  0000  FLOT4,  0
5544  5341          JMP .-3
5545  5546  FLOTT1, .+1
5546  6511          FLFR            /PEN-RIGHT
5547  6521          FLFL            /PEN-LEFT
5550  5551  FLOTT2, .+1
5551  6512          FLDU            /DRUM-UP
5552  6514          FLDD            /DRUM DOWN
5553  5554  FLOTT3, .+1
5554  6513          FLUR            /UP-RIGHT
5555  6523          FLUL            /UP-LEFT
5556  6515          FLDR            /DOWN RIGHT
5557  4760          JMS .+1         /DOWN-LEFT
5560  0000          0
5561  6514          FLDD
5562  6521          FLFL
5563  5760          JMP I .-3
5564  0000  FLOTFN, 0
5565  0000  FLOTNX, 0
5566  0000  FLOTNY, 0
5567  0000  FLOTDX, 0
5570  0000  FLOTDY, 0
5571  0000  FLOTNA, 0
5572  0000  FLOTMV, 0
5573  0000  FLOTWT, 0
5574  6501          FLSF            /WAIT FOR DONE FLAG
5575  5374          JMP .-1         /NOT YET
5576  6502          FLCF            /CLEAR FLAG
5577  5773          JMP I FLOTWT    /EXIT
                    *5600
              /FLOATING POINT INPUT FROM PAPERTAPE.
5600  0000  FLINTP, 0
5601  1565          TAD I GO1
5602  3136          DCA STOR1
5603  1536          TAD I STOR1     /NUMBER OF DIGITS
5604  7041          CIA
5605  3156          DCA COUNT
5606  2565          ISZ I GO1       /INCR.RETURN ADDR.
5607  4217          JMS DECONV

5610  1216          TAD C27
5611  3157          DCA EXP
5612  4407          FENTER
5613  7000          FNOR            /NORMALIZE F.P.
5614  0000          FEXT            /NUMBER
5615  5600          JMP I FLINTP
5616  0027  C27,    0027
              /DOUBLE PRECISION DECIMAL-BINARY
              /INPUT AND CONVERSION.
5617  0000  DECONV, 0
5620  7300          CLA CLL         /INITIALIZE
5621  3160          DCA HORD        /MANTISSA
5622  3161          DCA LORD
5623  4406          READ            /READ DIGIT
5624  4547          JMS I CONVRT    /IBM-BINARY
5625  3136          DCA STOR1
5626  4232          JMS MULT10
5627  2156          ISZ COUNT
5630  5223          JMP .-5         /NEXT DIGIT
5631  5617          JMP I DECONV
5632  0000  MULT10, 0               /MULTIPLY DOUBLE
5633  1161          TAD LORD        /PRECISION WORD
5634  3252          DCA LTEMP       /BY TEN(DECIMAL)
5635  1160          TAD HORD
5636  3253          DCA HTEMP
5637  3254          DCA REMAIN
5640  4255          JMS MULT2       /MULTIPLY BY TWO
5641  4255          JMS MULT2
5642  4271          JMS DUBLAD      /CALL DOUBLE ADD
5643  4255          JMS MULT2
5644  1136          TAD STOR1       /LAST DIGIT
5645  3252          DCA LTEMP       /RECEIVED
5646  3253          DCA HTEMP
5647  4271          JMS DUBLAD
5650  1254          TAD REMAIN      /EXIT WITH RE-
5651  5632          JMP I MULT10    /MAINDER IN AC.
5652  0000  LTEMP,  0               /DOUBLE PRECIS-
5653  0000  HTEMP,  0               /ION WORD.
5654  0000  REMAIN, 0
5655  0000  MULT2,  0               /MULTIPLY WORD,
5656  7300          CLA CLL         /LORD BY TWO.
5657  1161          TAD LORD
5660  7004          RAL
5661  3161          DCA LORD
5662  1160          TAD HORD
5663  7004          RAL
5664  3160          DCA HORD
5665  1254          TAD REMAIN
5666  7004          RAL
5667  3254          DCA REMAIN
5670  5655          JMP I MULT2
5671  0000  DUBLAD, 0               /DOUBLE PRECIS-
5672  7300          CLA CLL         /ION ADDITION.
5673  1161          TAD LORD
5674  1252          TAD LTEMP
5675  3161          DCA LORD
5676  7004          RAL
5677  1160          TAD HORD
5700  1253          TAD HTEMP
5701  3160          DCA HORD
5702  7004          RAL
5703  1254          TAD REMAIN
5704  3254          DCA REMAIN
5705  5671          JMP I DUBLAD
5706  0000  MSIGN,  0               /ROUTINE TO FORM
5707  7300          CLA CLL         /2S COMPLEMENT
5710  2323          ISZ SGN1        /IF MINUS
5711  5706          JMP I MSIGN     /SIGN=0000:EXIT
5712  1161          TAD LORD
5713  7041          CMA IAC
5714  3161          DCA LORD
5715  1160          TAD HORD
5716  7040          CMA
5717  7430          SZL
5720  7001          IAC
5721  3160          DCA HORD
5722  5706          JMP I MSIGN
5723  0000  SGN1,   0               /=0 IF+1=7777IF-
              /OUTPUT THE EXPONENT.
5724  0000  FEXC,   0
5725  7300          CLA CLL
5726  1157          TAD EXP
5727  7510          SPA
5730  7061          CMA IAC CML
5731  3157          DCA EXP
5732  1370          TAD C253
5733  7430          SZL
5734  1371          TAD C255
5735  4776          JMS I DGPT
5736  3160          DCA HORD
5737  1157          TAD EXP
5740  2160          ISZ HORD
5741  1372          TAD M144
5742  7500          SMA
5743  5340          JMP .-3
5744  1373          TAD C144
5745  3157          DCA EXP
5746  7040          CMA
5747  1160          TAD HORD
5750  7440          SZA
5751  4776          JMS I DGPT
5752  3160          DCA HORD
5753  1157          TAD EXP
5754  2160          ISZ HORD
5755  1374          TAD M12
5756  7500          SMA
5757  5354          JMP .-3
5760  1375          TAD C12
5761  3161          DCA LORD
5762  7240          CLA CMA
5763  1160          TAD HORD
5764  4776          JMS I DGPT
5765  1161          TAD LORD
```

```
5766  4276          JMS I IGET
5767  5714          JMP I FEXC
5770  7773  C253,   253-260
5771  0002  L255,   255-253
5772  7634  M144,   7634
5773  0144  L44,    0.44
5774  7766  M12,    7766
5775  0012  C12,    0012
5776  6145  DGET,   OUTDG
                    #6000
            /FLOATING OUTPUT PROGRAM.
6000  0000  FLOUTF, 0
6001  1565          TAD I GO1
6002  3136          DCA STOK1
6003  1536          TAD I STOK1
6004  0327          AND MASK2           /NUMBER OF
6005  7010          RAR                 /DIGITS.
6006  7110          CLL RAR
6007  7110          CLL RAR
6010  3166          DCA FORMAT
6011  1536          TAD I STOK1
6012  0330          AND MASK1           /DIGITS BEHIND '.'
6013  3167          DCA FORM
6014  2565          ISZ I GO1           /INCR.RETURN ADDR.
6015  1160          TAD HORD
6016  7210          SPA CLA
6017  1337          TAD SMINUS
6020  1155          TAI SPACE
6021  4405          TYPE                /'SPACE' OR '-'
6022  1334          TAD BEXF
6023  3010          DCA INDEX           /INIT. AUTO-INDEX
6024  5237          JMP FOUTCN          /CONVERT MANTISSA
6025  1331  RETN,   TAD BEXP           /STORE DECIMAL EXP
6026  3157          DCA EXP
6027  4741          JMS I FXAD          /OUTPUT NUMBER
6030  5600          JMP I FLOUTF        /FIXED POINT RETURN
6031  7200          CLA                 /FLOAT.POINT RETURN
6032  1332          TAD CHE
6033  4405          TYPE                /PRINT 'E'
6034  4744          JMS I FEXPPT        /OUTPUT EXPONENT
6035  7200          CLA
6036  5600          JMP I FLOUTF        /EXIT
6037  1160  FOUTCN, TAD HORD
6040  7700          SMA CLA
6041  5245          JMP .+4
6042  7040          CMA                 /NUMBER IS NEGA
6043  3741          DCA I SNPT          /TIVE.
6044  4740          JMS I MSNPT
6045  7240          CLA CMA             /SUBTR.1 FROM EX
6046  1157          TAD EXP             /PONENT,COMPEN
6047  3157          DCA EXP             /SATE AT FG04
6050  3331          DCA BEXP
6051  1157  FG02,   TAD EXP            / 4 EXP  1??
6052  7500          SMA
6053  5266          JMP FG03            /MULT.BY 1/10
6054  1336          TAD FOUR
6055  7700          SMA CLA
6056  5273          JMP FG04
6057  4407          FENTEN              /TIMES TEN
6060  3371          FMFY TEN
6061  0000          FEXT
6062  7240          CLA CMA
6063  1331          TAD BEXP
6064  3331          DCA BEXP
6065  5251          JMP FG02
6066  4407  FG03,   FENTEN
6067  3366          FMFY TENTH          /ONE TENTH
6070  0000          FEXT
6071  2331          ISZ BEXP
6072  5251          JMP FG02
6073  3136  FG04,   DCA STOR1          /MULT.BY TWO
6074  4743          JMS I M2PT          /IE.SHIFT LEFT
6075  4742          JMS I M10PT         /MULT.BY TEN
6076  7410          SKP
6077  4352          JMS DIVTWO          /COMPENSATE FOR
6100  2157          ISZ EXP             /BINARY EXP.
6101  5277          JMP .+2
6102  7450          SNA                 /FIRST DIGIT 0??
6103  5314          JMP FG07            /YES,IGNORE
6104  3410          DCA I INDEX
6105  1333  FG06,   TAD MINUS7
6106  3157          DCA EXP
6107  4742          JMS I M10PT
6110  3410          DCA I INDEX
6111  2157          ISZ EXP
6112  5307          JMP .-3
6113  5226          JMP RETN
6114  7240  FG07,   CLA CMA           /ION.FIRST DIGIT
6115  1331          TAD BEXP            /SUBTRACT 1 FROM
6116  3331          DCA BEXP            /DECIMAL EXP.
6117  1160          TAD HORD
6120  7640          SZA CLA
6121  5325          JMP .+4             /MANTISSA-0??
6122  1161          TAD LORD
6123  7650          SNA CLA
6124  3331          DCA BEXP            /YES:EXP-0
6125  7240          CLA CMA
6126  5305          JMP FG06
6127  0070  MASK2,  0070
6130  0007  MASK1,  0007
6131  0000  BEXP,   0                  /DECIMAL EXP.
6132  0305  CHE,    305
6133  7772  MINUS7, 7772
6134  6367  BFAST,  BUFFER-1
6135  6200  FXAD,   FIX1
6136  0004  FOUR,   0004
6137  0017  SMINUS, 255-240
6140  5706  MSNPT,  MSIGN
6141  5723  SNPT,   SGN.
6142  5632  M10PT,  MULT10
6143  5675  M2PT,   MULT2
6144  5724  FEXPPT, FEXP
6145  0000  OUTDG,  0                  /OUTPUT 1 DIGIT.

6146  1351          TAD C260
6147  4405          TYPE
6150  7745          JMP I OUTDG
6151  0260  C260,   0260
6152  0000  DIVTWO, 0                  /DIVIDE BY TWO,
6153  7110          CLL RAR             /IE.ROTATE RIGHT
6154  3365          DCA STOK
6155  1160          TAD HORD
6156  7010          RAR
6157  3160          DCA HORD
6160  1161          TAD LORD
6161  7010          RAR
6162  3161          DCA LORD
6163  1365          TAD STOK
6164  5752          JMP I DIVTWO
6165  0000  STOK,   0
6166  7775  TENTH,  7775               /.10
6167  3146          3146
6170  3147          3147
6171  0004  TEN,    0004               /10
6172  2400          2400
6173  0000          0000
                    #6700
            /IN THE COMMENTS BELOW W'
            /   B = NUMBER OF DIGITS TO BE OUTPUT
            /   D = NUMBER OF DECIMAL PLACES
            /   E = DECIMAL EXPONENT
            /   F = NUMBER OF PLACES REMAINING TO BE
            /       PRINTED BEFORE DECIMAL POINT
6700  0000  FIX1,   0
6701  1166          TAD FORMAT
6702  7450          SNA                 /FLOATING OUTPUT?
6703  5315          JMP K6              /YES,K.OF 6 PLACES
6704  7041          CIA
6705  1167          TAD FORM
6706  7510          SPA                 /F - B - 2 ?
6707  5314          JMP .+5             /YES
6710  7240          CLA CMA
6711  1166          TAD FORMAT
6712  3167          DCA FORM            /MAKE B = F
6713  7040          CMA
6714  1157          TAD X
6715  7500          SMA                 /F - B - E ?
6716  7200          CLA                 /NO,K OFF TO F PLACES
6717  1777          TAD FORMAT          /YES
6720  7510          SPA                 /DIF = 0
6721  5750          JMP FRNTI-1         /YES, NO ROUNDING
6722  1354          TAD MINO            /NO,ROUND OFF PLACES,
6723  7500          SMA                 /TO MAX.OF 6 PLACES
6724  7700          CLA
6725  1355  K6,     TAD K7
6726  3364          DCA TEMPX           /SAVE NUMBER OF
6727  1346          TAD BUFST           /PLACES TO ROUND
6730  1364          TAD TEMPX           /BUFF.ADDR. AT WHICH
6731  3366          DCA PLCE            /RD. OFF SHOULD START
6732  1364          TAD TEMPX
6733  7041          CIA                 /COUNT OF MAXIMUM NR
6734  3364          DCA TEMPX           /OF CHARS ALLOWABLE
6735  7107          CLL IAC RTL         /*4
6736  1366  RET,    TAD PLCE            /ADD 1 TO DIGIT
6737  1766          TAD I PLCE
6740  1355          TAD K10
6741  7710          SPA CLA             /CARRY REQUIRED?
6742  5751          JMP FRNTI           /NO, GO TO OUTPUT
6743  3766          DCA I PLCE          /YES,MAKE DIGIT A 0
6744  2364          ISZ TEMPX           /BUFFER REACHED?
6745  5343          JMP RET             /NO,DECREMENT, REPEAT
6746  7766          ISZ I PLCE          /YES, MANTISSA TO 0.1
6747  2157          ISZ EXP             /COMPENSATE BY INC'M
6750  7700          CLA
6751  1346  FRNTI,  TAD BUFST
6752  3010          DCA INDEX           /SET AUTO INDEX REG.
6753  1166          TAD FORMAT
6754  7450          SNA                 /F = 0 ?
6755  5342          JMP FLOP            /YES,FLOATING OUTPUT
6756  7041          CIA                 /NO, SET OF COUNT
6757  3367          DCA FCOUNT          /TO PRINT F PLACES
6760  1367          TAD FCOUNT
6761  11 7          TAD EXP
6762  7540          SMA SZA             /E F ?
6763  5317          JMP XXX             /YES, PRINT XS
6764  1167          TAI FORM
6765  7500          SMA                 /F - F D ?
6766  7700          CLA                 /NO, TAKE F - E
6767  7041          CIA                 /YES, TAKE F - F D
6770  1157          TAD EXP
6771  7041          CIA
6772  3364          DCA TEMPX           /SET D MINUS F
6773  1361          TAD M7
6774  3365          DCA COUNT           /MAX.NO OF SIG.FIGS.
6775  1157  BACK,   TAD EXP
6776  1764          TAD I TEMPX
6777  7650          SNA CLA             /F - E ?
6300  5330          JMP DIG             /YES, PRINT DIGIT
6301  1364          TAD TEMPX           /NO,
6302  7001          IAC
6303  7710          SPA CLA             /F - 1 ?
6304  1360          TAD SPCE            /YES,SPACE, NO/ZERO
6305  4323  IN,     JMS OUTX            /PRINT CHARACTER
6306  2364          ISZ TEMPX           /F CHARACTERS PRINTED?
6307  5775          JMP BACK            /NO
6310  1367          TAD POINT           /YES,
6311  4757          JMS I OUT           /PRINT DECIMAL POINT
6312  5775          JMP BACK
6313  7040  DECR,   CMA
6314  1366          TAD PLCE
6315  3366          DCA PLCE
6316  5336          JMP RET
6317  7200  XXX,    CLA
6320  1363          TAD CHX
6321  4323          JMS OUTX            /PRINT 'X'
6322  5320          JMP .-2             /AND REPEAT
6323  0000  OUTX,   0
```

```
6324  4757          JMS I OFUT      /PRINT CHARACTER
6325  2367          ISZ FCOUNT      /# CHARACTERS PRINTED?
6326  5723          JMP I OUTX      /NO, RETURN
6327  5600          JMP I FIX1      /YES, NUMBER FINISHED
6330  7040  DIG,    CMA
6331  1157          TAD EXP         /REDUCE E BY 1
6332  3157          DCA EXP
6333  2365          ISZ SCOUNT      /6 SIG.FIGS.PRINTED?
6334  5340          JMP .+4         /NO
6335  7040          CMA             /YES,
6336  3365          DCA SCOUNT      /RESET COUNT TO -1
6337  5305          JMP IN          /AND LEAVE C(AC) = 0
6340  1410          TAD I INDEX     /TAKE NEXT DIGIT
6341  5305          JMP IN
6342  1364  FLOF,   TAD MIN6       /PRINT 6 DIGITS
6343  3367          DCA FCOUNT      /AFTER DECIMAL POINT
6344  4757          JMS I OFUT      /PRINT "0"
6345  1363          TAD FOINT
6346  4757          JMS I OFUT      /PRINT "."
6347  2700          ISZ FIX1        / NOREM,RETURN ADDR.
6350  1410          TAD I INDEX     /TAKE NEXT DIGIT
6351  4823          JMS OUTX        /PRINT IT
6352  5350          JMP .-2         /AND REPEAT
6353  0007  N7,     7
6354  7772  MIN6,   -6
6355  7766  N10,    -12
6356  6367  BUFST,  BUFFER -1
6357  6140  OFUT,   OUTDG
6360  7760  SECT,   740-260
6361  7771  M7,     -7
6362  7776  FOINT,  256-260
6363  0050  CHX,    330-260
6364  0000  TEMPX,  0
6365  0000  SCOUNT, 0
6366  0000  FIX1,   0
6367  0000  FCOUNT, 0
6370  0000  BUFFER, 0
              /6371-6377: OUTPUT BUFFER
                      *6400
              /FLOATING POINT SINE.
6400  0000  FSIN,   0
6401  1160          TAD HORD        /X 0?
6402  7740          SMA SZA CLA
6403  5210          JMP .+5         /YES
6404  1160          TAD HORD
6405  7700          SMA CLA         /NO X 0?
6406  5600          JMP I FSIN      /YES SIN(0) 0
6407  4363          JMS FNEG        /SIN( X)  SIN(X)
6410  3347          DCA FNTR        /X MODULO 2PI
6411  4407          FENTER
6412  4317          FDIV TWOPI
6413  6330          FPUT XSQR
6414  0000          FEXT
6415  4547          JMS I FIXR
6416  4350          JMS FLOA
6417  4407          FENTER
6420  6325          FPUT X
6421  5330          FGET XSQR
6422  7325          FSUB X
6423  3317          FMPY TWOPI
6424  6325          FPUT X
6425  2347          FSUB PI         /X PI?
6426  0000          FEXT
6427  1160          TAD HORD
6430  7710          SPA CLA
6431  5241          JMP .+10        /YES
6432  4407          FENTER          /NO!
6433  6325          FPUT X          /SIN(X-PI)=-SINX
6434  0000          FEXT
6435  1347          TAD FNTR
6436  7650          SNA CLA
6437  7040          CMA
6440  3347          DCA FNTR
6441  4407          FENTER          /X PI/2?
6442  5325          FGET X
6443  7314          FSUB PIOT
6444  0000          FEXT
6445  1160          TAD HORD
6446  7710          SPA CLA
6447  5255          JMP .+6         /YES
6450  4407          FENTER          /NO
6451  5322          FGET PI         /SINX-SIN(PI-X)
6452  2325          FSUB X
6453  6325          FPUT X
6454  0000          FEXT
6455  4407          FENTER
6456  5325          FGET X
6457  4314          FDIV PIOT
6460  6325          FPUT X
6461  7325          FMPY X
6462  6330          FPUT XSQR
6463  5111          FGET C9
6464  3330          FMPY XSQR
6465  1336          FADD C7
6466  3330          FMPY XSQR
6467  1341          FADD C5
6470  3330          FMPY XSQR
6471  1344          FADD C3
6472  3330          FMPY XSQR
6473  1314          FADD PIOT
6474  3325          FMPY X
6475  0000          FEXT
6476  2347          ISZ FNTR
6477  5600          JMP I FSIN
6500  4363          JMS FNEG
6501  7200          CLA
6502  5600          JMP I FSIN
              /FLOATING POINT COSINE.
6503  0000  FCOS,   0
6504  4407          FENTER          /COSX=SIN(PI/2-X
6505  6325          FPUT X
6506  5314          FGET PIOT
6507  2325          FSUB X

6510  0000          FEXT
6511  1303          TAD FCOS
6512  3200          DCA FSIN
6513  5201          JMP FSIN+1
              /CONSTANTS AND POINTERS.
6514  0001  PIOT,   0001            /PI/2
6515  3110          3110
6516  3755          3755
6517  0003  TWOPI,  0003            /2*PI
6520  3110          3110
6521  3755          3755
6522  0002  PI,     0002            /PI
6523  3110          3110
6524  3755          3755
6525  0000  X,      0
6526  0000          0
6527  0000          0
6530  0000  XSQR,   0
6531  0000          0
6532  0000          0
6533  7764  C9,     7764
6534  2366          2366
6535  5735          5735
6536  7771  C7,     7771
6537  5466          5466
6540  6317          6317
6541  7775  C5,     7775
6542  2431          2431
6543  5053          5053
6544  0000  C3,     0000
6545  5325          5325
6546  0420          0420
6547  0000  FNTR,   0
              /FLOAT ACCU.
6550  0000  FLOA,   0
6551  3160          DCA HORD
6552  7300          CLA CLL
6553  3161          DCA LORD
6554  1362          TAD C13
6555  3157          DCA EXP
6556  4407          FENTER
6557  7000          FNOR
6560  0000          FEXT
6561  5750          JMP I FLOA
6562  0013  C13,    0013
              /NEGATION SUBROUTINE.
6563  0000  FNEG,   0
6564  4767          JMS I ACMIN     /CALL SUBROUTINE
6565  7240          CLA CMA         /IN INTERPRETER
6566  5763          JMP I FNEG
6567  7000  ACMIN,  ACMINS
              /FLOATING SQUARE SUBROUTINE.
6570  0000  SQUARE, 0
6571  4407          FENTER
6572  6162          FPUT FPAC1
6573  3162          FMPY FPAC1
6574  0000          FEXT
6575  5770          JMP I SQUARE
                    *6600
              /FLOATING POINT ARITHMETIC INTERPRETER.
6600  0000  FPNT,   0
6601  4773          JMS I NEXT2
6602  3173          DCA OVER1
6603  3174          DCA OVER2
6604  1600          TAD I FPNT      /GET NEXT INSTR-
6605  3254          DCA JUMP        /UCTION.
6606  1254          TAD JUMP
6607  0264          AND PAGENO      /GET PAGE BIT
6610  7650          SNA CLA         /PAGE ZERO?
6611  5214          JMP .+3         /YES
6612  1262          TAD MASK5       /NO
6613  0200          AND FPNT        /C(FPNT)0-4 CON-
6614  3257          DCA ADDR        /TAINS PAGE BITS
6615  1263          TAD MASK7       /GET 7BIT ADDRES
6616  0254          AND JUMP        /S
6617  1257          TAD ADDR
6620  3257          DCA ADDR
6621  1265          TAD INDRCT      /INDIRECT BIT=1?
6622  0254          AND JUMP
6623  7650          SNA CLA
6624  5774          JMP I DIR1      /NO-GO ON
6625  1657          TAD I ADDR      /YES DEFER
6626  3257          DCA ADDR
6627  4775          JMS I INDIR1
6630  2200  LOOF01, ISZ FPNT
6631  1657          TAD I ADDR
6632  3170          DCA EX1         /EXPONENT
6633  1257          TAD ADDR
6634  3260          DCA SAVE
6635  2260          ISZ SAVE
6636  1660          TAD I SAVE
6637  3171          DCA AC1H        /HIGH ORDER MANTISSA
6640  2260          ISZ SAVE
6641  1660          TAD I SAVE
6642  3172          DCA AC1L        /LOW ORDER MANTISSA
6643  1254          TAD JUMP
6644  7106          CLL RTL
6645  4776          JMS I RESET1
6646  0261          AND MASK3       /GET BITS 0-2
6647  1266          TAD TABLE       /OPCODE LOOKUP
6650  3255          DCA JUMP2       /IN TABLE
6651  1655          TAD I JUMP2
6652  3255          DCA JUMP2
6653  5655          JMP I JUMP2     /GO THERE
6654  0000  JUMP,   0
6655  0000  JUMP2,  0
6656  0000  GO2,    0
6657  0000  ADDR,   0
6660  0000  SAVE,   0
6661  0017  MASK3,  0017
6662  7600  MASK5,  7600
6663  0177  MASK7,  0177
6664  0200  PAGEND, 0200
```

```
6665  0400  INDRCT, 0400
6666  6667  TABLE,  .+1
6667  6742          EXIT            /TABLE USED IN
6670  6721          FLAD            /INTERPRETING
6671  6720          FLSU            /BITS 0 2 OF
6672  6761          FLMY            /PSEUDO INSTRUCT
6673  7310          FLDV            /ION.IF OPCODE 0
6674  6677          FLGT            /GO TO EXIT AND
6675  6706          FLPT            /INTERPRET
6676  6737          NORF            /BITS 8-11
6677  1170  FLGT,   TAD EX1         /FGET=5
6700  3157          DCA EXP
6701  1171          TAD AC1H
6702  3160          DCA HORD
6703  1172          TAD AC1L
6704  3161          DCA LORD
6705  5201          JMP FFNT+1
6706  1157  FLPT,   TAD EXP         /FPUT-6
6707  4777          JMS I STORE2
6710  3657          DCA I ADDR
6711  2257          ISZ ADDR
6712  1160          TAD HORD
6713  3657          DCA I ADDR
6714  2257          ISZ ADDR
6715  1161          TAD LORD
6716  3657          DCA I ADDR
6717  5201          JMP FFNT+1
6720  4741  FLSU,   JMS I OPMINS   /FSUB-2
6721  4771  FLAD,   JMS I ALGN      /FLAD 1 FIRST
6722  5201          JMP FFNT+1      /ALIGN EXPONENTS
6723  4772          JMS I UNORM
6724  1173          TAD OVER1       /TRIPLE PRECIS-
6725  1174          TAD OVER2       /ION ADDITION
6726  3174          DCA OVER2       /SINCE BITS ARE
6727  7004          RAL             /SHIFTED RIGHT.
6730  1172          TAD AC1L
6731  1161          TAD LORD
6732  3161          DCA LORD
6733  7004          RAL
6734  1171          TAD AC1H
6735  1160          TAD HORD
6736  3160          DCA HORD
6737  4770  NORF,   JMS I NORM      /NORMALIZE
6740  5201          JMP FFNT+1
6741  7412  OPMINS, MINUS2
6742  1254  FXIT,   TAD JUMP        /OPCODE-0
6743  0261          AND MASK3       /ARE BITS 8-11=0
6744  7450          SNA
6745  5600          JMP I FPNT      /YES=FEXT
6746  1360          TAD ACON6       /LOOKUP ON TABLE
6747  3255          DCA JUMP2
6750  1655          TAD I JUMP2
6751  3255          DCA JUMP2
6752  1200          TAD FPNT
6753  3256          DCA G02
6754  4655          JMS I JUMP2     /CALL AS SUBROUTINE
6755  1256          TAD G02         /RESTORE F.P.
6756  3200          DCA FPNT        /POINTER
6757  5201          JMP FFNT+1
6760  7544  ACON6,  TABLE6-1
6761  7201  FLMY,   CLA IAC         /FMPY-3
6762  1170          TAD EX1
6763  1157          TAD EXP         /ADD EXPONENTS
6764  3157          DCA EXP
6765  4767          JMS I MULT      /MULTIPLY
6766  5201          JMP FFNT+1
6767  7221  MULT,   DMULT
6770  7600  NORM,   DNORM
6771  7020  ALGN,   ALIGN
6772  7564  UNORM,  DUNORM
6773  4334  NEXT2,  NEXT1
6774  4340  DIR1,   DIR
6775  4320  INDIR1, INDIR
6776  4325  RESET1, RESET
6777  4331  STORE2, STORE1
              *7000
7000  0000  ACMINS, 0               /ROUTINE TO PER-
7001  7300          CLL CLA         /FORM TRIPLE
7002  1174          TAD OVER2       /PRECISION
7003  7041          CMA IAC         /NEGATION OF
7004  3174          DCA OVER2       /FLOATING AC
7005  1161          TAD LORD
7006  7040          CMA
7007  7430          SZL
7010  7101          CLL IAC
7011  3161          DCA LORD
7012  1160          TAD HORD
7013  7040          CMA
7014  7430          SZL
7015  7101          CLL IAC
7016  3160          DCA HORD
7017  5600          JMP I ACMINS
7020  0000  ALIGN,  0               /SUBR.TO ALIGN
7021  1160          TAD HORD        /BINARY POINTS
7022  7640          SZA CLA         /FOR ADD SUBTR.
7023  5227          JMP .+4
7024  1161          TAD LORD        /MANTISSA=0?
7025  7650          SNA CLA
7026  5354          JMP NOWHERE     /YES
7027  1171          TAD AC1H        /OPERAND=0?
7030  7640          SZA CLA
7031  5235          JMP .+4
7032  1172          TAD AC1L
7033  7650          SNA CLA
7034  5620          JMP I ALIGN     /BOTH ZERO-EXIT
7035  1170          TAD EX1
7036  7041          CMA IAC
7037  1157          TAD EXP
7040  7450          SNA             /EX NTS EQUAL?
7041  5330          JMP DONE        /YES
7042  7510          SPA
7043  7041          CMA IAC
7044  3366          DCA AMOUNT

7045  1366          TAD AMOUNT
7046  1367          TAD TEST        /CAN EXPONENTS
7047  7710          SPA CLA         /BE ALIGNED
7050  5256          JMP .+6         /YES
7051  4446          JMS OUTGO       /NO
7052  7410          SZL
7053  1374          TAD TAG2
7054  1373          TAD TAG1
7055  5342          JMP NOGO
7056  4333          JMS OUTGO
7057  7420          SNL             /SET UP ADDRESS
7060  1374          TAD TAG2
7061  1373          TAD TAG1
7062  3370          DCA TEST3
7063  1366          TAD AMOUNT
7064  1770          TAD I TEST3
7065  3770          DCA I TEST3
7066  2370          ISZ TEST3
7067  1370          TAD TEST3
7070  3371          DCA TEST4
7071  2371          ISZ TEST4
7072  1371          TAD TEST4
7073  3372          DCA TEST5
7074  2372          ISZ TEST5
7075  7240          CLA CMA         /SUBTR.1  NUM SHIFT
7076  1366          TAD AMOUNT      /COUNT FOR ASR
7077  3304          DCA SHIFT3      /INSTRUCTION
7100  1771          TAD I TEST4     /LOW ORDER
7101  7421          MQL
7102  1770          TAD I TEST3     /HIGH ORDER
7103  7415          ASR
7104  0000  SHIFT3, 0
7105  3304          DCA SHIFT3      /HIGH ORDER
7106  7501          MQA             /ORDER ALIGNMENT
7107  3333          DCA UNTGO       /LOW ORDER
7110  1366          TAD AMOUNT      /ORDER ALIGNMENT
7111  1332          TAD MINUS
7112  7510          SPA
7113  5257          JMP TEST15      /LESS THAN 15 SHIFTS
7114  3371          DCA .+5         /AMOUNT .> SHIFTS.
7115  1771          TAD I TEST4     /LOW ORDER
7116  7421          MQL
7117  1770          TAD I TEST3     /HIGH ORDER.
7120  7417          LSR
7121  0000  SHIFT2, 0
7122  7701          MQA CLA
7123  3772          DCA .+5         /OVERFLOW
7124  1504          TAD SHIFT3
7125  3770          DCA I TEST3
7126  1333          TAD UNTGO
7127  3771          DCA .+4
7130  7000  DONE,   NOP             /ALIGN
7131  5600          JMP I ALGN
7132  7763  MINUS,  -5
7133  0000  OUTGO,  0               / DETERMINE WHICH
7134  1170          TAD EX1         /TO ADJ
7135  7041          CMA IAC
7136  1157          TAD EXP
7137  7004          RAL
7140  7200          CLA             /L NK ON IF EXT EXP
7141  5733          JMP I OUTGO
7142  1770  NOGO,   DCA I TEST3     /CANT BE ALIGNED
7143  1770          TAD I TEST3     /LARGEST GOES IN D
7144  3157          DCA EXP         /AM
7145  2370          ISZ TEST3
7146  1770          TAD I TEST3
7147  3160          DCA HORD
7150  2370          ISZ TEST3
7151  1770          TAD I TEST3
7152  3161          DCA LORD
7153  5670          JMP I ALIGN
7154  1170  NOWHERE, TAD EX1         /MANTISSA 0
7155  3157          DCA EXP
7156  5630          JMP DONE
7157  7240  TEST15, CLA CMA         /SUBTR.1 FROM SHIFT
7160  1366          TAD AMOUNT      /COUNT FOR LESS
7161  3371          DCA SHIFT2      /IN INSTRUCTION.
7162  1772          TAD I TEST5     /OVERFLOW
7163  7421          MQL
7164  1771          TAD I TEST4     /LOW ORDER
7165  5320          JMP SHIFT2 I
7166  0000  AMOUNT, 0
7167  7760  TEST2,  -20
7170  0000  TEST3,  0
7171  0000  TEST4,  0
7172  0000  TEST5,  0
7173  0157  TAG1,   EXP
7174  0011  TAG2,   EX1 EXP
7175  0000  EX.TA,  0               / DUMMY SUBROUTINE
7176  5775          JMP   EXTRA
              *7200
7200  0000  DIVL,   0               /SHIFT FAC RIGHT
7201  7300          CLA CLL
7202  1160          TAD HORD
7203  7510          SPA
7204  7130          CLL CML
7205  7010          RAR
7206  3160          DCA HORD
7207  1161          TAD LORD
7210  7010          RAR
7211  3161          DCA LORD
7212  1174          TAD OVER2
7213  7010          RAR
7214  3174          DCA OVER2
7215  7100          CLL
7216  1157          TAD EXP
7217  7000          NOP
7220  5600          JMP I DIV
7221  0000  DMULT,  0               / DOUBLE PRECI. MULT
7222  7300          CLA CLL         /SAVE PROD TRIPLE
7223  4330          JMS I SIGN      /PRECISION.
7224  1173          TAD A CC        /MULT BY A ITEM
7225  5230          DCA .+3
```

```
/ 6    6          TAD LORD
7227  24 ,        MQA MUY
2430  0000  D,    0
7231  3174        DCA OVER.
7232  1160        TAD HORD
7233  5256        DCA .+3
7234  1177        TAD ACIL
7235  7435        MQL MUY
7236  0000  KEEP,  0
7237  3230        DCA D
7240  7501        MQA
7241  1174        TAD OVER?
7242  3174        DCA OVER?
7243  7004        RAL
7244  1230        TAD D
7245  3230        DCA D
7246  1171        TAD ACIH
7247  5253        DCA .+3
7250  1177        TAD LORD
7251  7435        MUY MUY
7252  0000        0
7253  3156        DCA KEEP
7254  7501        MQA
7255  1174        TAD OVER?
7256  3174        DCA OVER.
7257  7004        RAL
7260  1156        TAD KEEP
7261  1230        TAD D
7262  5253        D A B
7263  7004        RAL
7264  3156        DCA KEEP
7265  1160        TAD HORD
7266  5271        DCA .+3
7267  1171        TAD ACIH
7270  7435        MQL MUY
7271  0000        0
7272  1160        DCA HORD
7273  7401        MQA
7274  1230        TAD D
7275  3161        DCA LORD
7276  7004        RAL
7277  1160        TAD HORD
7300  1256        TAD KEEP
7301  3150        DCA QUOT
7302  4747        JM  I NEGM
7303  5174        DCA OVER
7304  7341        CLA SGN
7305  6671        JM  I DMULT
7306  4747        JMS I MINT
7307  6671        JMP I DMULT
7310  1177  DIVV, TAD ACIH
7311  7640        SZA CLA
7312  5316        JMP .+4
7313  1177        TAD ACIH
7314  7650        SNA CLA
7315  5266        JMP I ERROR     /DIVISION BY 0
7316  1170        TAD EXP
7317  7041        CMA IAC
7320  1057        TAD EXP
7321  3157        D A EXP         /SUBTRACT 20+2
7322  4330        JMS  IGN        /SET UP SIGN
7323  4750        JM  I DIVIDE    /DIVIDE
7324  7377        AD  43
7325  31          DCA DMULT
7326  5340        JMP FIDV 2
7327  5660        RENT4I
7330  0000  SIGN,  0              /TEST SIGN OF
7331  1357        TAD KEEP        /KEEP TEST IN AC
7332  3351        DCA IGN         /MY MULTIPLY
7333  1160        TAD HORD        /AND DIVID
7334  7700        SMA CLA
7335  5340        JMP  .+3
7336  4754        JMS I MINS
7337  2351        ISZ  IGN
7340  1171        TAD ACIH
7341  7700        SMA CLA
7342  5740        JMP I IGN
7343  4754        JMS I MINS
7344  2351        ISZ SGN
7345  7600        NOP
7346  5730        JMP I SIGN
7347  7600  NORMF,  .NORM
7350  7401  DIVIDE, .+1
7351  0000  SGN,   0
7352  0076  KEEP,  7776
7353  7412  MINS,  MINS2          / ADDRESS
7354  7600  MINT,  AMIN
7355  7401  ERROR, ERROR1
7356  0000  DIV ,  0              /SHIFT OF AND
7357  7300        CLA CLL         /RIGHT=TRUE
7360  1177        TAD ACIH        /DIVISION
7361  7110        SPA
7362  7100        CLL CML
7363  7010        RAR
7364  3171        DCA ACIH
7365  1172        TAD ACIL
7366  7010        RAR
7367  3172        DCA ACIL
7370  1173        TAD OVER1
7371  7010        RAR
7372  3173        DCA OVER1
7373  7100        CLL
7374  5756        JMP I DIV2
                  #7400
7400  6601  RETN2,  RETN1
7401  0000  ERROR1,  TAD GOOF        /DIVISION BY ZERO
7402  3157        D A EXP         /SET TO LARGEST
7403  1211        TAD GOOF        /EVALUE
7404  3160        DCA HORD
7405  7040        MA
7406  3161        DCA LORD
7407  2377        ISZ FLAG        /SET FLAG
7410  7600        JMP I RETN.
```

```
7411  3777  GOOF,  3777
7412  0000  MINUS,  0              /NEGATE OPERAND
7413  7300        CLA CLL         /TRIPLE PRECISION
7414  1173        TAD OVER1
7415  7041        CMA IAC
7416  3173        DCA OVER1
7417  1172        TAD AC1L
7420  7040        CMA
7421  7430        SZL
7422  7101        CLL IAC
 423  3172        DCA AC1L
7424  1171        TAD AC1H
7425  7040        CMA
7426  7430        SZL
7427  7101        CLL IAC
7430  3171        DCA AC1H
7431  5612        JMP I MINUS2
                  /DOUBLE PRECISION DIVIDE
7432  0000  DUBDIV,  0              /OPERANDS NORMALIZED
7433  3353        DCA DVFLG       /C  AS F AC.
7434  1172        TAD AC1L        /SHIFT DIVISOR LEFT
7435  7104        CLL RAL         /1 BIT TO AVOID
7436  1 ??        .CA IV3         /OVERFLOW
7437  1171         AT AC1H
7440  7004        RAL
7441  3276        DCA IV4
7442  1276        TAD IV4
7443  3250        DCA DV2
7444  1161        TAD LORD
7445  7421        MQL             /HORD*LORD*2**-12
7446  1160        TAD HORD        /     ----
7447  7407        DVI             /     AC1H
7450  0000  DV2,   0
7451  3250        DCA DV2         /REMAINDER
7452  7501        MQA
7453  3160        DCA HORD        /QUOTIENT
7454  7405        MUY             /QUOTIENT*AC1L*2**-12
7455  0000  DV3,   0
7456  7141        CLL CMA IAC
7457  1250        TAD DV2
7460  7450        SNA
7461  5303        JMP DV5         /H.PROD.-REMAINDER
7462  7470        SNL
7463  5315        JMP DV6         /H.PROD. REMAIN.ER
7464  3255        DCA DV5         /REMAINDER H PROD.
7465  7040        CMA
7466  3333        ICA DVFLG
7467  7501        MQA             /SUBTR...ER PRODUCT
7470  7141        CLL CMA IAC     /FROM DV3+2**-24
7471  7421        MQL
7472  7420        SNL
7473  7040        CMA             /SUBTRACT 1 FROM DV3
7474  1255        TAD DV3
7475  7407        DVI             /REM QUOT*AC1L*2** 12
7476  0000  DV4,   0              /     -
7477  7701        MQA CLA         /       AC1H
7500  7100        CLL CML         /FOR REM. H.PROD.
7501  2333        ISZ DVFLG       /WAS REM. H.PROD.
7502  7141        CMA IAC CLL     /NO
7503  3161  DV5,   DCA LORD      /YES
7504  7470        SNL
7505  7040        CMA             /SUBTRACT 1 FROM
7506  1160        TAD HORD        /H.O.QUOTIENT
7507  7410        SFA
7510  5334        JMP DV7         /QUOTIENT R GHT 1 BIT
7511  5160        ICA HORD
7512  5637        JMP I DUBDIV    /EXIT
7513  7041  IV6,   CMA IAC
7514  3250        DCA DV2         /H.PROD. REMAINDER
7515  1276        TAD IV4         /WATCH OUT FOR
7516  7141        CLL CMA IAC     /DIVIDE OVERFLOW
7517  1250        TAD DV2
7520  7430        SNL
7521  5326        JMP .+5
7522  3250        DCA DV2         /FFF.DECREASE HIGH
7523  7040        CMA             /H.ORD.QUOT.BY 1 AND
7524  1160        TAD HORD        /INCR.REMAINDER BY
7525  3160        DCA HORD        /HIGH ORDER DIVISOR
7526  7200        CLA
7527  1250        TAD DV2
7530  7440        SZA
7531  5275        JMP DV4-1
7532  5301        JMP DV5 1
7533  0000  DVFLG,  0
7534  7110  DV7,   CLL RAR        /SHIFT 2 WORD QUOT.
7535  3160        DCA HORD        /RIGHT 1 BIT AND
7536  1161        TAD  ORD        /AI.ST EXPONENT
7537  7010        RAR
7540  3161        DCA LORD
 541  2157        ISZ EXP
7542  5663        JMP I DUBDIV
7543  5632        JMP I DUBDIV
7544  7456  RAR3,  DIV3
7545  6570  TABLE,  SQUARE       /TABLE FOR INTER
7546  7665        SQRDOT          /RETATION OF
7547  6400        SIN             /BITS 0 11
7550  6503        COS
7551  7775        ABS
7552  4506        FDF0
7553  4513        FDF1
7554  7000        ACMINS
7555  5600        FLINTP
7556  6000        FLCUTF
7557  7175        EXIT6
7560  7175        EXIT6
7561  7175        EXIT6
7562  7175        EXIT6
7563  7175        EXIT6
7564  0000  DUNORM,  0
7565  4744        JMS I RAR3      /SHIFT OPERAND RIGHT
7566  4772        JMS I RAR1
7567  2170        ISZ EXI
7570  7000        NOP
```

```
7571  7764          JMP I DNORM
7572  7200  AAA1,   DIVI
                    #3600
7600  0000  DNORM,  0                 /SUBR. TO NORMALIZE
7601  7320          CLA CLL CML       /FLOATING AC
7602  1160          TAD MQRD
7603  7710          SPA CLA           /IS MANTISSA NEG.
7604  4772          JMS I NEG         /YES
7605  7430          SZL               /O LINK IF NEG
7606  7040          CMA
7607  3376          DCA SIGN1
7610  1160          TAD MQRD
7611  7640          SZA CLA           /IS MANTISSA 0
7612  5225          JMP LOF           /NO.
7613  1161          TAD LORD
7614  7510          SPA
7615  5226          JMP LOF+1         /NO.
7616  3160          DCA MQRD          /SHIFT LEFT 12 BITS.
7617  1174          TAD OVER2
7620  3161          DCA LORD
7621  3174          DCA OVER1
7622  1763          TAD FOURTN
7623  1157          TAD EXP

7624  3157          DCA EXP
7625  1161  LOF,    TAD LORD
7626  7421          MQL
7627  1160          TAD MQRD
7630  7411          NMI
7631  7450          SNA
7632  3157          DCA EXP           /MANTISSA=0
7633  3160          DCA MQRD
7634  7441          SCA               /GET STEP COUNTER.
7635  7450          SNA
7636  5255          JMP EX+1          /NO. SHIFTING.
7637  7041          CMA IAC
7640  1157          TAD EXP
7641  3157          DCA EXP
7642  7441          SCA
7643  1764          TAD ONE
7644  3251          DCA SHIFT
7645  1174          TAD OVER2
7646  7421          MQL
7647  1161          TAD LORD
7650  7413          SHL
7651  0000  SHIFT,  0                 /NUMBER OF SHIFTS 1
7652  3161          DCA LORD
7653  7501          MQA
7654  3174          DCA OVER2
7655  2262  EXIT1,  ISZ SIGN1
7656  4772          JMS I NEG
7657  4661          JMS I FAT 41
7660  5600          JMP I DNORM
7661  4346  FATCH1, FATCH
7662  0000  SIGN1,  0
7663  7764  FOURTN,  14
7664  7777  ONE,    -1
7665  0000  SQROOT, 0                 /FLOAT,SQUARE ROOT
7666  3371          DCA FLAG1         /TAKES ROOT OF ABS.
7667  1160          TAD MQRD          /VALUE
7670  7700          SMA CLA
7671  5274          JMP .+3
7672  4772          JMS I NEG         /NUMBER IS NEGATIVE
7673  2371          ISZ FLAG1
7674  4407          FENTER
7675  6365          FPUT SQRT
7676  0000          FEXT              /NEWTONS METHOD.
7677  1157          TAD EXP           /NUMBER
7700  7100          CLL               /-  -      +AN
7701  7510          SPA               /   AN
7702  7020          CML               /-  ---      -AN+1
7703  7010          RAR               /    2
7704  7430          SZL               /MAKE FIRST APPROX.
7705  7001          IAC
7706  3362          DCA ITER1
7707  1370          TAD SQCON1        /3015
7710  3363          DCA ITER1+1
7711  3364          DCA ITER1+2
7712  1366          TAD SQRT+1
7713  7640          SZA CLA
7714  5325          JMP CLCU
7715  1367          TAD SQRT+2
7716  7640          SZA CLA
7717  5325          JMP CLCU
7720  3157          DCA EXP           /NUMBER 0
7721  5665          JMP I SQROOT
7722  4407  ROOTGO, FENTER
7723  6362          FPUT ITER1
7724  0000          FEXT
7725  4407  CLCU,   FENTER
7726  6365          FOFF SQR1
7727  4362          FDIV ITER
7730  1362          FADD ITER1
7731  0000          FEXT
7732  7240          CLA CMA
7733  1157          TAD EXP
7734  3357          DCA EXP
7735  1157          TAD EXP
7736  7041          CMA IAC
7737  1362          TAD ITER1
7740  7640          SZA CLA           /EXPONTS EQUAL?
7741  5322          JMP ROOTGO        /NO
7742  1160          TAD MQRD          /ALL HIGH ORDER
7743  7041          CMA IAC           /MANTISSAS EQUAL
7744  1363          TAD ITER1+1
7745  7640          SZA CLA
7746  5322          JMP ROOTGO        /NO
7747  1161          TAD LORD
7750  7041          CMA IAC
7751  1364          TAD ITER1+2       /DO LOW ORDER
7752  7500          SMA               /MANTISSAS AGREE
7753  7041          CMA IAC           /WITHIN 1 BIT?
7754  7001          IAC

7755  7710          SPA CLA
7756  5361          JMP ROOTGO        /NO
7757  1371          TAD FLAG1
7760  3177          DCA FLAG
7761  5665          JMP I SQROOT
7762  0000  ITER1,  0
7763  0000          0
7764  0000          0
7765  0000  SQRT,   0
7766  0000          0
7767  0000          0
7770  3015  SQCON1, 3015
7771  0000  FLAG1,  0
7772  7000  NEG,    ACMIN;
                    /ABSOLUTE VALUE  IF FLOATING POINT NUMBER
7773  0000  ABS,    0
7774  1160          TAD MQRD
7775  7710          SPA CLA
7776  4772          JMS I NEG
7777  5773          JMP I ABS;
                    /
```

SYMBOL	TABLE
AB	7773
ACMIN	6567
ACMINS	7000
ACON6	6760
ACIH	0171
ACIL	0172
ADDR	6657
A_GN	6771
ALIGN	7070
AMOUNT	7166
ANS	4233
ANSWER	0147
ANSWR	0140
ANS1	4706
ASC	4515
ASCII	4534
ASCIX	0150
ASLIY	0151
ASR	7415
BACK	6275
BCKSL	4235
BCKWRD	5706
BEXF	6131
BFRST	6134
BKWRD	0144
BLKTP	0115
BLOCK	4155
BLOCKN	4156
BUFIER	6370
BUFST	6356
BUG	0135
BUG1	4365
CHAR	4521
CHARAC	4771
CHF	6131
CHX	6363
CLCU	7725
CONV	5230
CONVRT	0147
CONV1	5236
COS	0004
COUNT	0156
CNLF	5365
C12	5775
C13	6562
C144	5773
C256	5770
C255	5771
C260	6151
C27	5616
C3	6544
C5	6541
C7	6536
C9	6533
D	7230
DECONV	5617
DELR	6313
DF0	4344
DF1	4345
DGFT	5776
DIG	6330
DIGIT	5264
DIR	4140
DIR1	6774
DIVIDE	7350
DIVTWO	6152
DIV1	7200
DIV2	7356
DMULT	7221
DNORM	7600
DONE	7130
DUBDIV	7432
DUBLAD	5671
DUNORM	7564
DUFLG	7513
DVI	7407
DV1	4177
DV2	7450
DV3	7455
DV4	7476
DV5	7503
DV6	7513
DV7	7534
ERROR	7355
ERROR1	7401
EXIT	6742
EXIT1	7655
EXIT6	7175
EXF	0157
EXF1	0175
EX1	0170
FABS	0005
FADD	1000
FCDF0	0006
FCDF1	0007
FCOS	6503
FCOUNT	6467
FDF0	4306
FDF1	4313
FDIV	4000
FENTER	4407
FFXC	5774
FEXFPT	6144
FEXT	0000
FGET	5000
FG02	6051
FG03	6066
FG04	6071
FG06	6101
FG07	6114
FIX	4157
FIXR	6142
FIX1	6700
FLAD	6731
FLAG	0177
FLAGTF	0134
FLAG1	7771
FLAG2	5363
FLDV	7310
FLG1	6677
FLINTF	5600
FLMY	6761
FLOA	6550
FLOAT	0143
FLOF	6342
FLOLTP	6000
FLFT	6706
FLSU	6720
FMPY	3000
FNEG	6563
FNOR	7000
FORM	0167
FORMAT	0166
FORWRD	5217
FOUR	6136
FOUTN	7663
FOUTN	6037
FPAC	0162
FINT	6600
FPUT	6000
FRWRD	0145
FSIN	6400
FSUB	2000
FXAD	6146
GOOF	7411
GO1	0165
GO2	6656
HOLD	4305
HORD	0160
HTEMP	5634
IBM	5265
IBMTBL	5266
IN	6330
INDEX	0010
INDEXC	0011
INDIN	4370
INDIK1	6775
INDRCT	6662
INFUT	0011
ITFF1	7717
JUMF	6654
JUMP2	6655
KEEP	7246
KKBX	4200
K7	6353
LESS15	7157
LF	5674
LOOF01	6630
LOF	7675
LOKD	0161
LSR	7417
LTEMF	5651
MASKX	4526
MASKY	4525
MASK1	6130
MASK2	6177
MASK3	6661
MASK5	6663
MASK7	6663
MASK77	4514
MATRIX	4522
MATRX	4524
MEMO	4044
MESS	4373
MINS	7354
MINS2	7353
MINUS2	7412
MINUS7	6133
MIN10	5301
MIN15	7132
MIN6	6354
MOA	7501
MOL	7421
MOLMUY	7425
MRTRN	4233
MRUB	4234
MSIGN	5706
MSKADR	4477
MSKNUM	7741
MSKFFN	4527
MSNFT	6130
MTRXN	4523
MULT	6767
MULT10	5636
MULT2	5655
MUY	7405
M10PT	6142
M12	5774
M13	4176
M144	5772
M2FT	6143
M260	4303
M7	6361
NEG	7777
NEGATE	0010
NEXT	4530
NEXT1	4334
NEXT2	6773
NMI	7411
NOGO	7142
NOHERE	7154
NORF	6717
NORM	6770
NORMF	7347
N10	6335
ONE	7664
OFMINS	6741
OFUT	6317
ONTENT	0154
OUTDG	6145
OUTGO	7133
OUTFUT	0015
OUTX	6325
OVERK1	0173
OVERP	0174
PAGFNO	6664
PATCH	4346
PATCH1	7661
PCRLF	0146
PI	6535
PIOT	6514
PIASC1	4442
PIASC2	4442
PICF	6366
PLCF	6503
PLCNT	4517
PLDD	6514
PLDK	6515
PLDU	6517
PLOT	4403
PLOTA	5470
PLOTDN	5534
PLOTDX	5567
PLOTDY	5570
PLOTMV	5572
PLOTNA	5571
PLOTNX	5565
PLOTNY	5566
PLOTFN	5564
PLOTSL	5330
PLOTT1	5545
PLOTT2	5550
PLOTT3	5553
PLOTWT	5573
PLOTX	5400
PLOT1	5427
PLOT2	5475
PLOT3	5516
PLOT4	5543
PLPD	6524
PLPL	6521
PLPR	6511
PLPU	6504
PLSF	6501
PLTASC	4400
PLUD	6522
PLUL	6523
PLUR	6513
PNTR	6547
POINT	6362
PRNT1	6351
PSIZE1	4533
QUOL	0176
RAR1	7572
RAR3	7544
RBA	6631
RBS	6631
RDTAPE	0132
RDTF	4117
READ	4406
READTF	4115
READ1	5200
REMAIN	5654
RESET	4325
RESETL	6726
REST	7352
RET	6236
RETN	6025
RETN2	7400
RETRN	4232
RFD	6654
RODTBO	7722
R6	6225
SAVE	6660
SCA	7441
SCOUNT	6365
SGN	7351
SGN1	5723
SHIFT	7641
SHIFT2	7151
SHIFT3	7104
SHL	7413
SICNV	0141
SICONV	4235
SICTBL	4370
SIGN	7330
SIGN1	7667
SIMASK	4301
SIM271	4304
SIN	0003
SINFUT	4263
SIZE	0153
SIZE1	4635
SIZE2	4704
SIZE4	4715
SMINUS	6137
SNPT	6141
SPACE	0155
SPCE	6360
SQCON1	7770
SQNE	0001
SQROOT	7645
SQRRT	0002
SQRT	7765
SQUARE	6770
SQR	7161
STOKEL	4331
STOKE2	6777
STORL	0136
SZECNT	4716
TABLE	6666
TABLE6	7545
TAG1	7173
TAG2	7174
TEMFX	6364
TEN	6171
TENTH	6166
TEST	7167
TEST3	7170
TEST4	7171
TEST5	7172
TNM1M	5362
TNM37	5360
TN100	5363
TN215	5361
TN237	5364
TN77	5357
TFBLK	4061
TFCNT	4154
TFFLAG	4047
TWOFI	6517
TYFF	4405
TYFF1	5302
TYFNT	5337
TYFFLT	0152
TYPX	5321
TYPY	5340
UNORM	6772
WRITE	4404
WRITTF	4035
WRTAFF	0131
WRTTF	4041
WRTTF1	4074
X	6525
XCRD	4717
XCRD1	4531
XSQR	6530
XXX	6317
YCRD	4720
YCRD1	4532

SUMMARY

This thesis deals with the investigation of the temperature- and magnetic field-dependence of the photoconductivity spectra of shallow donors and acceptors present in high purity germanium. These spectra lie in the difficult region of the far infrared. To enter this region a Michelson interferometer has been constructed capable to cover the wave number range of 5-350 cm^{-1}. This instrument, the relevant detector system (bolometer cooled with liquid helium) and the experimental arrangement for photoconductivity measurements are described in Chapter II. This latter system allows measurements at controlled temperatures between 1 and 15 K.

In the progress of these investigations it was discovered that a substantial deviation from the real spectrum may be caused by radiation which is reflected back into the interferometer due to reflection on the sample. In Chapter III, which starts with the elementary theory of Fourier spectroscopy on which our experimental method is based, the theoretical and experimental investigation of this reflection-effect is discussed.

In Chapter IV the application of the interferometer to the study of the photoconductivity in ultra-pure germanium is treated. Using the technique of photo-thermal ionization spectroscopy the impurities, which are present in extremely low concentrations of 10^{10}-10^{11} atoms/cm^3, are analyzed. The binding energies of the electron/hole of the donor/acceptor impurities were determined very accurately from the temperature dependence of the peak-intensity in the hydrogen-like excitation spectra. The complete temperature dependence of the photo-thermal conductivity signal was thoroughly investigated, both theoretically and experimentally.

From measurements in a magnetic field, the linear and quadratic Zeeman-terms were determined for all lines of the boron acceptor excitation spectrum. The relevant values for these levels are compared with the available values from the literature. Some of the lines showing up in a magnetic field could be identified as states associated with light-hole Landau levels.

The computer programs developed for the processing of the measured interferogram data and executing the Fourier transform to get the frequency spectrum are collected in an Appendix. These programs are suitable for a PDP-12 (or, with slight modifications, for a PDP-8) laboratory computer.

Dit proefschrift behandelt het onderzoek naar de temteratuur- en magneetveld-afhankelijkheid van de fotogeleidings spektra van ondiep liggende donors en acceptors die aanwezig zijn in ultra-zuiver germanium. Deze spektra liggen in het moeilijke gebied van het verre infrarood. Om door te dringen in dit gebied werd een Michelson interferometer gekonstrueerd die een bereik heeft van golfgetallen tussen 5 en 350 cm^{-1}. Dit instrument, het bijbehorende detektor systeem (bolometer, gekoeld met vloeibaar helium) en de experimentele opstelling voor foto-geleidings metingen worden beschreven in Hoofdstuk II. Dit laatstgenoemde systeem maakt metingen mogelijk bij een gekontroleerde temperatuur tussen 1 en 15 K.

In de loop van het onderzoek werd ontdekt dat een aanzienlijke afwijking van het werkelijke spektrum kan worden veroorzaakt door straling die ten gevolge van reflektie op het sample wordt teruggekaatst in de interferometer. In Hoofdstuk III, dat begint met de elementaire theorie over Fourier spektroskopie waarop onze experimentele methode is gebaseerd, wordt het theoretische en experimentele onderzoek van dit reflektie-effekt besproken.

In Hoofdstuk IV wordt de toepassing van de interferometer bij het bestuderen van de foto-geleiding in ultra-zuiver germanium behandeld. De onzuiverheden, die aanwezig zijn in extreem lage concentraties van 10^{10}-10^{11} atomen/cm^3, worden geanalyseerd door gebruikmaking van de techniek van fotothermische ionisatie spektroskopie. De bindings-energieën van het elektron/gat van de donor/acceptor onzuiverheden werden zeer nauwkeurig bepaald uit de temperatuur-afhankelijkheid van de intensiteit van de pieken in de waterstof-achtige excitatie spektra. De volledige temperatuur-afhankelijkheid van het foto-thermische geleidings-signaal werd grondig onderzocht, theoretisch zowel als experimenteel.

Uit metingen in een magneetveld werden de lineaire en kwadratische Zeeman-termen bepaald voor alle lijnen van het excitatie spektrum van de borium acceptor. De desbetreffende waarden voor deze niveau's worden vergeleken met de beschikbare waarden uit de literatuur. Enige van de lijnen die ontstaan in een magneetveld konden worden geidentificeerd als toestanden die verbonden zijn met Landau niveau's van lichte gaten.

De computer programma's die werden ontwikkeld voor het verwerken van de gemeten interferogram data en het uitvoeren van de Fourier transformatie om

het frekwentie spektrum te verkrijgen zijn verzameld in een Appendix. Deze programma's zijn geschikt voor een PDP-12 (of, met geringe wijzigingen, voor een PDP-8) laboratorium computer.

CURRICULUM VITAE

H.W.H.M. Jongbloets

Geboren	:	22 december 1943, Nijmegen
1950 - 1956	:	Lagere school, Nijmegen
1956 - 1961	:	Dominicus College, Nijmegen; HBS-b
1961 - 1963	:	Technische Hogeschool, Eindhoven Elektrotechniek
1964 - 1965	:	Militaire dienst
1965 - 1972	:	Katholieke Universiteit, Nijmegen Natuurkunde studie, in april 1972 afgesloten met het doctoraal examen Experimentele Natuurkunde, hoofdvak Vaste Stoffysica
1972 - 1978	:	Promotie-onderzoek Experimentele Vaste Stoffysica, als F.O.M. medewerker bij de afdeling Experimentele Natuurkunde 4, Faculteit der Wiskunde en Natuurwetenschappen, Katholieke Universiteit Nijmegen, groepsleider: Prof.Dr. P. Wyder
april-okt. 1979	:	In dienst van de vakgroep Vaste Stoffysica van de afdeling der Technische Natuurkunde van de T.H.-Eindhoven voor een tijdelijk onderzoek gestationeerd in Nijmegen, groepsleider: Prof.Dr. M.J. Steenland

STELLINGEN

I

De extrinsieke geleiding van halfgeleiders wordt in het algemeen bepaald door de absolute waarde van het verschil van de donor- en acceptor-koncentraties Onder bepaalde omstandigheden echter dragen donors en acceptors afzonderlijk bij tot de geleiding

II

Bij de bestudering van de bandenstructuur van materialen als $Cd_3As_{2-x}P_x$ via optische effecten kan de nauwkeurigheid van de analyse sterk worden vergroot door naast reflectie en transmissie-metingen de absorptie te bepalen via de kalorische methode

M.J. Gelten, A. van Lieshout, C. van Es and F.A.P. Blom, J. Phys. C 11, 227 (1978)

III

Anders dan bij metalen kunnen bij halfmetalen veranderingen in de effectieve massa van de electronen als gevolg van de electron-fonon interaktie niet worden verwaarloosd bij fonon-spektroskopie met behulp van de puntkontakt methode

A.G.M. Jansen, F.M. Mueller and P. Wyder, Science 199, 1037 (1978)

IV

Door een ongunstige verhouding tussen golflengte en bundel-diameter treden bij verre infrarood apparatuur vaak diffractie-problemen op, die vermeden kunnen worden door bundels met een gaussische intensiteits-verdeling te gebruiken Een dergelijke intensiteits-verdeling zou kunnen worden verkregen door toepassing van metaal-maas filters met een kontinu verlopende strip-breedte

D.H. Martin and J. Lesurf, Infrared Physics 18, 405 (1978)

De optische eigenschappen van bepaalde materialen kunnen worden bestudeerd door de spiegels van een Fabry-Perot interferometer met deze materialen te bedekken De werking van de interferometer kan worden geoptimaliseerd via de bedekkingsgraad

C.G C.M. de Kort, Proefschrift, Nijmegen 1979

VI

Smith en Loewenstein geven een uitdrukking voor de efficiency van een beamsplitter, waarbij ook de absorptie in rekening wordt gebracht Deze formule geeft echter alleen betrouwbare resultaten indien rekening wordt gehouden met de invalshoek-afhankelijkheid van de absorptie term

D.R. Smith and E.V. Loewenstein, Appl. Opt. 14, 2473 (1975)

VII

Het is mogelijk verre infrarood straling te detecteren via de gelijkrichtende werking van een puntkontakt tussen normale metalen bij lage temperatuur

VIII

Indien camera's in een lichte kleur zouden worden uitgevoerd i p v het gebruikelijke zwart, zou de opwarming ten gevolge van geabsorbeerde zonnestraling en daardoor de kans op afwijkingen in de film veel geringer zijn

IX

Daar er geen direct verband bestaat tussen het brandstof-verbruik en de lawaai-produktie van de verschillende auto-modellen, zal de inning van de heffing geluidshinder wegverkeer via een prijsverhoging voor de brandstoffen wel een stimulans zijn om te kiezen voor zuinige, maar niet voor geluidsarme auto's

H.W H M Jongbloets

Nijmegen, 13 maart 1980